HEINRICH HEINE
UNIVERSITÄT DÜSSELDORF

Aberrant protein accumulation associated with proteostasis impairments in brain aging and disease

Inaugural-Dissertation

zur Erlangung des Doktorgrades
der Mathematisch-Naturwissenschaftlichen Fakultät
der Heinrich-Heine-Universität Düsseldorf

vorgelegt von

Philipp Ottis

aus München

Düsseldorf, Juli 2013

aus dem Institut für Neuropathologie
der Heinrich-Heine Universität Düsseldorf

Gedruckt mit der Genehmigung der
Mathematisch-Naturwissenschaftlichen Fakultät der
Heinrich-Heine-Universität Düsseldorf

Referent: Prof. Dr. Carsten Korth
Korreferent: Prof. Dr. Dieter Willbold

Tag der mündlichen Prüfung: 24.09.2013

Betreffend die vorgelegte Dissertation:

Aberrant protein accumulation associated with proteostasis impairments in brain aging and disease

Ich versichere an Eides Statt, dass die Dissertation von mir selbständig und ohne unzulässige fremde Hilfe unter Beachtung der„Grundsätze zur Sicherung guter wissenschaftlicher Praxis an der Heinrich-Heine-Universität Düsseldorf“ erstellt worden ist.

Des Weiteren versichere ich, dass diese Dissertation zuvor keiner anderen Universität oder Fakultät vorgelegt wurde und ich bislang keinerlei andere Promotionsversuche getätigt habe.

Düsseldorf, den 29. Juli 2013

Ph. Ottis

Philipp Ottis

Abstract

Protein homeostasis (”Proteostasis”), the cellular maintenance of a soluble and functional proteome, constitutes an extremely sensitive equilibrium of protein metabolism and folding. Disturbance of this equilibrium by intrinsic processes or environmental factors usually results in the accumulation of damaged, misfolded proteins, often of poor solubility and degradability. Such aberrant protein agglomerations have been directly linked to cellular pathology. The investigation of proteostasis impairments and the related disease-associated accumulation of polypeptides therefore constitutes an important step towards diagnostics and potential intervention in cellular pathology via novel therapeutic targets.

In this cumulative dissertation, two of the three studies described, analyze protein precipitation associated with normal aging, a known condition of decreased proteostasis, particularly in neurons, and the mechanistic implications for the pathophysiology of brain aging.

In the first study presented here, proteomic characterization of the age-associated lysosomal lipid and protein agglomeration, lipofuscin, yielded in the novel description of human and rat brain lipofuscin proteome. A comparison between the lipofuscin proteomes of rat and human, and a comparison with published reports on the proteomic composition of lipofuscin-like material of age-related macular degeneration, demonstrated an apparently conserved cellular mechanism between different species as well as between tissues of the same species.

In another study, investigating age-related changes of proteostasis in the rat hippocampus, age-associated disturbances in protein homeostasis were demonstrated by the description of compositional changes in the insoluble hippocampal proteome. Taking a systems biology approach and linking quantitative hippocampal proteomics data of aged rats to respective performance and learning scores of those animals, a molecular circuitry of three synaptic proteins was identified. The insolubility status of these three proteins, ARP3, NEB2 and BRAG2, correlated with cognitive performance and learning, thus implying a role of synaptic plasticity and memory formation in age-associated cognitive dysfunction.

Apart from aging as an intrinsic factor of disturbed proteostasis, specific disease conditions can either cause or manifest themselves in proteostasis impairments and protein insolubility. Therefore, effects, secondary to the previously described aggregation of the mental illness susceptibility protein DISC1 were subject of investigation. This resulted in the demonstration of co-aggregation with another protein, dysbindin, independently also strongly genetically linked to mental illness. This co-aggregation, modeled *in vitro* and in cell culture, was successfully validated in *post-mortem* brain material of cases with chronic mental illness.

All in all, the studies presented here highlight the widespread, pathognomonic and far-reaching effects of impairments of proteostasis, associated with states of diseases as well as with normal aging in the central nervous system – presumably all contributing in unison to the challenges inflicted upon the sensitive equilibrium of the functional cellular proteome.

Zusammenfassung

Proteinhomöostase („Proteostase“), das Aufrechterhalten eines löslichen und funktionellen, zellulären Proteoms, stellt ein äußerst sensibles Gleichgewicht des Proteinmetabolismus und der Proteinfaltung dar. Eine Störung dieses Gleichgewichts durch intrinsische Prozesse oder Faktoren der Umwelt können in der Akkumulation beschädigter, fehlgefalteter Proteine resultieren, welche oft schlecht löslich und schwer abzubauen sind. Ein direkter Zusammenhang zwischen derart aberranten Proteinaggregaten und zellulärer Pathologie ist beschrieben. Die Untersuchung von Störungen in der Proteostase und daraus abgeleiteten, krankheitsassoziierten Proteinaggregaten, stellt daher einen wichtigen Schritt im Bereich der Diagnostik dar, sowie auch einen molekularen, pharmakologischen Zielkomplex einer potentiellen Intervention in die zelluläre Pathologie.

Ausgehend von der bekannten Verschlechterung der zellulären Proteostase, insbesondere der des Gehirns, im Zuge des Alterungsprozesses, beschäftigen sich zwei der drei Studien der vorliegenden, kumulativen Dissertationsarbeit, mit altersassoziierter Proteinpräzipitation und den daraus abgeleiteten Implikationen für die Pathophysiologie der Hirnalterung.

In der ersten hier dargelegten Studie wird die proteomische Charakterisierung der altersassoziierten lysosomalen Lipid- und Proteinakkumulation, Lipofuszin, beschrieben. Ein Vergleich des Lipofuszinproteoms von Ratte und Mensch sowie ein weiterer Vergleich mit der bereits beschriebenen proteomischen Zusammensetzung der lipofus-

zinähnlichen Ablagerungen in altersbedingter Makuladegeneration, deuten auf einen konservierten zellulären Mechanismus zwischen unterschiedlichen Spezies sowie zwischen verschiedenen Geweben in der gleichen Spezies hin.

In der zweiten Studie, welche die Untersuchung altersabhängiger Veränderungen der Proteostase des Rattenhippocampus beschreibt, werden altersassoziierte Störungen in der Proteinhomöostase anhand der Charakterisierung von Veränderungen in der Zusammensetzung des unlöslichen Proteoms nachgewiesen. Einem systembiologischen Ansatz folgend, wurden die quantitativen proteomischen Daten des unlöslichen Hippokampusproteoms alter Ratten den jeweiligen Werten für kognitive Leistung und Lernen der individuellen Tiere gegenübergestellt. Diese Untersuchungen zeigen eine Korrelation zwischen dem Löslichkeitsstatus dreier Proteine, ARP3, NEB2 und BRAG2, und der kognitiven Leistung, beziehungsweise der Lernfähigkeit alter Ratten, und weisen damit auf einen Zusammenhang zwischen synaptischer Plastizität sowie Gedächtnisformierung und altersassoziierter kognitiver Dysfunktion hin.

Neben dem Prozess des Alterns als intrinsischer Faktor für eine gestörte Proteinhomöostase, können sich auch krankheitsassoziierte Bedingungen in Beeinträchtigungen der Proteostase sowie Proteinunlöslichkeiten manifestieren. In diesem Sinne wurden die Auswirkungen der Aggregation des mit mentalen Erkrankungen in Verbindung stehenden DISC1-Proteins auf andere Proteine untersucht. Als Ergebnis zeigte sich eine Co-Aggregation von DISC1 mit Dysbindin, einem anderen, unabhängigen, genetisch stark mit mentalen Erkrankungen assoziierten Protein. Diese, *in vitro* und in Zellkultur dargestellte Co-Aggregation, konnte erfolgreich in *post-mortem* Hirngewebe von Patienten mit chronischen mentalen Erkrankungen bestätigt werden.

Zusammenfassend zeigen die hier dargelegten Studien die stark verbreiteten, krankheitscharakteristischen und weitreichenden Effekte von Proteostasestörungen auf, welche eng mit Krankheitsbildern und dem normalen Alterungsprozess des Zentralnervensystems verbunden sind. Es darf angenommen werden, dass diese Effekte und Pro-

zesse gemeinsam zu einer weiteren Destabilisierung des sensiblen Gleichgewichts beitragen, in welchem sich das funktionelle zelluläre Proteom befindet.

Contents

1 Introduction

1.1 Protein folding

1.1.1 Assembly of functional protein structure

The structural determinants of protein folding have been conceived to be encoded in a protein's primary structure, i.e. its sequence of amino acids (Anfinsen, 1973). Already parallel to the translation process, the nascent polypeptide chain assembles its secondary structure, which consists of several individual, independently folding domains (Netzer and Ulrich Hartl, 1998). The driving thermodynamic force in the process of protein folding is established by the gain of free energy that compensates for the loss of conformational entropy (Brooks et al., 2001).

The energy landscape of the folding process can be viewed as a funnel, which is entered by the newly synthesized, unfolded protein (Figure 1) (Hartl et al., 2011). In the course of the funnel towards its narrow end the protein folds into subsequent conformations of energetically favorable states, following an overall decline of energy (Dobson, 2003).

While small polypeptide chains can fold into their native state unaided in a matter of microseconds (Kubelka et al., 2004), larger, multidomain proteins may take up to several hours to accomplish folding without aid (Herbst et al., 1997). Hence, to accomplish protein folding in an efficient timeframe, *in vivo* folding, in many cases, is accompanied by the acquisition of molecular chaperones, proteins that interact with the

nascent polypeptide chain and aid in the process of folding by shielding hydrophobic surfaces or shifting the folding environment [process reviewed by (Hartl, 1996; Hartl et al., 2011)].

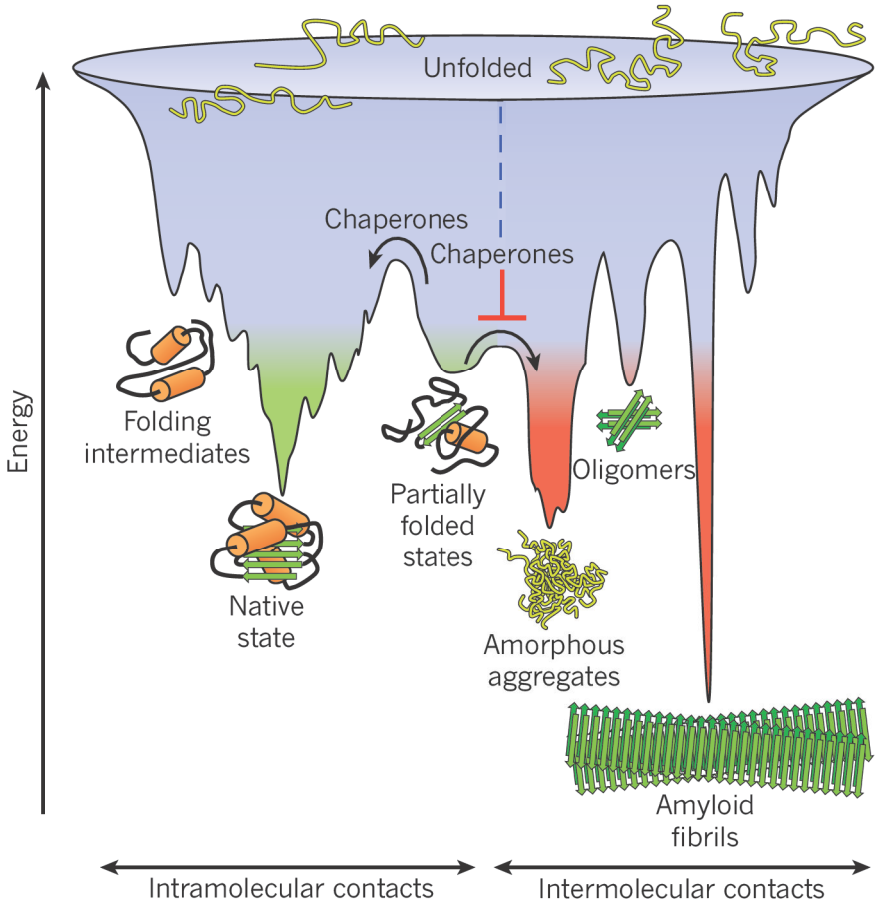

Figure 1: The energy landscape of protein folding.
Funnel-view of the decreasing free energy in protein folding. Unfolded proteins enter the process of protein folding with a relatively high amount of free energy and low entropy and, driven by the continuous release of energy, fold towards states of low energy and higher entropy. Pitfalls of non-native low energy conformations may only be overcome by the help of molecular chaperones. *Reprinted by permission from Macmillan Publishers Ltd: Nature (Hartl et al., 2011), copyright 2011.*

1.1.2 Misfolding

However, proteins may not always exit the folding process in their functional native conformations but get stuck in a folding state at low conformational entropy and in states of energy too low to allow for spontaneous refolding into their functional states (Figure 1) (Hartl et al., 2011). Under normal conditions within a cell, a refolding event is then again aided via the recruitment of specialized chaperones (Hartl et al., 2011). Yet, if the chaperone system does not work properly, e.g. due to cellular stress, the incorrectly folded protein might pass a point of no return and thus becomes ultimately misfolded.

As described, the chemical nature of the protein's side chains and the environment in which it folds provide critical forces for the folding. It is therefore conclusive that a change in the chemical nature of the protein, e.g. by mutation or aberrant post-translational modification, as well as changes in the protein's environment, i.e. the cell homeostasis, can shift the state of lowest energy away from the functional conformation towards a misfolded state (Fink, 1998; Uversky, 2003; Wetzel, 1994). Misfolding of a protein can occur from various intermediate states of the folding procedure and can lead to different types of aberrantly folded proteins (Figure 1) (Dobson, 2003). Under normal conditions, these misfolded proteins become rapidly degraded via the cell's proteolytic systems (Buchberger et al., 2010).

1.2 Proteostasis

The maintenance of a functional cellular proteome, also called protein homeostasis, or proteostasis, requires action from hundreds of components (Hartl et al., 2011) and is a challenging task for cells constantly subject to various changes of intra- and extracellular environment throughout their lifetime (Balch et al., 2008). The proteostasis network comprises multiple cellular pathways allowing for the modulation of all aspects of protein fate, from transcription initiation to terminal degradation (Balch et al., 2008),

enabling the cell to answer to homeostatic stress inflicted upon its proteome (Åkerfelt et al., 2010; Haynes and Ron, 2010; Ron and Walter, 2007). Apart from modulation of transcription, translation, and degradation to regulate protein concentrations, proteostasis networks also encompass pathways influencing protein folding, processing and modification, trafficking and localization, as well as assembly and disassembly of protein complexes (Balch et al., 2008; Douglas and Dillin, 2010). Herein, cellular principles of post-protein folding proteostasis maintenance shall be discussed in more detail.

1.2.1 Quality control and assisted folding and refolding

As mentioned above, polypeptide chains do not always fold towards their native, functional states straight away but often get trapped in some intermediate or misfolded state (Figure 1). In order to recognize non-native conformers and proteins damaged by aberrant modifications or uncontrolled chemical reactions introducing covalent bonds, e.g. oxidation, cells have evolved a mechanism of quality control to detect non-functional proteins (Buchberger et al., 2010).

Polypeptides in their non-native state are detected by exposed stretches of hydrophobic amino acids, otherwise buried in the core of the functionally folded proteins (Buchberger et al., 2010). In a first line of response such hydrophobic motifs are recognized by chaperones (Rüdiger et al., 1997a; Rüdiger et al., 1997b) and chaperonins (Sigler et al., 1998). These molecular machines shield the hydrophobic surfaces, thus preventing unwanted interactions and aggregation, and modulate their substrate's environment (Hartl et al., 2011). In case of protein aggregation, a special set of chaperones actively forces unfolding of protein complexes and untangles its substrate to loosen the aggregation (Sharma et al., 2009). In this concert action involving ATP-driven, repeated sequences of binding and release of the non-native substrate protein (Hartl et al., 2011), the chaperone system attempts disaggregation to induce refolding of the substrate in its native conformation, indicated by the absence of the recognized hydrophobic patches

(Buchberger et al., 2010; Wickner et al., 1999). If these attempts of refolding fail, the sequential actions of the chaperone system are terminated and the aberrantly folded substrate enters the proteolytic pathway (Buchberger et al., 2010; Connell et al., 2001; Wickner et al., 1999).

1.2.2 Proteolytic systems

Intracellular damaged and misfolded proteins pose a potential toxic threat to the cell as they enable non-native interactions with their abnormally folded and presented polypeptide chains (Bolognesi et al., 2010). In order to dispose of conformers that resist refolding, such substrates are subjected to one of the cell's two major protein degradation machineries (Buchberger et al., 2010). Modulation of either of these proteolytic machineries has been demonstrated to directly affect the accumulation of aggregation-prone proteins (Carew et al., 2010; Ravikumar et al., 2004; Waelter et al., 2001; Ward et al., 1995).

Proteasomal degradation

The ubiquitin proteasome system (UPS) is the main degradation machinery for the regulatory turnover of short-lived, functional proteins (Hershko and Ciechanover, 1998). However, it also takes a substantial part in the cell-clearing degradation of soluble misfolded proteins from the cytosol or endoplasmic reticulum (Hiller et al., 1996; Kaganovich et al., 2008). Proteins destined for proteasomal degradation become marked for destruction by the concert action of ubiquitin conjugating enzymes, catalyzing the subsequent covalent addition of multiple ubiquitin monomers to the substrate protein (Hershko and Ciechanover, 1998; Jung et al., 2009). Suchlike 'labeled' proteins are then degraded by the proteasome (Hershko and Ciechanover, 1998; Jung et al., 2009). Yet, as the entering of the substrate protein into the proteasome lumen requires unfolding of the substrate (Benaroudj et al., 2003; Groll et al., 2000), degradation of misfolded

proteins by the UPS is limited to monomeric and soluble proteins (Ding and Yin, 2008; Hershko and Ciechanover, 1998).

Lysosomal-autophagosomal degradation

Insoluble or long-lived proteins on the other hand, are usually targeted towards the macroautophagy-lysosome system for degradation (Ding and Yin, 2008). This system, henceforth just referred to as autophagy, shows less specificity than the UPS (Ding and Yin, 2008). Autophagy, therefore, makes up the major proteolytic pathway for insoluble proteins and protein aggregates (Bjorkoy et al., 2005; Ravikumar et al., 2002). Additionally, also the turnover of large protein complexes, such as the proteasome, and whole cell organelles, such as mitochondria, is executed via this lysosomal pathway (Cuervo et al., 1995; De Duve and Wattiaux, 1966; Kim et al., 2007). The mechanism of autophagy and lysosomal degradation has been studied and reviewed extensively (De Duve and Wattiaux, 1966; Luzio et al., 2007; Mizushima et al., 2008; Mizushima et al., 2002). Generally, cytosolic protein oligomers and organelles are engulfed by an autophagic isolation membrane forming the autophagosome, an enclosed, double membrane compartment surrounding the material destined for degradation (Mizushima et al., 2002). The autophagosome then fuses with a lysosome, which provides the acidic environment and the lytic enzymes required for proteolysis (Luzio et al., 2007).

1.2.3 Living on the edge hypothesis

The maintenance of a functional proteome is a challenging business for the cell. Especially, as co-translational misfolding of newly synthesized polypeptides alone can account for up to 30% of all freshly synthesized proteins (Princiotta et al., 2003; Schubert et al., 2000). Together with proteins marked for degradation due to normal turnover, regulatory elimination or irreparable damage, this constitutes a continuous flux of protein substrates through the cellular proteolytic systems (Ding and Yin, 2008). Since

misfolding and aggregation in particular, are therefore very costly and thus pose a great burden to the cell, highly expressed proteins tend to be more soluble than others (Drummond and Wilke, 2008, 2009; Tartaglia et al., 2007, 2009; Tartaglia and Vendruscolo, 2009; Vendruscolo, 2012; Winkelmann et al., 2010) and protein evolution is marked by the constant attempt to keep the proteins' aggregation propensity at the lowest level possible (Chen and Dokholyan, 2008; De Baets et al., 2011; Drummond and Wilke, 2008, 2009; Monsellier and Chiti, 2007; Monsellier et al., 2007; Vendruscolo, 2012). Yet, the findings by Tartaglia and colleagues, having plotted log-transformed expression levels of multiple proteins versus their respective measured, log-transformed aggregation rates, describe a direct correlation of those parameters, with correlation coefficients reaching an astonishing 0.97, indicating an almost perfect correlation (1.00) (Tartaglia et al., 2007; Tartaglia and Vendruscolo, 2009). This also suggests that aggregation is only avoided at the expression levels present, but with hardly any margin of safety to establish protein solubility under genetic or environmental challenge (Tartaglia et al., 2007). Tartaglia and co-workers termed this a "life on the edge" (Tartaglia et al., 2007), taking into account that protein evolution shaped polypeptides by two continuous opposing forces: The need for structural stability and the conformational flexibility required for proper functionality (DePristo et al., 2005; Gidalevitz et al., 2011; Kamerzell and Middaugh, 2008). This hypothesis indicates that protein expression levels *in vivo* are leveled out with the respective co-evolved aggregation propensity, fine-tuning protein concentrations to optimal efficiency, however with only marginal solubility (Tartaglia et al., 2007). Balancing on that 'edge' even minor environmental changes, such as oxidative stress, or changes of expression levels, e.g. in the course of aging, may result in the loss of protein solubility and subsequent aggregation (Gidalevitz et al., 2011; Tartaglia et al., 2007). Such an increase in misfolded and aggregated proteins in turn, results in an increased demand of the cell's proteostasis machinery, such as chaperones and the proteolytic systems (Taylor and Dillin, 2011). Eventually, this may result in a deple-

tion of the available chaperone and proteolysis machineries, consequently triggering precipitation of other metastable proteins prone to misfolding (Cuervo et al., 2010). A direct impairment of the ubiquitin-proteasome system by protein aggregates has been demonstrated (Bence et al., 2001). Thus, even minor increases of levels of misfolded proteins may have drastic effects (Taylor and Dillin, 2011). Destabilization of unrelated metastable components of the proteome in response to proteostatic challenge, e.g. by the introduction of labile or folding-incompetent protein species, has repeatedly been demonstrated (Gidalevitz et al., 2006; Gidalevitz et al., 2009; Gidalevitz et al., 2011; Olzscha et al., 2011). Conducting such an approach, Olzscha and co-workers identified a whole metastable sub-proteome aggregating in response to the expression of an artificial, aggregation-prone polypeptide (Olzscha et al., 2011).

This hypothesis of the 'life on the edge' is supported by increasing numbers of studies and could explain the dramatic effects seen upon age, stress or genetic mutation induced shifts of protein homeostasis (Gidalevitz et al., 2011; Vendruscolo, 2012).

1.3 Protein accumulation in its various forms

1.3.1 Protein aggregation

The aberrant accumulation of proteins, which are usually misfolded and mislocalized, is one of the first signs of a declining, stressed and impaired proteostasis system in which the substrates exceed the system's capacity (Ben-Zvi et al., 2009; Carew et al., 2010; Douglas and Dillin, 2010; Gupta et al., 2011; Waelter et al., 2001; Ward et al., 1995). Once a critical concentration of misfolded proteins is reached, their exposed hydrophobic parts can no longer be effectively shielded by the chaperone system (Hartl et al., 2011). As a consequence, these non-native conformers interact with other hydrophobic surfaces of their own protein species or of unrelated polypeptides, resulting in loss of solubility and aggregation (Kopito, 2000; Olzscha et al., 2011).

Only recently has protein aggregation been broadly recognized as an inherent molecular principle (Dobson, 1999) and a common cellular phenomenon (David et al., 2010; Narayanaswamy et al., 2009; Tartaglia et al., 2007; Vendruscolo, 2012; Vendruscolo et al., 2011). In 2000, Ron Kopito reviewed various reported characteristics of protein aggregates and proposed to define them as "oligomeric complexes of non-native conformers that arise from non-native interactions among structured, kinetically trapped intermediates in protein folding or assembly (Haase-Pettingell and King, 1988; London et al., 1974; Wetzel, 1994)" (Kopito, 2000). Aggregates are further characterized by their poor solubility in aqueous or detergent solvents and the mislocalization of the entrapped proteins (Fink, 1998). This insolubility of protein aggregates renders them metabolically stable under physiological conditions (Kopito, 2000).

Accumulating, insoluble proteins tend to agglomerate either in highly ordered, fibrillar structures, called amyloids, with exposed β-sheets forming hydrogen bonds with other β-sheet-rich proteins (Douglas and Dillin, 2010; Nelson et al., 2005), or as aggregates of disordered polypeptide chains lacking discernible organization (Zettlmeissl et al., 1979) (Figure 1). However, there is evidence that protein aggregation, ordered and disordered, underlie structural principles that are not yet fully understood. Those principles seem to allow – in some cases – strict protein-specificity for apparently disorganized accumulations (Rajan et al., 2001; Speed et al., 1996), whilst – at least in one case using artificial polypeptides – substantial co-aggregation with structured, amyloid-like precipitates has been demonstrated (Olzscha et al., 2011).

1.3.2 Aggresomes - aggregates of aggregates

Usually, intracellular misfolded and insoluble proteins initially precipitate forming mini-aggregates ($\sim$ 200 nm) throughout the cell (Garcia-Mata et al., 2002). These small aggregates are then transported along microtubules in a retrograde fashion towards the perinuclear microtubule organization center (MTOC) at the centrosome (Figure 2)

(García-Mata et al., 1999; Johnston et al., 1998; Wigley et al., 1999). An ATP-driven dynein/dynactin-mediated transport has been proposed for this mechanism (Johnston et al., 2002).

At the MTOC, the smaller particles accumulate and form larger aggregates (1 - 3 μm) (Figure 2), which reportedly also encompass members of the proteasome along with enzymes of the ubiquitination system, and proteins of the chaperone family (Lee et al., 2002; Wigley et al., 1999) [reviewed in (Garcia-Mata et al., 2002; Kopito, 2000)]. Reports on the presence of ubiquitin in the inclusions are inconsistent (Anton et al., 1999; García-Mata et al., 1999; Johnston et al., 2000; Johnston et al., 1998; Wigley et al., 1999). These microtubule dependent inclusions are called aggresomes (Johnston et al., 1998; Kopito, 2000). This term was introduced for the large perinuclear accumulations to replace the more widely used term 'inclusion body', which refers to an aggregate of aggregates, as well as to the respective foci of accumulation (Kopito, 2000).

Electron-microscopic investigations showed aggresomes as massive accumulations of tightly packed electron-dense matter near the centrosome (Johnston et al., 1998). Their formation is often accompanied by a collapse of intermediate filament networks. Vimentin, in particular, has been shown to form cage-like structures surrounding the aggresomes, as demonstrated by Johnston et al. (Johnston et al., 1998) and Garcia-Mata and colleagues (García-Mata et al., 1999). Such a cage of collapsed filaments might contribute to the exceptional stability of aggresomes (Kopito, 2000).

1.3.3 Aggresome formation - an inherent cellular mechanism

Although aggresomes are usually not observed in healthy, unstressed cells Ron Kopito and his group raised the idea of the aggresomal pathway being an underlying cellular process operating continuously to prevent intracellular accumulation of aggregated, misfolded proteins (Johnston et al., 1998; Kopito, 2000). Only if this pathway is overwhelmed, e.g. by cellular stress or by persistent aggregation of a certain protein species,

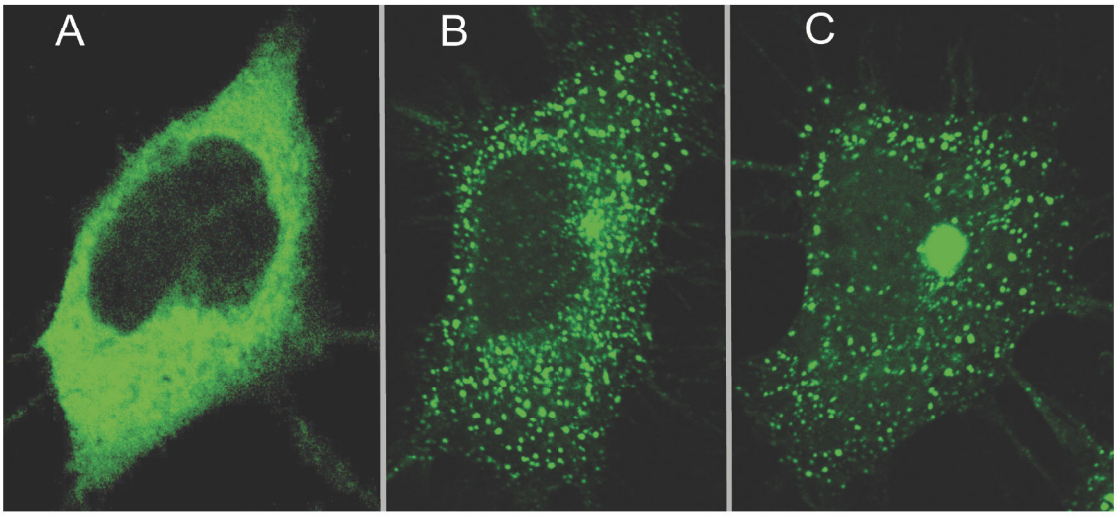

Figure 2: Aggresome formation at the MTOC.
Displayed are three CAD mouse neuroblastoma cells at different time points following transient transfection with metastable DISC1 protein, N-terminally fused to green fluorescent protein. Initially, the metastable polypeptide is equally distributed in the cytosol (A). Upon passing a certain capacity threshold, the cellular proteostasis system can no longer maintain the protein's solubility and small aggregates form throughout the cell (B). Subsequently, the small aggregates get actively transported towards the MTOC in a microtubule dependent mechanism. Here, the aggregates agglomerate and form large aggresomes (C). See also a review on this process in (Garcia-Mata et al., 2002).

the perpetual delivery system accumulates more and more mini-aggregates leading to bigger, actually detectable aggregates and eventually to aggresomes (Kopito, 2000) (Figure 2).

Sequestration of smaller aggregates into one or a few distinct aggresomes limits the misfolded proteins' surface exposed to the cytosol, were they might interact aberrantly with other proteins and may cause proteotoxicity. This cell-protective effect of aggresome formation has repeatedly been reported (Behrends et al., 2006; Cohen et al., 2006; Douglas et al., 2008; Tanaka et al., 2004; Taylor et al., 2003; Wang et al., 2009; Wolfe and Cyr, 2011).

Rafael Garcia-Mata and colleagues reviewed the formation of aggresomes at the MTOC and the different shapes in which they may assemble (Garcia-Mata et al., 2002).

They reported an apparent connection between the aggresomes' shape and their respective protein substrate, and also the cellular milieu in which the aggregation takes place. As a result, they describe two different types of aggresomes, single round-shaped spheres (Figure 2) and extended ribbons.

1.4 Implications of disturbed proteostasis and aberrant protein accumulation

1.4.1 Cellular effects of protein aggregation

Besides the precipitation of a small group of distinct proteins, whose aggregation does not result from proteostasis impairment but serves beneficial signaling purposes (Newby and Lindquist, 2013), there are two cellular effects arising upon protein aggregation: A loss-of-function and a gain-of-function effect. The gain of cytotoxic effects by the aberrant accumulation of misfolded polypeptides appears to be predominant (Taylor et al., 2002; Winklhofer et al., 2008) and, as a consequence of the toxicity, triggers the loss of normal cellular function (Winklhofer et al., 2008). This cytotoxic effect can be composed of various cellular affections, such as aberrant protein interactions and sequestration (Olzscha et al., 2011), disrupted ion homeostasis, oxidative stress, membrane damage and mitochondrial lesions (Bossy-Wetzel et al., 2004; Terman et al., 2006), and also inflammatory processes, transcriptional deregulation and aberrant trafficking (Bossy-Wetzel et al., 2004). The comparably rather weak effect of a loss of native function of the aggregating protein has so far only been conclusively demonstrated for the Huntington's disease protein huntingtin (Cattaneo et al., 2001; Dragatsis et al., 2000).

1.4.2 Aging

The process of aging is characterized by a progressive decline in proteostasis (Ben-Zvi et al., 2009; Douglas and Dillin, 2010; Lopez-Otin et al., 2013; Taylor and Dillin, 2011).

As illustrated by Peter Douglas and Andrew Dillin, there are substantial decreases in all protein homeostasis network components throughout the whole "proteostasis landscape" when comparing young and old organisms (Douglas and Dillin, 2010). The most serious losses in terms of maintenance of proteome solubility are changes in the protein quality control and degradational systems. In this context, age-associated decreases in the chaperone heat shock response (Fargnoli et al., 1990) (Heydari et al., 1993) as well as in the lysosomal protein degradation system (Cuervo and Dice, 2000; Simonsen et al., 2008) have been described. Reports concerning proteasomal activity in aging, however, are not consistent (Carrard et al., 2002; Ferrington et al., 2005; Keller et al., 2004). The close relationship of chaperone activity and aging has been further demonstrated by causatively linking it to longevity and accelerated aging (Hsu et al., 2003; Min et al., 2008; Morrow et al., 2004; Swindell et al., 2009; Walker and Lithgow, 2003). Positive effects on longevity were also shown for enhanced autophagy (Simonsen et al., 2008). These observed aging-associated changes in proteostasis capacity eventually can lead to the inability to maintain metastable proteins in their native, soluble conformation (Ben-Zvi et al., 2009; Douglas and Dillin, 2010). Such impairment, furthermore, consequently results in an excess of substrates and the subsequent accumulation of misfolded, insoluble and aggregated proteins (Ben-Zvi et al., 2009; David et al., 2010) leading to proteotoxic stress (Morimoto, 2008). Therefore, aging is now widely considered a major risk factor for protein conformational diseases (Amaducci and Tesco, 1994; Douglas and Dillin, 2010; Morawe et al., 2012).

Generally, cellular aging can be viewed as a specific pathophysiological condition (Terman and Brunk, 2004) and it has been proposed that the event of aging is a mere collapse of proteostasis (Ben-Zvi et al., 2009; Taylor and Dillin, 2011). This view could possibly also unify with the "lysosomal-mitochondrial axis theory of aging" (Brunk and Terman, 2002), which founds in the idea that, especially in post-mitotic cells, reactive oxygen species (ROS) severely damage proteins and organelles, mainly mitochondria,

leading to an impairment in their lysosomal degradation. Protein debris and damaged mitochondria, hence, accumulate in the cytosol and as an undigestable material within lysosomes, the so-called lipofuscin (Terman et al., 2006). In a vicious circle, lipofuscin and damaged mitochondria are thought to further increase the production of ROS. This theory was reviewed and further extended by Ulf Brunk, Alexei Terman and their co-workers (Brunk and Terman, 2002; Terman et al., 2006; Terman et al., 2010).

It is therefore reasonable to argue that the global, age-associated decrease in proteostasis capacity, due to impairments in degradation (Cuervo and Dice, 2000; Simonsen et al., 2008), not only leads to intra- and extracellular protein aggregation (Braak et al., 2011), but also to intra-lysosomal accumulation of hardly digestible substrates such as lipofuscin (Terman and Sandberg, 2002). Similar to gradual protein aggregation over lifetime (Braak et al., 2011), lipofuscin has been shown to accumulate almost linearly with age (Nakano et al., 1995).

1.4.3 Diseases of protein accumulation

As a consequence of the proposed 'living on the edge' (Tartaglia et al., 2007), it is not surprising that with the exhibited metastability of a major part of the proteome (Olzscha et al., 2011; Pace and Hermans, 1975) the introduction of certain allele mutations, such as missense single-nucleotide polymorphisms (Matthews, 1993; Pakula and Sauer, 1989), or environmental stressors (Farina et al., 2013; Gupta et al., 2011) into this sensitive equilibrium, can trigger protein destabilization, leading to protein misfolding, accumulation and, eventually, to diseases derived thereof (Chiti and Dobson, 2006). Up to 70% of low-frequency missense alleles in humans are therefore considered at least mildly deleterious (Kryukov et al., 2007) and create a cellular environment of enhanced predisposition for diseases. Events of proteostasis collapse and progressive aberrant accumulation of proteins manifest themselves especially in post-mitotic cells as these cells lack the ability to dilute their load of massed up proteins by cell division (Terman

et al., 2007). Some of the cells, most vulnerable to protein misfolding, accumulation and aggregation, are neurons (Drummond and Wilke, 2008; Lee et al., 2006).

Neurodegenerative diseases

The best-known group of diseases characterized by agglomerations in neurons are the neurodegenerative diseases. Among those, the Alzheimer's disease (AD) (Alzheimer, 1907) and the Creutzfeldt-Jakob's disease (CJD) (Creutzfeldt, 1920) are prominent examples of neuronal degeneration associated with extracellular protein aggregation. Intra-neuronal protein aggregation, on the other hand, characterizes maladies such as Parkinson's disease (PD) (Parkinson, 1817), Huntington's disease (HD) (Huntington, 1872), amyotrophic lateral sclerosis (ALS) (Rosen et al., 1993) and age-related macular degeneration (AMD) (Suter et al., 2000). In AD, additional to the extracellular accumulations of amyloid-β (Aβ) peptide, intracellular depositions of tau protein, so-called neurofibrillary tangles (NFTs), are typical (Nelson et al., 2009).

These neurodegenerative diseases with incidents partly as high as 17% in the case of AD (Beiser et al., 2000) and about 2% for PD (Elbaz et al., 2002) have in common that they occur in familial forms with inherited genetic mutations as well as sporadically (Mayeux, 2003). While sporadic forms usually are characterized by late onset, familial forms often already start in adulthood (Mayeux, 2003). In any case, a certain lag-phase is needed to set off the molecular disease cascade (Braak et al., 2011; Morawe et al., 2012). The deposition of NFTs and Aβ has been described to occur long before the potential onset of AD (Amieva et al., 2008; Lemere et al., 1996; Leverenz and Raskind, 1998; Ohm et al., 1995), beginning as early as in childhood and progressing continuously throughout life (Braak et al., 2011).

These observations and characteristics of neurodegenerative diseases point towards a compensatory role of the proteostasis network in maintaining a functional proteome in neurons challenged by disease proteins (Douglas and Dillin, 2010). The late onset of

these diseases suggests that the constant presence or gradual increase of disease proteins at some point meets the age-declining capacity threshold of the proteostasis machinery (Ben-Zvi et al., 2009), resulting in a loss of the compensation, and eventually to neurotoxicity (Douglas and Dillin, 2010; Morawe et al., 2012; Morimoto, 2008).

In many cases, oligomers, rather than the larger aggregates seem to mediate the toxic function [summarized in (Douglas and Dillin, 2010)], consistent with idea of a protective role of aggresomes and amyloids discussed above.

Non-neurodegenerative diseases

Non-neurodegenerative diseases of aberrant protein accumulation can be classified into systemic and localized, according to the pattern of affection within an organism. Examples for systemic protein conformational pathologies are the familial mediterranean fever, familial amyloidotic polyneuropathy and various amyloidoses of apolipoproteins, lysozyme and other proteins [reviewed by (Chiti and Dobson, 2006)].

Localized diseases of protein accumulation comprise maladies such as type II diabetes, cataract, pituitary prolactinoma [reviewed by (Chiti and Dobson, 2006)], and alcoholic liver disease (Hirano et al., 2009). Recently, disease-specific insoluble proteins were demonstrated to accumulate also in schizophrenia and other chronic mental diseases (Bader et al., 2012; Leliveld et al., 2008).

The present study focused on mammalian brain protein accumulation occurring as a result of impairments in proteostasis associated with psychiatric disease and normal aging. It attempts to contribute to the overall understanding of cellular mechanisms leading to the accumulation of misfolded and undegradable proteins in cells challenged by disease or aging. The described investigations on composition of protein accumulations and on the mechanism of secondary co-precipitation of intrinsically stable proteins through mutual interactions with aggregation-prone polypeptides are matched to

respective states of mental disease, aging or cognitive impairments. This study, thus shall contribute insight into the close relation of disturbed proteostasis and the cellular and organismal effects arising from this impairment.

2 Synopsis

2.1 Publication I

In the first study, the proteomic composition of brain-derived rat and human lipofuscin, an autofluorescent sedimentation in lysosomes of post-mitotic cells, directly related to aging, was analyzed. The findings suggest the existence of common cellular mechanisms underlying lipofuscin accumulation, conserved between species and tissues. These implications were substantiated by the identification of a set of 49 lipofuscin protein components – mainly mitochondria, cell membrane and cytoskeleton derived – present in the autofluorescence-enriched fractions of aged human subjects. An intra-species validation further produced an overlap of 64%, comparing the lipofuscin proteomic compositions of human and rat brain. The additional comparison with published proteomic data on cytotoxic lipofuscin derived from retinal pigment epithelium cells showed a substantial overlap in proteins of mitochondrial and cytoskeletal origin, indicating similar cellular processes for lipofuscin accumulation in different tissues. With lipofuscin sedimentation constituting the manifestation of a presumably inherently imperfect lysosomal degradation, these data may enable further research on age-associated pathophysiologies related to proteostasis impairments by lysosomal dysfunction.

2.2 Publication II

The second study, addressing age-associated disturbances in proteostasis, continues investigations on aging-related protein insolubility, initiated by work in the nematode *Caenorhabditis elegans*, where proteostasis collapse resulting in protein aggregation was demonstrated to be a phenotype of aging. The results presented here demonstrate this phenomenon to also occur in the course of mammalian brain aging. This is illustrated by the description of quantitative changes in the proteomic composition of the hippocampal insoluble proteome of adult and aged wild-type rats. Moreover, additional analysis of the proteomic data on each individual aged rat with regard to the respective behavioral data, assessed for each animal, identified a molecular circuitry of three post-synaptic proteins – ARP3, NEB2 and BRAG. These proteins, correlating in their solubility with performance levels as well as learning scores in a trial of spacial cognition, could all be implicated in the neuronal phenomenon of long-term depression mediated synaptic plasticity, underlying memory formation.

The novel demonstration of substantial changes in the proteostasis of the aging mammalian brain, along with specific changes being directly attributable to cognitive impairment in aged rats, will contribute to the understanding of the far-reaching effects of age-associated disturbances of the sensitive proteostatic equilibrium, particularly in post-mitotic neurons, which are especially vulnerable to such changes. Specifically the findings related to inferior cognition in the aged might give rise to novel approaches on the human mild cognitive impairment, a pre-pathological state of cognition and a major risk factor for the development of Alzheimer's disease.

2.3 Publication III

Following up on a recent report demonstrating insolubility of the mental illness susceptibility protein DISC1 in a subgroup of patients suffering from chronic mental diseases, this study presented here aimed to highlight further potential cellular consequences arising from disturbed DISC1 proteostasis. Led by the initial observation of DISC1 forming large aggresomes upon overexpression in cells, aggregation of this protein was modeled by transient transfection of cells in culture. Motivated by recent reports on substantial co-aggregation of metastable proteins following the disturbance of protein homeostasis by an initial aggregation event, the co-sedimentation of DISC1 with dysbindin, another unrelated protein highly implicated in schizophrenia, could be demonstrated. Subsequent *in vitro* experiments proved a direct interaction of recombinant dysbindin with soluble DISC1 oligomers, forming soluble multimeric structures. The resulting hypothesis of dysbindin – a second protein, separately identified as being linked to schizophrenia – passively co-precipitating with the presumably initially aggregating DISC1, could be demonstrated in *post-mortem* brains for a subgroup of patients of chronic mental diseases.

3 Publications

3.1 Publication I

Human and rat brain lipofuscin proteome

Philipp Ottis, Katharina Koppe, Bruce Onisko, Irina Dynin, Thomas Arzberger, Hans Kretzschmar, Jesus R. Requena, Christopher J. Silva, Joseph P. Huston and Carsten Korth

Proteomics 12 (2012) 2445-2454

Supplementary information can be accessed online via:
http://onlinelibrary.wiley.com/doi/10.1002/pmic.201100668/suppinfo

Author's contribution:
The author performed 4 out of 6 lipofuscin purifications and *post-hoc* analyses of all 6 proteomic data sets.
In particular, the author's contributions covered:

- Revision of experimental setup
- Tissue preparation (rats)
- Microscopic analyses
- Biochemical purification of lipofuscin material
- Fluorescence spectrometric analyses
- Separation and sampling of proteins for mass-spectrometry
- *Post-hoc* analyses of proteomic data sets using the Scaffold proteome software
- Gene-ontology analyses
- Writing the manuscript

RESEARCH ARTICLE

Human and rat brain lipofuscin proteome

Philipp Ottis[1], Katharina Koppe[1], Bruce Onisko[2,3], Irina Dynin[3], Thomas Arzberger[4], Hans Kretzschmar[4], Jesus R. Requena[5], Christopher J. Silva[3], Joseph P. Huston[6] and Carsten Korth[1]

[1] Department of Neuropathology, Heinrich Heine University of Düsseldorf, Düsseldorf, Germany
[2] OniPro, Kensington, CA, USA
[3] USDA, Albany, CA, USA
[4] Department Neuropathology, Ludwig-Maximilians-Universität München, München, Germany
[5] Department of Medicine and CIMUS Biomedical Research Institute, University of Santiago de Compostela-IDIS, Santiago, Spain
[6] Center for Behavioral Neuroscience, Department Experimental Psychology, Heinrich Heine University of Düsseldorf, Düsseldorf, Germany

Received: December 26, 2011
Revised: March 11, 2012
Accepted: March 26, 2012

The accumulation of an autofluorescent pigment called lipofuscin in neurons is an invariable hallmark of brain aging. So far, this material has been considered to be waste material without particular relevance for cellular pathology. However, two lines of evidence argue that lipofuscin may play a yet unidentified role for pathological cellular functions: (i) Genetic forms of premature accumulation of similar autofluorescent material in neuronal ceroid lipofuscinosis indicate a direct disease-associated link to lipofuscin; (ii) Retinal pigment epithelium cell lipofuscin is mechanistically linked to age-associated macular degeneration. Here, we purified autofluorescent material from the temporal and hippocampal cortices of three different human individuals by a two-step ultracentrifugation on sucrose gradients. For human brain lipofuscin, we could identify a common set of 49 (among > 200 total) proteins that are mainly derived from mitochondria, cytoskeleton, and cell membrane. This brain lipofuscin proteome was validated in an interspecies comparison with whole brain rat lipofuscin (total > 300 proteins), purified by the same procedure, yielding an overlap of 32 proteins (64%) between lipofuscins of both species. Our study is the first to characterize human and rat brain lipofuscin and identifies high homology, pointing to common cellular pathomechanisms of age-associated lipofuscin accumulation despite the huge (40-fold) difference in the lifespan of these species. Our identification of these distinct proteins will now allow research in disturbed molecular pathways during age-associated dysfunctional lysosomal degradation.

Keywords:
Aging / ATP synthase / Biomedicine / Fluorescence detection / Mitochondria / Oxidative phosphorylation

1 Introduction

Lipofuscin, first described in neurons by Hannover in 1842 [1] as a yellow-brown pigment, is found in postmitotic cells such as neurons, cardiac myocytes, retinal pigment epithelium (RPE) cells, and skeletal muscle fibers (reviewed in [2]). It appears chemically and morphologically polymorphous and, due to its assumed lysosomal origin, is widely considered to be waste material [3]. Lipofuscin consists of electron-dense material and features autofluorescence with characteristic spectral properties, showing emission at wavelengths between 460 and 630 nm when excited at wavelengths between 320 and 480 nm (Fig. 1) [4]. These pigment granules consist of approximately two-thirds protein and one-third lipids [5, 6]. Furthermore, small amounts of carbohydrates as well as traces of metal—mainly iron—have been reported to be contained in lipofuscin [5–7], while the lipid constituents

Correspondence: Dr. Carsten Korth, Neurodegeneration Unit, Department Neuropathology, University of Duesseldorf Medical School, Moorenstrasse 5, 40225 Duesseldorf, Germany.
E-mail: ckorth@uni-duesseldorf.de
Fax: +49-211-8117804

Abbreviations: AMD, age-associated macular degeneration; **HNE**, 4-hydroxy-2-nonenal; **MDA**, malondialdehyde; **NCL**, neuronal ceroid lipofuscinosis; **RPE**, retinal pigment epithelium

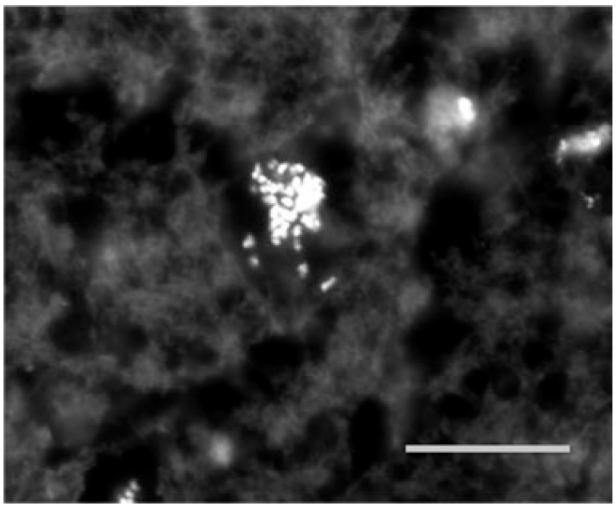

Figure 1. Fluorescent lipofuscin accumulation in a neuron of human brain (65 years). Cryosection of cortex under a fluorescence microscope with an excitation of 450–490 nm and detection at 520 nm. Visible are autofluorescent lipofuscin granules in a cortical neuron. Scale bar 20 μm.

have been characterized as triglycerides, free fatty acids, cholesterol, phospholipids, dolichols, and phosphorylated dolichols [3].

So far, most research into lipofuscin has focused on RPE-lipofuscin. The proteomic content of RPE lipofuscin has been investigated [8, 9] and retinoid derivatives were reported in these lipopigments [10]. In contrast, for the analysis of brain lipofuscin, only candidate protein identification rather than a systematic proteomic analysis has been performed. For example, amyloid β-protein was detected in neuronal lipofuscin [11]. The presence of undegraded macromolecules derived from phagocytosed long-lived proteins and damaged organelles, mainly mitochondria, appears to be a common feature of these lipopigments [8, 9, 12–14].

Lipofuscin, often referred to as "aging pigment," is located primarily in secondary lysosomes or residual bodies of post-mitotic cells [15–17] and accumulates in a linear relation to age [18–20]. For human myocardial cells, an accumulation of approximately 0.067% pigment growth per year and cell volume was determined [20] and for canine myocardium and the nervous system of *Callinectes sapidus* (blue crabs) such a correlation with age has also been shown [18, 19]. Lipofuscin is, therefore, considered to be a hallmark of aging. It has been difficult to ascribe a pathogenetic role for lipofuscin in physiological aging and, amazingly, lipofuscin accumulation adding up to 75% of the soma volume in aged neurons is still not considered to be abnormal [2]. Furthermore, the varying amount of lipofuscin accumulation in different neuronal subtypes remains unexplained [21].

The current concept of how lipofuscin originates [22] is that intracellular macromolecules and organelles such as mitochondria, destined for lysosomal degradation, get engulfed by a membranous phagophore in a phagocytotic process, resulting in the formation of an autophagosome. Extracellular material is taken up by phagocytosis, forming an early endosome. Fusion of these organelles with vesicles from the trans-Golgi network or with a mature resting lysosome delivers the proteolytic lysosomal enzymes together with an acidic environment, resulting in the formation of an autolysosome and in the degradation of the enclosed molecules. In a perfect process, this would result in complete degradation of the engulfed material, yielding an "empty" mature, resting lysosome. However, in the case of lipofuscin, lysosomal degradation is incomplete, leaving behind undegradable material that is not exocytosed and accumulates in the lysosomes over time (reviewed in ref. [22]).

Lipofuscin-like material present in genetic forms of premature lipopigment accumulation, termed neuronal ceroid lipofuscinoses (NCLs), is called ceroid and clearly has to be distinguished by nomenclature from mere age-related lipofuscin, as ceroids are not age-associated, but occur prematurely as a result of genetic mutational diseases (e.g. NCLs) [4, 23–26].

Purified lipofuscin granules have been demonstrated to show biological effects: Studies conducted with nonpathological lipofuscin-loaded cells, or cells treated with exogenous, purified lipofuscin granules, report a decrease in lysosomal hydrolase activity, antioxidant enzymes, and glutathione levels in those cells [27]. These experiments suggest a subsequent decay of the cells' capability to cope with potential stress factors will eventually lead to reduced viability and oxidative stress-induced apoptosis [28]. These studies, combined with our understanding of the role of RPE lipofuscin in age-associated macular degeneration (AMD) [29], suggest that the presence of lipofuscin is indicative of more than just a benign accumulation of "cellular garbage."

We hypothesized that due to the linear increase in the accumulation of lipofuscin with age, its pathogenic role in AMD and genetic NCLs, an analysis of the lipofuscin proteome might reveal candidate proteins involved in or hinting at the cellular circuitry that is deficient in the lysosomal failure during lipofuscin generation. Here, we analyzed the proteomic composition of human brain lipofuscin in three independent samples and validated this analysis by the analysis of rat brain lipofuscin.

2 Material and methods

2.1 Tissue

Animal brain tissue derived from whole brains of seven 20- to 21-month-old Wistar rats. Rats were anesthetized by inhalation of carbon dioxide directly before termination by decapitation and subsequent brain removal. For the first experiment (in the following depicted as "rat A"), the brain tissue of five rats was briefly kept on ice, pooled, and, subsequently homogenized and subjected to lipofuscin purification. The two remaining rat brains were snap-frozen in liquid nitrogen

directly after removal and were stored at –80°C until they were separately homogenized and subjected to lipofuscin purification.

Human brain tissue was obtained via the European BrainNet with informed consent and with consideration of all relevant ethical issues (outlined on http://www.brainnet-europe.org). In addition, experimentation with human brain tissue was approved by the Ethics Committee of the Medical Faculty of the University of Düsseldorf (#1978/2002 and 3224/2009).

The brains underwent a thorough neuropathological exam which led to the neuropathological diagnosis of beginning Alzheimer's disease in one case (human A) or the complete absence of brain disease (human B, human C). "Human brain A" was from temporal cortex of a 64-year-old female individual where the occurrence of neurofibrillary tangles at Braak stage IV had been noted [30] and CERAD-grade C was determined [31]. Human brain samples B and C were pieces of gyrus parahippocampalis from two female subjects, 85 years and 83 years old, respectively. Human B was noted to show no amyloid plaques and was classified Braak stage I. Human C was noted to show a few plaques in the gyrus hippocampalis and was classified Braak stage II. Both, human B and human C, were assigned the CERAD-grade 0. No other brain pathology or clinical disease was reported for the human samples.

2.2 Lipofuscin purification

All experimental steps were carried out on ice with prechilled buffers. All centrifugation steps were performed at 4°C. Lipofuscin was isolated using a method described by Boulton and Marshall [32]. Briefly, the deep frozen or fresh brain tissue was homogenized in presence of VRL buffer (50 mM Hepes, 0.25 M sucrose, 5 mM EDTA, 0.1 M potassium acetate, pH 7.5) supplemented with protease inhibitors (cOmplete, EDTA-free Protease Inhibitor Cocktail Tablets/Roche Applied Science, Mannheim, Germany) in a Dounce homogenizer to yield a 20% homogenate. The homogenate was centrifuged at 60 × *g* for 7 min. The resulting supernatant was removed and then centrifuged (6000 × *g*; 10 min). The pellet was resuspended in VRL-buffer (0.7 mL per gram of brain tissue). The suspension was layered on top of a discontinuous gradient consisting of five different concentrations of sucrose in VRL-buffer: 1.6, 1.5, 1.4, 1.2, 1.0 M. One large-scale preparation (rat A: 1, 1.2, 1.4 M, 5 mL each; 1.5, 1.6, 1.8 M, 3.5 mL each; human A: 1, 1,2, 1.4 M, 7 mL each; 1.5, 1.6 M, 3.5 mL each) and two small-scale preparations were performed (human B, C, rat B, C: each sucrose fraction was 0.75 mL and sample was 0.7 mL. All in a 5-mL Eppendorf ultracentrifugation tube).

Gradient separation was achieved by centrifugation at 100 000 × *g* for 1 h in a swing-bucket rotor (MLS-50, Beckman Coulter, Fullerton, CA, USA). The lipofuscin-containing interface was identified by its characteristic fluorescence excitation/emission spectrum [9, 32] (Fig. 2). The lipofuscin-containing interface fraction was diluted with phosphate-buffered saline (PBS) and pelleted at 6000 × *g* for 10 min. The pellet was resuspended in VRL-buffer and a second gradient separation with subsequent fluorescence 3D-scans of the interfaces was performed as described above. Finally, the identified lipofuscin fraction was diluted with PBS, pelleted, and washed two times in PBS (all 6000 × *g*; 10 min).

2.3 Fluorescence 3D scans

Identification of the lipofuscin-containing fractions was achieved by analyzing the excitation wavelengths and emission spectra of the different samples. This was performed in a Safire microplate reader (Tecan, Switzerland) using black 96-well microtiter plates. Emission spectra were recorded between 400 and 500 nm for the excitation wavelengths: 325, 340, 355, 365, 370, 375, 385 nm (Fig. 2).

2.4 SDS-PAGE 1D-separation and sampling

Purified and washed lipofuscin, derived from 0.75 g brain tissue, was mixed with SDS-loading buffer supplemented with 1% beta-mercaptoethanol, heated to 95°C for 5 min, and was loaded onto an SDS gel. Separation of the polypeptides was achieved by electrophoresis with application of 180 V for approximately 1 h. Following this, the gel was stained for proteins with the Colloidal Blue Staining Kit (Invitrogen, Darmstadt, Germany; see Supporting Information Figs. S1–S4). The resulting visualized smear of proteins was excised from the gel and was cut into small gel bands. The excised bands were cut into 1 mm sized cubes, placed in 96-well digestion trays (INTAVIS Bioanalytical Instruments AG, Bergisch Gladbach, Germany) according to their apparent molecular weight in the gel. Subsequently, these gel cubes were subjected to in-gel trypsin digestion.

2.5 In-gel digestion and processing of peptides

In-gel digestion of the 96-well digestion trays was done with a DigestPro (INTAVIS Bioanalytical Instruments AG, Koeln, Germany). Following washing, reduction with DTT, alkylation with iodoacetamide, and tryptic digestion, the peptides were eluted with 40 μL of 10% formic acid containing 0.1% trifluoroacetic acid.

2.6 LC/MS/MS

NanoLC/ESI/MS/MS analysis for human B, C, and rat B, C samples was done with an Applied Biosystems (ABI/MDS SCIEX, Toronto, Canada) model QStar Pulsar equipped with a Proxeon Biosystems (Odense, Denmark) nanoelectrospray source. Digested samples (20 μL) were loaded automatically

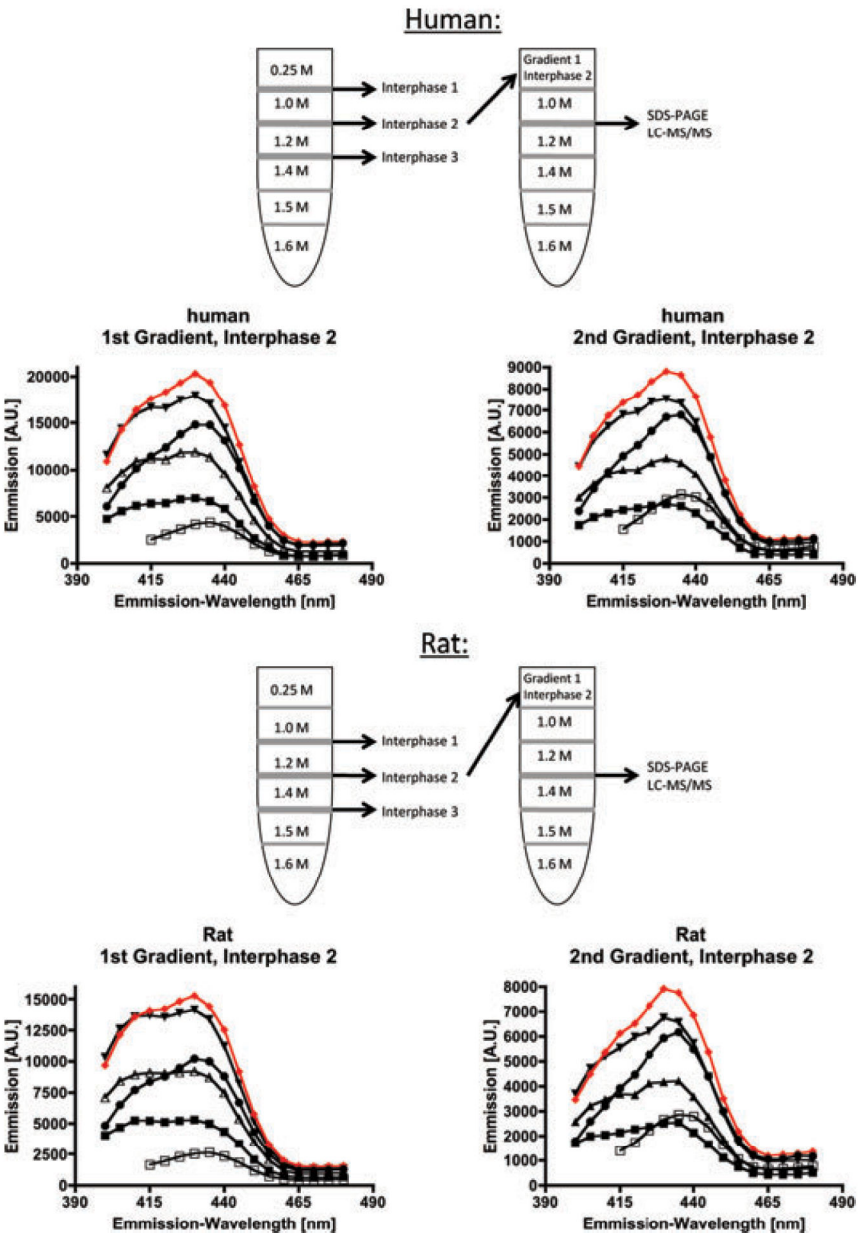

Figure 2. Flowchart of lipofuscin purification by sucrose gradients out of human (top panel) and rat (bottom panel) brain homogenates, as well as 3D fluorescence scans of selected lipofuscin fractions. A schematic tube with layers consisting of discontinuous sucrose concentrations is shown on top of both panels. Below are the fluorescence scans for human and for rat lipofuscin fractions showing emission spectra at variable excitation wave lengths for the first and the second sucrose gradient. The second purification step led to a reduction in fluorescence intensity of the selected fraction approximately 50%. Characteristic emission maximum with 370 nm excitation is highlighted in red. In each of the 3D fluorescence scans, the emission spectra of the following excitation wavelengths are depicted: Filled squares 325 nm, open triangles 340 nm, filled triangles 355 nm, filled red diamonds 370 nm, black diamonds 385 nm, open squares 400 nm.

onto a C-18 trap cartridge and chromatographed on a RP column (EASY-Column, 75 μm × 100 mm; Thermo Scientific; Waltham, MA, USA) fitted at the effluent end with stainless steel emitter spray tip (Thermo Scientific). A nanoflow LC system (EASY-nLC II, Thermo Scientific) with autosampler, column-switching device, loading pump, and nanoflow solvent delivery system was used. Elution solvents were A (0.1% formic acid in water) and B (0.1% formic acid in ACN). Samples were eluted at 250 nL/min with the following gradient profile: 15% B at 0 min to 25% B in a 25-min linear gradient; 45% B at 25 min to 60% B in a 5-min linear gradient; 60% B at 30 min to 80% B in a 5-min linear gradient; held at 80% B for 5 min then back to 15% B for 5 min. The QStar Pulsar was externally calibrated daily and operated above a resolution of 8000. The acquisition cycle time of 6 s consisted of a single 1-s MS "survey" scan followed by a 5-s MS/MS scan. Ions between m/z 400 and 2500 of charge states between +2 and +4 having intensities greater than 40 counts in the survey scan were selected for fragmentation to improve spectra quality. A new 1-s survey scan was then repeated to find the next best precursor for MS/MS. The dynamic exclusion window was set to exclude previously fragmented masses for the next 45 s to prevent repeated MS/MS analysis of the same peptide, but to allow other peptides with similar precursors, but different retention times to be analyzed. Collision energy optimized for charge state and m/z was automatically selected by the Analyst QS software after adjusting parameters to obtain satisfactory fragmentation of human [Glu^1]-fibrinopeptide B (+2).

Nitrogen was used for the collision gas, and the pressure in the collision cell ranged from 3×10^{-6} to 6×10^{-6} torr.

In between the analysis of human A/rat A samples and the respective B and C samples, the nanoLC-system had to be replaced; therefore, the gradient settings were slightly different. Elution solvents for the A samples were A (0.5% acetic acid in water) and B (0.5% acetic acid in 80% ACN/20% water) in a 15-min linear gradient from 2% B at 0 min to 80% B, held at 80% B for 5 min, returned to 2% B over 10 min from a RP column (Vydac, Grace Davison Discovery Sciences, Deerfield, IL, 238EV5.07515, 75 μm × 150 mm) fitted with a coated spray tip (FS360–50-5-CE; New Objective, Inc., Woburn, MA). NanoLC ESI MS/MS was done with an AB QStar Pulsar, with a Proxeon Biosystems nano-electrospray source, with resolution >10 000. A 5-s MS/MS scan followed a 1-s survey scan. Ions between m/z 400 and 1000, charges between +2 and +5, and intensities >40 counts were fragmented.

2.7 Database searching

MS/MS spectra were extracted in a deconvoluted and deisotoped charge state by Analyst QS version 1.1. All MS/MS samples were analyzed using Mascot (Matrix Science, London, UK; version Mascot) and X! Tandem (The GPM, thegpm.org; version CYCLONE [2010.12.01.1]). Mascot was set up to search the human or rat subset of the UniProt-database [33]. X! Tandem was set up to search the subset databases (state: June 2011, 41 471 entries for human and 33 954 entries for rat), assuming a digestion of the proteins with trypsin. Conducting the searches Mascot and X! Tandem allowed for fragment ion mass tolerance of 0.100 Da and a parent ion tolerance of 0.200 Da. The iodoacetamide derivative of cysteine was specified in Mascot and X! Tandem as a fixed modification, whereas oxidation of methionine was specified as a variable modification.

2.8 Criteria for protein identification

Scaffold (version Scaffold_3.2.0, Proteome Software Inc., Portland, OR, USA) was used to validate MS/MS-based peptide and protein assignments. Peptide identifications were accepted if they could be established at greater than 95.0% probability as specified by the Peptide Prophet algorithm [34]. Protein identifications were accepted if they could be established at greater than 99.9% probability and included at least three different identified peptides. Protein probabilities were assigned by the Protein Prophet algorithm [35]. Proteins that contained similar peptides and could not be differentiated based on MS/MS analysis alone were grouped to satisfy the principles of parsimony.

2.9 Data analyses

Detected proteins were checked for probability with regard to their approximate molecular weight observed in the gel and the amount of the corresponding peptides together with the resulting total sequence coverage. Peptides matched to unidentified proteins were manually reinvestigated for fitting to other known polypeptides. Fully uncharacterized proteins, whose peptides could not be mapped to other characterized proteins, were excluded from the final listing.

Gene ontology (GO) analyses were performed using the online DAVID Bioinformatics Resources 6.7 tool [36, 37] applying a brain subset of human or rat UniProt database [33] as background. *p*-Values stated were calculated by the DAVID tool and were corrected according to Bonferroni.

3 Results

3.1 Identifying lipofuscin guided by its fluorescence characteristics in sucrose gradients

Lipofuscin was purified from brain homogenates using the methods of Boulton and Marshall [32], and Schutt et al. [9]. The presence of the lipofuscin fractions was revealed by their characteristic fluorescent excitation using 3D-fluorescence scans. (Fig. 2) [8, 9].

After each ultracentrifugation step for both rat and human samples, three articulate interfaces formed, with the topmost containing a brown flocculent suspension. For the human samples, this fraction did not enter the gradient, but was present between the sample and the 1.0 M sucrose fraction (Fig. 2). For the rat sample, that upper interface formed between 1.0 and 1.2 M sucrose. Though this fraction had the highest emission maxima in the fluorescence scans for some of the samples, this interface presumably consisted to a large proportion of lipids and cell debris that was not readily separated by the gradient. Therefore, it was not analyzed further. The middle and lower interfaces are formed between 1.0 and 1.2 M sucrose, and between 1.2 and 1.4 M for the human samples. For the rat samples, they are formed between 1.2 and 1.4 M, and between 1.4 and 1.5 M. With the middle interface giving the highest characteristic emission maximum at 430 nm with 370 nm excitation wavelength (Fig. 2), these fractions at 1.0 M/1.2 M for human and 1.2 M/1.4 M for rat samples, respectively, were subjected to a second purification step on the same sucrose gradient.

After the second ultracentrifugation, the same interfaces as in the first gradient, 1.0 M/1.2 M (human), and 1.2 M/1.4 M (rat), respectively, were processed further (Fig. 2). These fractions were then washed, concentrated, separated via SDS-PAGE, and analyzed by MS as described.

Figure 2 displays representative plots of 3D-fluorescence-scans performed on those lipofuscin gradient interfaces used for further processing. Apparent are the emission maxima at 430 nm that reach their peak at an excitation wavelength of 370 nm. These observed spectra are consistent with the reported characteristics of lipofuscin granules isolated from RPE cells by Schutt et al. [9] and indicated purity.

Table 1. Major human brain lipofuscin proteins.

Entry Human	Entry Rat	Protein name	Subcellular location
P62258		14–3-3 protein epsilon	Cytoplasm/Melanosome
P61981		14–3-3 protein gamma (Protein kinase C inhibitor protein 1)	Cytoplasm
P63104	**P63102**	14–3-3 protein zeta/delta (Protein kinase C inhibitor protein 1)	Cytoplasm/Melanosome
P09543	**P13233**	2′,3′-cyclic-nucleotide 3′-phosphodiesterase	Cytoplasm/ Melanosome/Membrane
P10809	**P63039**	60 kDa heat shock protein, mitochondrial	Mitochondrion
***P60709**	**P60711**	Actin, cytoplasmic 1 (Beta-actin)	Cytoplasm/Cytoskeleton
*P02511		Alpha-crystallin B chain (Heat shock protein beta-5)	Cytoplasm
***P25705**	**P15999**	ATP synthase subunit alpha, mitochondrial	Mitochondrion/Membrane
***P06576**	**P10719**	ATP synthase subunit beta, mitochondrial	Mitochondrion/Membrane
*O75947	**P31399**	ATP synthase subunit d, mitochondrial	Mitochondrion/Membrane
P48047	**Q06647**	ATP synthase subunit O, mitochondria	Mitochondrion/Membrane
P80723		Brain acid soluble protein 1	Cell membrane
Q9UQM7		Calcium/calmodulin-dependent protein kinase type II subunit alpha	Synapse
Q00610		Clathrin heavy chain 1	Cytoplasm/Vesicle/Membrane
***P12277**	**P07335**	Creatine kinase B-type	Cytoplasm
P12532		Creatine kinase U-type, mitochondrial	Mitochondrion/Membrane
*P20674	**P11240**	Cytochrome c oxidase subunit 5A, mitochondrial	Mitochondrion/Membrane
Q16555	P47942	Dihydropyrimidinase-related protein 2	Cytoplasm
Q05193		Dynamin-1	Cytoplasm
*P09104	P07323	Gamma-enolase (Neuron-specific enolase)	Cytoplasm/Membrane
*P14136		Glial fibrillary acidic protein (GFAP)	Cytoplasm
***P04406**	**P04797**	Glyceraldehyde-3-phosphate dehydrogenase (GAPDH)	Cytoplasm
P62873	**P54311**	Guanine nucleotide binding protein G(I)/G(S)/G(T) subunit beta-1	Cell membrane
*P09471	**P59215**	Guanine nucleotide binding protein G(o) subunit alpha	Cell membrane
Q08722		Leukocyte surface antigen (CD antigen CD47)	Cell membrane
Q13449		Limbic system associated membrane protein (LSAMP)	Cell membrane
*O75489		NADH dehydrogenase [ubiquinone] iron-sulfur protein 3, mitochondr.	Mitochondrion/Membrane
P07196		Neurofilament light polypeptide (NF-L)	Cytoplasm
P62937	**P10111**	Peptidyl-prolyl cis-trans isomerase A (PPIase A)	Cytoplasm
P13637	**P06687**	Sodium/potassium-transporting ATPase subunit alpha-3	Cell membrane
Q13813	**P16086**	Spectrin alpha chain, brain	Cytoplasm
Q01082	Q6XD99	Spectrin beta chain, brain 1	Cytoplasm
P60880	P60881	Synaptosomal-associated protein 25 (SNAP-25)	Synapse/Membrane
P61266	**P61265**	Syntaxin-1B	Cell membrane
P61764	**P61765**	Syntaxin-binding protein 1	Cytoplasm/Vesicle/Membrane
P04216	**P01830**	Thy-1 membrane glycoprotein (CD antigen CD90)	Cell membrane
P60174	**P48500**	Triosephosphate isomerase (TIM)	Cytoplasm
***P68363**	**Q6P9V9**	Tubulin alpha-1B chain	Cytoplasm/Cytoskeleton
P68366	Q5XIF6	Tubulin alpha-4A chain	Cytoplasm/Cytoskeleton
***Q13885**	**P85108**	Tubulin beta-2A chain	Cytoplasm/Cytoskeleton
***P68371**	**Q6P9T8**	Tubulin beta-2C chain	Cytoplasm/Cytoskeleton
***Q13509**		Tubulin beta-3 chain	Cytoplasm/Cytoskeleton
*P04350		Tubulin beta-4 chain	Cytoplasm/Cytoskeleton
*P07437		Tubulin beta-5 chain	Cytoplasm/Cytoskeleton
O94811		Tubulin polymerization-promoting protein (25 kDa, brain-specific)	Cytoplasm
P09936	Q00981	Ubiquitin carboxyl-terminal hydrolase isozyme L1	Cytoplasm
P36543	Q6PCU2	V-type proton ATPase subunit E 1	Cytoplasm/Vesicle/Membrane
P63027	**P63045**	Vesicle-associated membrane protein 2 (VAMP-2)	Cytoplasm/Vesicle/Membrane
***P21796**	Q9Z2L0	Voltage-dependent anion-selective channel protein 1	Mitochondrion/Membrane

Only those proteins that were identified in at least two of three independent analyses of human lipofuscin are depicted. Human orthologs, having been detected in at least two of three independent analyses of rat lipofuscin, are indicated by listing of the rat accession number. Proteins identified in all three experiments for human and for rat are highlighted in bold. Polypeptides, identified in RPE-derived human lipofuscin in the study conducted by Schutt et al. in 2002 [9], are marked with an asterisk.

3.2 Validation of human lipofuscin proteome content by intra- and interspecies comparisons

The initial experiment with "human A" and "rat A" brain samples employed three SDS gels of different acrylamide content (7.5%, 4–15%, 4–20%) in order to identify the best resolution for lipofuscin proteins and to enable detection of low-abundance proteins. By combining the MS/MS data of all peptides identified in the three different gels, we were able to identify 175 proteins for "human A" and 205 proteins for "rat A" (Supporting Information Tables S1 and S2). In order to validate the more abundant proteins as being the key players in lipopigment composition, two further experiments using MS/MS analysis of purified lipofuscin were performed for human ("human B" and "human C") and for rat ("rat B" and "rat C") samples. Here, only one gel (4–12% acrylamide) was used to separate the samples' proteins. This resulted in the clear identification of 33 proteins for "human B" and 49 proteins for "human C." For the rat samples, 57 lipofuscin-derived proteins could be identified in "rat B" and 66 in "rat C" (Supporting Information Table S2). Keratins and myelin-related proteins were excluded from the protein listings shown, as they are most likely contaminants and impurities that co-sediment with the pigment granules. Only proteins identified in at least two of the three experiments performed per species were considered to be validated and, therefore, are presented here as possible lipofuscin components (Table 1). The Venn diagrams in Fig. 3 visualize the amount of proteins identified in multiple samples and across species in rat and human lipopigments. Within the human triplicate analysis, 29 proteins were identified in two of the three experiments and 20 were found to be present in all human samples, together accounting for 49 proteins detected in more than two analyses of human lipofuscin. For the rat analyses, 27 proteins could be confirmed to be present in all three data sets, whereas 35 were identified in two separate experiments. Hence, a total of 62 rat proteins detected could be verified in at least one additional approach. The lower two diagrams in Fig. 3 display the overlap of lipofuscin proteins present in human and rat.

3.3 Analysis of validated top protein hits in human brain lipofuscin

All human proteins identified in at least two experiments are listed in Table 1 alongside the rat orthologs. Although most proteins could be identified at approximately the expected height in the gels with best sequence coverage, many proteins were found in clusters appearing at various positions in the gels, presumably due to crosslinking and different proteolytic processing. It is believed that uncontrolled oxidation within lipofuscin granules favors intermolecular crosslinking [22, 38]. GO analysis of the human proteins in Table 1 highlighted the significant enrichment ($p = 0.01$) of proteins of the mitochondrial membrane together with the 60 kDa heat shock protein, mainly located in the mitochondrial matrix. Apart from this heat shock protein and the voltage-dependent anion-selective channel protein 1 in the outer mitochondrial membrane, this protein cluster is composed of the U-type creatin kinase and subunits of the ATP synthase, of NADH dehydrogenase (Complex I), and of cytochrome c oxidase. All these subunits are part of the mitochondrial oxidative phosphorylation pathway.

Another identified cluster contains the cytoskeleton proteins beta-actin, together with tubulin alpha and beta chains, the intermediary filaments glial fibrillary acidic protein (GFAP) and neurofilament light polypeptide (NFL), as well as polypeptides associated with the cytoskeleton in terms of its maintenance and stability (tubulin polymerization promoting protein), remodeling (dihydropyrimidase-related protein 2), movement (spectrin alpha and beta chain), and transport (dynamin).

4 Discussion

To our knowledge, this is the first description of the proteomic composition of brain lipofuscin purified from human and rat brain. We validated our results by running several independent within-species analyses, as well as analyses of another species (rat). We used lipofuscin's characteristic autofluorescence to guide our purification, an approach previously employed to isolate RPE lipofuscin [8, 9]. This purification method relies on the integrity of binding of the autofluorescent pigments to the other proteins and it is not clear how strong this is; therefore, for further experiments focusing on the proteome content of brain lipofuscin, it would be helpful to have additional protein markers independent of the poorly defined autofluorescent brain lipofuscin pigments. One goal of the present study was to present lipofuscin protein candidates worth further investigation in future experiments to assess their value as autofluorescence-indpendent, tracking markers for brain lipofuscin.

The distribution of fractions formed during the separation of the homogenates in the sucrose gradient differed between human and rat. The fractions with the strongest characteristic excitation/emission spectra appeared to be shifted in their different sedimentation characteristics (by 0.2 M sucrose) toward heavier fractions in rat samples, even though the fluorescence characteristics of these interfaces were equal. These differences could be caused by different sizes of lipofuscin particles or differences in their relative lipid content, with a higher lipid content increasing buoyancy. For example, species differences in myelin content have been described to correlate with brain size, with bigger brains having higher myelin content [39], consistent with the increased buoyancy of human lipofuscin (Fig. 2).

We identified mitochondrial and cytoskeletal polypeptides as the main clusters of proteins present in neuronal lipofuscin. The proteome of retinal (RPE) lipofuscin had been identified previously [9] and in our data on brain lipofuscin, 19 of the 49 proteins (38%) listed in Table 1 were identical (marked with an asterisk in the table). Disregarding the

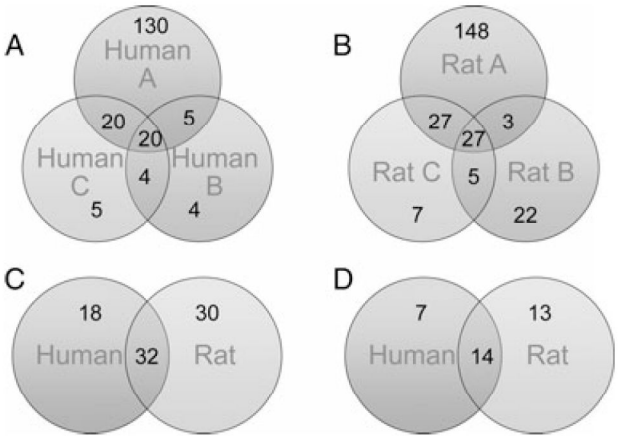

Figure 3. Venn diagrams of overlapping proteomic identification results. Values indicate the number of proteins clearly identified in each experiment. (A) Interrelation of the results for human lipofuscin with the three experiments Human A, B, and C. (B) Interrelation of the results for rat lipofuscin with the three experiments Rat A, B, and C. (C) Cross species overlap of proteins identified in at least two separate experiments for human and for rat. (D) Cross species overlap of proteins identified in all three separate experiments for human and for rat.

proteins of the visual cycle being present in RPE-lipopigments, the similarity of proteins indicates the existence of a general mechanism involved in lipofuscin formation. However, the fact that RPE lipofuscin is toxic and causes AMD whereas brain lipofuscin is at least not overtly neurotoxic to the brain suggests that either remaining differences in their protein, lipid, other organic or inorganic contents, or that different cellular susceptibility is responsible for the differences in the effects of accumulating lipofuscin.

The likelihood of general mechanisms of lipofuscin deposition is also highlighted by our findings of a 64% overlap of proteins clearly identified in both, human and rat, and also independent of Alzheimer disease neuropathology (present in the brain of human A). In particular, a majority of the polypeptides assigned to the two prominent protein clusters were shown to be present in neuronal lipofuscin of both species. On an absolute time scale, lipofuscin in humans appears much later in humans than it does in rats and the absolute age of neurons from rat and from human brain differed by a factor of 30–40 (investigated rat age: 21 months versus investigated human age: 64–85 years). The high similarity between human and rat lipofuscin protein content despite the large absolute time difference therefore indicates that that lipofuscin is likely to arise through distinct cellular processes rather than simple accumulation as a function of time and suggests a similarity in the still unknown age-associated lysosomal failure during brain aging in both species.

Many of the detected proteins were found at various positions in the gel and often also in high molecular weight fractions. Similar results were observed for the RPE pigments [9]. This indicates that those proteins were further processed by directed posttranslational modifications, proteolytic progression, and other undirected modifications occurring in the course of lipofuscin formation and deposition. Such undirected modifications may be, apart from oxidation [40], the attachment of advanced glycosylation end-products (AGEs) [41–43], modifications by malondialdehyde (MDA) and by 4-hydroxy-2-nonenal (HNE) [43, 44]. The latter two modifying components, MDA and HNE, are very reactive electrophilic aldehydes capable of crosslinking lysine residues and other primary amines. Both MDA and HNE are products of the reactive oxygen species (ROS) induced peroxidation of polyunsaturated lipids [44, 45] and around 40% of the hits reported for RPE-lipofuscin have been demonstrated to show MDA immunoreactivity [43]. In general, oxidative stress has been proposed to be the major trigger in lipofuscin formation [46]. ROS (primarily hydrogen peroxide) are mainly generated by mitochondria as byproducts of imperfect oxidative phosphorylation. They are assumed to diffuse into the lysosomes where they react with accumulated ferrous iron, Fe (II), in a Fenton-like reaction to generate highly reactive oxygen radicals, such as the hydroxyl radical, which then react with lipids to yield MDA and HNE or directly react with proteins present in the lysosome (reviewed by the group of Ulf T. Brunk [22, 38]). In addition, senescent mitochondria, producing increased amounts of ROS, have been proposed to accumulate in aged postmitotic cells, and thus, to act as the major cause of aging itself in these cells [38].

Curiously, many of the identified polypeptides are so-called housekeeping proteins. So far, most of these housekeeping proteins have not been shown to have any cytotoxic properties. Therefore, it has to be assumed that the reported toxic and stress-inducing effects of lipofuscin are related to the induced modifications occurring in the process of lipofuscin formation, as suggested by Schutt et al. [9]. However, there have been demonstrations of very abundant housekeeping genes showing important, previously unconsidered cellular functions. For example, the glyceraldehyde-3-phosphate dehydrogenase (GAPDH) was identified in all six experiments conducted here. This abundant protein, widely known for its role in the glycolytic pathway, was recently demonstrated to be involved in regulating apoptosis [47] in an aggregation-dependent manner and in oxidative stress induced cell death [48].

It should be noted that a proportion of our identified proteins is found among the top hits continuously reported in the majority of proteomic studies [49]. This especially applies to the various forms of tubulins and actin, but also to the 14–3-3 protein family and ATP synthase beta chain. However, in the case of brain lipofuscin, the group of ATP synthase subunits detected together with other proteins of the mitochondrial inner membrane indicates the specificity of these proteins as components of lipofuscin.

ATPase has been previously identified as a principal target of ROS-induced protein oxidative damage in rat liver mitochondria; in particular, as a target of oxidative modification by HNE [50]. In brain, it has been identified as a prominent target of modification by MDA [51]. Furthermore, an

age-related increase of oxidized ATP synthase has been found in interfibrillar heart mitochondria of rats [52].

While many of the proteins identified in neuronal lipofuscin in human and rat brain appear to be abundant housekeeping proteins, there is a striking overlap of the most prominent protein cluster of mitochondrial oxidative phosphorylation with the main components of pathologic ceroids reported for the genetic forms of premature lipofuscin-accumulation, the NCLs. The main components are ATP synthase subunit c and cytochrome c oxidase subunit 4 [23, 53, 54]. Even though these specific subunits could not be detected in our analyses, it remains highly intriguing that these polypeptides belong to the same protein complexes we identified as being the most prominent group in our data sets. This becomes even more interesting, considering that the symptoms observed in most of the NCLs, such as psychomotorical and cognitive impairments [4, 23], are also symptoms strongly associated with the "pathology" of aging. Hence, these findings may imply that ceroids in NCLs and lipofuscin in normal aging are not that different and they might share the same principle involved in the accumulation of nondegradable material affecting cell viability. It also supports the emerging view that lipofuscin is not just inert waste material, but, that on the contrary, it resembles ceroid accumulations, at least in part contributing to the pathology of NCLs, which, in turn, shares features also seen in the course of normal aging.

Further investigations regarding the proteomic composition of pathological ceroids versus age-associated lipopigments in the brain, the organ most susceptible to toxicity and oxidative stress, together with appropriate cell-culture models will help to contribute to the study of both lipopigment granules and their respective effects on the cell.

This research has been funded by grant from the EU-FP7 PRIORITY to C. K. and J. R. R., and grants form the DFG (GRK1033) and KNDD-Demtest to C. K., and Hu 306/27-2 to J.P.H.

The authors have declared no conflict of interest.

5 References

[1] Hannover, A., Mikroskopiske undersögelser af nervesystemet. *Kgl. Danske Vidensk. Kabernes Selskobs Naturv. Math. Afh. (Copenhagen)* 1842, *10*, 1–112.

[2] Terman, A., Brunk, U. T., Lipofuscin, Mechanisms of formation and increase with age. *APMIS* 1998, *106*, 265–276.

[3] Brunk, U. T., Terman, A., Lipofuscin, Mechanisms of age-related accumulation and influence on cell function. *Free Radic. Biol. Med.* 2002, *33*, 611–619.

[4] Seehafer, S. S., Pearce, D. A., You say lipofuscin, we say ceroid: defining autofluorescent storage material. *Neurobiol. Aging* 2006, *27*, 576–588.

[5] Jolly, R. D., Douglas, B. V., Davey, P. M., Roiri, J. E., Lipofuscin in bovine muscle and brain: a model for studying age pigment. *Gerontology* 1995, *41*(Suppl. 2), 283–295.

[6] Porta, E. A., Advances in age pigment research. *Arch. Gerontol. Geriatr.* 1991, *12*, 303–320.

[7] Essner, E., Novikoff, A. B., Human hepatocellular pigments and lysosomes. *J. Ultrastruct. Res.* 1960, *3*, 374–391.

[8] Warburton, S., Southwick, K., Hardman, R. M., Secrest, A. M. et al., Examining the proteins of functional retinal lipofuscin using proteomic analysis as a guide for understanding its origin. *Mol. Vis.* 2005, *11*, 1122–1134.

[9] Schutt, F., Ueberle, B., Schnölzer, M., Holz, F. G. et al., Proteome analysis of lipofuscin in human retinal pigment epithelial cells. *FEBS Lett.* 2002, *528*, 217–221.

[10] Murdaugh, L. S., Avalle, L. B., Mandal, S., Dill, A. E. et al., Compositional studies of human RPE lipofuscin. *J. Mass Spectrom.* 2010, *45*, 1139–1147.

[11] Bancher, C., Grundke-Iqbal, I., Iqbal, K., Kim, K. S. et al., Immunoreactivity of neuronal lipofuscin with monoclonal antibodies to the amyloid beta-protein. *Neurobiol. Aging* 1989, *10*, 125–132.

[12] Elleder, M., Sokolová, J., Hrebícek, M., Follow-up study of subunit c of mitochondrial ATP synthase (SCMAS) in Batten disease and in unrelated lysosomal disorders. *Acta. Neuropathol.* 1997, *93*, 379–390.

[13] Gray, D. A., Woulfe, J., Lipofuscin and aging: a matter of toxic waste. *Sci. Aging Knowledge Environ.* 2005, DOI: 10.1126/sageke.2005.5.re1.

[14] Nilsson, E., Yin, D., Preparation of artificial ceroid/lipofuscin by UV-oxidation of subcellular organelles. *Mech. Ageing Dev.* 1997, *99*, 61–78.

[15] Samorajski, T., Keefe, J. R., Ordy, J. M., Intracellular localization of lipofuscin age pigments in the nervous system. *J. Gerontol.* 1964, *19*, 262–276.

[16] Feeney, L., Lipofuscin and melanin of human retinal pigment epithelium. Fluorescence, enzyme cytochemical, and ultrastructural studies. *Invest. Ophthalmol. Vis. Sci.* 1978, *17*, 583–600.

[17] Essner, E., Novikoff, A. B., Localization of acid phosphatase activity in hepatic lysosomes by means of electron microscopy. *J. Biophys. Biochem. Cytol.* 1961, *9*, 773–784.

[18] Ju, S.-J., Secor, D. H., Harvey, H. R., Growth rate variability and lipofuscin accumulation rates in the blue crab *Callinectes sapidus*. *Mar. Ecol. Prog. Ser.* 2001, *224*, 197–205.

[19] Munnell, J. F., Getty, R., Rate of accumulation of cardiac lipofuscin in the aging canine. *J. Gerontol.* 1968, *23*, 154–158.

[20] Strehler, B. L., Mark, D. D., Mildvan, A. S., Gee, M. V., Rate and magnitude of age pigment accumulation in the human myocardium. *J Gerontol* 1959, *14*, 430–439.

[21] Mann, D. M., Yates, P. O., Stamp, J. E., The relationship between lipofuscin pigment and ageing in the human nervous system. *J. Neurol. Sci.* 1978, *37*, 83–93.

[22] Kurz, T., Eaton, J. W., Brunk, U. T., Redox activity within the lysosomal compartment: implications for aging and apoptosis. *Antioxid. Redox Signal* 2010, *13*, 511–523.

[23] Weimer, J. M., Kriscenski-Perry, E., Elshatory, Y., Pearce, D. A., The neuronal ceroid lipofuscinoses: mutations in different proteins result in similar disease. *Neuromolecular Med.* 2002, *1*, 111–124.

[24] Santavuori, P., Haltia, M., Rapola, J., Raitta, C., Infantile type of so-called neuronal ceroid-lipofuscinosis. 1. A clinical study of 15 patients. *J. Neurol. Sci.* 1973, *18*, 257–267.

[25] Haltia, M., Rapola, J., Santavuori, P., Keranen, A., Infantile type of so-called neuronal ceroid-lipofuscinosis. 2. Morphological and biochemical studies. *J. Neurol. Sci.* 1973, *18*, 269–285.

[26] Haltia, M., Rapola, J., Santavuori, P., Infantile type of so-called neuronal ceroid-lipofuscinosis. Histological and electron microscopic studies. *Acta. Neuropathol.* 1973, *26*, 157–170.

[27] Shamsi, F. A., Boulton, M., Inhibition of RPE lysosomal and antioxidant activity by the age pigment lipofuscin. *Invest. Ophthalmol. Vis. Sci.* 2001, *42*, 3041–3046.

[28] Terman, A., Abrahamsson, N., Brunk, U. T., Ceroid/lipofuscin-loaded human fibroblasts show increased susceptibility to oxidative stress. *Exp. Gerontol.* 1999, *34*, 755–770.

[29] Luibl, V., Isas, J. M., Kayed, R., Glabe, C. G. et al., Drusen deposits associated with aging and age-related macular degeneration contain nonfibrillar amyloid oligomers. *J. Clin. Invest.* 2006, *116*, 378–385.

[30] Braak, H., Braak, E., Neuropathological staging of Alzheimer-related changes. *Acta. Neuropath.* 1991, *82*, 239–259.

[31] Mirra, S. S., Heyman, A., McKeel, D., Sumi, S. M. et al., The consortium to establish a registry for Alzheimer's disease (CERAD). Part II. Standardization of the neuropathologic assessment of Alzheimer's disease. *Neurology* 1991, *41*, 479–486.

[32] Boulton, M., Marshall, J., Repigmentation of human retinal pigment epithelial cells in vitro. *Exp. Eye Res.* 1985, *41*, 209–218.

[33] UniProt-Consortium, Ongoing and future developments at the Universal Protein Resource. *Nucleic Acids Res.* 2011, *39*, D214–D219.

[34] Keller, A., Nesvizhskii, A. I., Kolker, E., Aebersold, R., Empirical statistical model to estimate the accuracy of peptide identifications made by MS/MS and database search. *Anal. Chem.* 2002, *74*, 5383–5392.

[35] Nesvizhskii, A. I., Keller, A., Kolker, E., Aebersold, R., A statistical model for identifying proteins by tandem mass spectrometry. *Anal. Chem.* 2003, *75*, 4646–4658.

[36] Huang da, W., Sherman, B. T., Lempicki, R. A., Bioinformatics enrichment tools: paths toward the comprehensive functional analysis of large gene lists. *Nucleic Acids Res.* 2009, *37*, 1–13.

[37] Huang da, W., Sherman, B. T., Lempicki, R. A., Systematic and integrative analysis of large gene lists using DAVID bioinformatics resources. *Nat. Protoc.* 2009, *4*, 44–57.

[38] Terman, A., Kurz, T., Navratil, M., Arriaga, E. A. et al., Mitochondrial turnover and aging of long-lived postmitotic cells: the mitochondrial-lysosomal axis theory of aging. *Antioxid. Redox Signal* 2010, *12*, 503–535.

[39] Zhang, K., Sejnowski, T. J., A universal scaling law between gray matter and white matter of cerebral cortex. *Proc. Natl. Acad. Sci. USA* 2000, *97*, 5621–5626.

[40] Stadtman, E. R., Protein oxidation and aging. *Science* 1992, *257*, 1220–1224.

[41] Shimokawa, I., Higami, Y., Horiuchi, S., Iwasaki, M. et al., Advanced glycosylation end products in adrenal lipofuscin. *J. Gerontol. A Biol. Sci. Med. Sci.* 1998, *53*, B49–B51.

[42] Brownlee, M., Advanced protein glycosylation in diabetes and aging. *Annu. Rev. Med.* 1995, *46*, 223–234.

[43] Schutt, F., Bergmann, M., Holz, F. G., Kopitz, J., Proteins modified by malondialdehyde, 4-hydroxynonenal, or advanced glycation end products in lipofuscin of human retinal pigment epithelium. *Invest. Ophthalmol. Vis. Sci.* 2003, *44*, 3663–3668.

[44] Esterbauer, H., Schaur, R. J., Zollner, H., Chemistry and biochemistry of 4-hydroxynonenal, malonaldehyde and related aldehydes. *Free Radic. Biol. Med.* 1991, *11*, 81–128.

[45] Requena, J. R., Fu, M. X., Ahmed, M. U., Jenkins, A. J. et al., Quantification of malondialdehyde and 4-hydroxynonenal adducts to lysine residues in native and oxidized human low-density lipoprotein. *Biochem. J.* 1997, *322*(Pt 1), 317–325.

[46] Terman, A., Gustafsson, B., Brunk, U. T., The lysosomal-mitochondrial axis theory of postmitotic aging and cell death. *Chem. Biol. Interact.* 2006, *163*, 29–37.

[47] Sen, N., Hara, M. R., Kornberg, M. D., Cascio, M. B. et al., Nitric oxide-induced nuclear GAPDH activates p300/CBP and mediates apoptosis. *Nat. Cell Biol.* 2008, *10*, 866–873.

[48] Nakajima, H., Amano, W., Kubo, T., Fukuhara, A. et al., Glyceraldehyde-3-phosphate dehydrogenase aggregate formation participates in oxidative stress-induced cell death. *J. Biol. Chem.* 2009, *284*, 34331–34341.

[49] Petrak, J., Ivanek, R., Toman, O., Cmejla, R. et al., Deja vu in proteomics. A hit parade of repeatedly identified differentially expressed proteins. *Proteomics* 2008, *8*, 1744–1749.

[50] Guo, J., Prokai-Tatrai, K., Nguyen, V., Rauniyar, N. et al., Protein targets for carbonylation by 4-hydroxy-2-nonenal in rat liver mitochondria. *J. Proteomics* 2011, *74*, 2370–2379.

[51] Pamplona, R., Dalfo, E., Ayala, V., Bellmunt, M. J. et al., Proteins in human brain cortex are modified by oxidation, glycoxidation, and lipoxidation. Effects of Alzheimer disease and identification of lipoxidation targets. *J. Biol. Chem.* 2005, *280*, 21522–21530.

[52] Chung, W. G., Miranda, C. L., Maier, C. S., Detection of carbonyl-modified proteins in interfibrillar rat mitochondria using N'-aminooxymethylcarbonylhydrazino-D-biotin as an aldehyde/keto-reactive probe in combination with Western blot analysis and tandem mass spectrometry. *Electrophoresis* 2008, *29*, 1317–1324.

[53] Kominami, E., Ezaki, J., Muno, D., Ishido, K. et al., Specific storage of subunit c of mitochondrial ATP synthase in lysosomes of neuronal ceroid lipofuscinosis (Batten's disease). *J. Biochem.* 1992, *111*, 278–282.

[54] Ezaki, J., Tanida, I., Kanehagi, N., Kominami, E., A lysosomal proteinase, the late infantile neuronal ceroid lipofuscinosis gene (CLN2) product, is essential for degradation of a hydrophobic protein, the subunit c of ATP synthase. *J. Neurochem.* 1999, *72*, 2573–2582.

3.2 Publication II

Aging-induced proteostatic changes in the rat hippocampus identify ARP3, NEB2 and BRAG2 as a molecular circuitry for cognitive impairment

Philipp Ottis, Bianca Topic, Maarten Loos, Ka Wan Li, Angelica de Souza, Daniela Schulz, August B. Smit, Joseph P. Huston and Carsten Korth

PLoS One, ***manuscript under review***

Author's contribution:

- Design of experimental setup
- Establishment of conditions for protein purification suitable for follow-up applications (e.g. trypsin digestion, iTRAQ-labeling) prior to start of experiments
- Biochemical purification of insoluble proteins
- Preparation for quantitative mass spectrometry (trypsin digestion, iTRAQ-labeling of peptides)
- F-actin precipitation assay
- *Post-hoc* statistical analyses of quantitative proteomic data sets
- Gene-ontology analyses
- Design of Figure 4
- Writing the manuscript

meanwhile published: Ottis, P., et al. (2013). PLoS One 8, e75112 [open access]

Aging-induced proteostatic changes in the rat hippocampus identify ARP3, NEB2 and BRAG2 as a molecular circuitry for cognitive impairment

Philipp Ottis[1], Bianca Topic[2], Maarten Loos[3,4], Ka Wan Li[3], Angelica de Souza[2], Daniela Schulz[2,#], August B. Smit[3], Joseph P. Huston[2], Carsten Korth[1]*

[1] Department of Neuropathology, Heinrich Heine University of Düsseldorf, Düsseldorf, Germany

[2] Center for Behavioral Neuroscience, Department Experimental Psychology, Heinrich Heine University of Düsseldorf, Düsseldorf, Germany

[3] Department of Molecular and Cellular Neurobiology, Faculty of Earth and Life Sciences, Center for Neurogenomics and Cognitive Research, Neuroscience Campus Amsterdam, VU University, Amsterdam, The Netherlands

[4] Synaptologics B.V., Amsterdam, The Netherlands

[#]Present address: Department of Neurobiology and Behavior, Stony Brook University, Stony Brook, NY, USA

* Corresponding author:

Carsten Korth, MD, PhD

Department of Neuropathology

Heinrich Heine University of Dusseldorf

Moorenstrasse 5

40225 Dusseldorf

Germany

Tel +49-211-811 6153

email: ckorth@uni-duesseldorf.de

Abstract:

Disturbed proteostasis as a particular phenotype of the aging organism has been advanced in *C. elegans* experiments and is also conceived to underlie neurodegenerative diseases in humans. Here, we investigated whether particular changes in non-disease related proteostasis can be identified in the aged mammalian brain, and whether a particular signature of aberrant proteostasis is related to behavioral performance of learning and memory.

Young (adult, n= 30) and aged (2 years, n= 50) Wistar rats were tested in the Morris Water maze (MWM) to test for superior and inferior performers. For both young and old rats, the best and worst performers in the MWM were selected and the insoluble proteome, termed aggregome, was purified from the hippocampus as evidence for aberrant proteostasis. Quantitative proteomics (iTRAQ) was performed. The aged inferior performers were considered as a model for spontaneous, age-associated cognitive impairment.

Whereas variability of the insoluble proteome increased with age, absolute changes in the levels of insoluble proteins were small compared to the findings in the whole *C. elegans* insoluble proteome. However, we identified proteins with with aberrant proteostasis in aging. For the cognitively impaired rats, we identified a molecular circuitry of proteins selectively involved in F-actin remodeling, synapse building and long term depression: actin related protein 3 (ARP3), neurabin II (NEB2) and IQ motif and SEC7 domain-containing protein 1 (BRAG2).

We demonstrate that aberrant proteostasis is a specific phenotype of brain aging in mammals. We identify a distinct molecular circuitry where changes in proteostasis are characteristic for poor learning and memory performance in the wild type, aged rat. Our findings 1. establish the search for aberrant proteostasis as a successful strategy to identify neuronal dysfunction in deficient cognitive behavior, 2. reveal a previously unknown functional network of proteins (ARP3, NEB2, BRAG2) involved in age-associated cognitive dysfunction.

Introduction:

The unraveling of the specific 'pathophysiology' of natural, non disease-associated brain aging is only emerging. Whereas general principles of cellular aging like telomere shortening [1], mitochondrial dysfunction leading to increased intracellular oxidative stress [2], or the involvement of insulin/IGF-1 (insulin-like growth factor 1)-like signaling [3] are well established, the specific molecular features of cellular aging in post-mitotic neurons of the brain are still not well understood.

Changes in protein homeostasis (proteostasis), i.e. the orderly life cycle of synthesis and degradation of proteins, have been described for the aged mammalian brain in terms of gene expression [4], epigenetic changes [5], and protein composition (reviewed by VanGuilder and Freeman in 2011 [6]). Proteomic changes comparing aged and young rodents primarily have been assigned to cellular processes such as glucose metabolism [7,8,9,10,11,12], signal transduction [7,8,9,10,11,13], oxidative stress [9,13], and cytostructure regulation [8,12]. Changes in the expression of proteins that are involved in synaptic processes appear to be more specific to changes in cognition rather than aging [14,15,16,17]. Peter Douglas and Andrew Dillin reviewed the potential effects of age-associated proteostasis changes on neuronal health [18].

Studies on the nematode *Caenorhabditis elegans* [19,20] revealed increases in the overall content of insoluble proteins with age in the whole organism. Subsequent experiments demonstrated that RNAi knockdown of some of the identified insoluble proteins increased the worms' lifespan [19]. This suggested that a decreased clearance of insoluble proteins may contribute to age-associated pathophysiology.

These findings also indicated that, at least in *C. elegans*, the mechanisms for quality control in proteostasis undergo an age-associated decline independent of any disease. Consequently, the analysis of specific proteins accumulating as a result of clearance dysfunction may reveal insights into the cellular mechanisms of neuronal aging, and provide

potential targets for therapeutic intervention. In humans, one phenotype associated with brain aging is mild cognitive impairment (MCI) [21,22]. MCI is defined as a decrease in cognitive abilities in elderly subjects that is clearly discernible but not yet interfering with tasks of daily life [22]. As such, this condition often precedes Alzheimer's disease [23,24].

As humans and animals age, individual differences become apparent across various behavioral domains [25,26]. While some aged subjects maintain performance levels comparable to that of young ones, termed successful or healthy aging [27,28], a fraction of aged individuals show impaired performances. This spontaneously arising increase in variability, found in aged cohorts of outbred rat strains, has been extensively studied in relation to learning and memory in aged rodents (e.g. [29,30,31,32]).

Here, the Morris water maze (MWM) represents a widely used task to assess individual differences in aging-related decrements in spatial learning and memory, with the spatial performance in this task being dependent on the functional integrity of the hippocampus [33].

In this study we aimed to answer 1. whether aging-associated disturbances in proteostasis, reflected by the segregation of distinct proteins into the insoluble proteome, can be observed in the rat brain, and 2. whether such segregation of certain insoluble proteins is functionally related to changes in learning and memory in aged rats.

Using quantitative proteomics, we demonstrate an age-dependent change in hippocampal proteostasis, indicated by compositional changes in the insoluble proteome. Focusing on changes specific for the aged rats showing impaired performance compared to their age-matched superior performers, we identify a molecular circuitry related to synaptic plasticity.

Material and methods:

Animals

The present study continues a report of results presented in Schulz *et al.* (2007) [34] using a subset of the same animals. Drug-naive adult (n = 30; 3 months) and aged (n= 50, 24 months) male outbred Wistar rats were obtained from the animal facilities of the University of Düsseldorf and were maintained under a reversed light-dark cycle (lights went on at 7 p.m. for 12 h). They were housed in standard Macrolon cages of Type IV in groups of 2-3 old or 5 young animals per cage, and had free access to water and standard laboratory chow (Ssniff Spezialdiät). Over a period of three months the animals were behaviorally characterized by assessing their performance in the open field test, black-white box, elevated plus maze as well as learning and extinction trials in the Morris water maze (MWM). Behavioral testing was conducted during the dark period between 09:00 am and 06:00 pm and took place every 48 h (see also Schulz et al., 2007 [34]). All experiments were carried out in accordance with and approved by the German Animal Protection Law (Bezirksregierung Düsseldorf), as well as National and European Regulations.

Water maze

The procedure, experimental design and water maze apparatus have been described in detail elsewhere [34]. Briefly, the water maze consisted of a black circular swimming pool made of polyethylene that was filled with water (20 ± 1 °C) up to a depth of 30 cm. The diameter of the pool was 185 cm. For the cued version of the water maze a 0.5 cm diameter metal peg (height: 22 cm) with black and white stripes was fixed onto the circular platform (18 cm in diameter, 1.5 cm under the water surface level) with a clip and tagged with vanilla aroma. Within one day, rats were released into the water maze for four successive trials with the platform cued. If a rat did not escape onto the platform within 1.5 min, it was gently guided to it by the experimenter. Two days later, the animals were trained in the hidden platform place version of the water maze for 6 days with two training trials per day (one in the

morning and one in the afternoon). During this phase, the platform was fixed 1.5 cm below the water surface in the center of one quadrant of four equally large virtual quadrants of the maze. The platform location was randomly varied between all rats, but was maintained in a fixed location for a given rat during each task. A trial ended either when a rat escaped onto the hidden platform, or after 2.5 min had elapsed. After each training trial in the water maze, the animals were dried under a red-light heating lamp, before being returned to their home cages.

The behavioral analysis during the acquisition trials for each rat comprised the distance to platform (cm) and the time spent within the platform quadrant (PQ, expressed as percentage of total trial duration) as well as the swimming speed (cm/sec), which were automatically recorded via the EthoVision tracking software (Version 3, Noldus, Wageningen, The Netherlands).

Since 11 animals (10 aged and 1 adult) exhibited obvious signs of physical weakness (such as body tumors, eye infection) during the course of experimental testing, their data were excluded from the behavioral analyses, resulting in aged: $n = 40$ and adults: $n = 29$.

Clustering of animals according to their learning abilities

In the present report, we examined whether subgroups of superior and inferior learners in the water maze also exhibit differences in the insoluble hippocampal proteome. For classification of superior *vs.* inferior learners, we calculated the mean distance to the platform over all hidden platform place-learning trials for each rat to establish an overall score of learning performance. In resemblance to other studies on individual differences in learning and memory [30,35,36] the animals were ranked according to their overall score. This was done separately for each age group. Of each age group 8 of the best performers were assigned to the superior group and 8 of the worst to the inferior performers (see Figure 3 A), again, taking special care not to include animals showing signs suggestive of any disease or motoric disabilities.

Statistical analysis of behavioral data

Data are presented as mean ± standard error of the mean (*SEM*). For the water maze, the mean curve level A_0, assessed as total mean distance to platform, as well as the time spent in the platform quadrant (expressed as percentage of trial duration) was taken as an index of the average performance, and the linear trend component a_1, describing the slope of the curve, was calculated as an estimate of the rate of behavioral change over the course of training [37]. Three-way repeated measures analyses of variance (ANOVAs) with pairwise multiple comparisons using Bonferroni adjustment were conducted for statistical analysis, with 'age' and 'learning performance' (superior and inferior learners) as between-groups factors and days as the repeated measures factor for the water maze acquisition (computed on mean of trials per day) data. For the cued version of the water maze, trials were used as the repeated measures factor. When appropriate, t-tests for independent groups were carried out using the A_0 and a_1 values to determine differences between superior and inferior learners within each age group and also superior and inferior learners between the age groups. The level of significance was set to $p \leq 0.05$.

Tissue and protein extraction

From a total of 32 animals comprising four groups (8 'adult inferior', 8 'adult superior', 8 'aged inferior', and 8 'aged superior') hippocampi were dissected, homogenized and aliquoted. Each rat hippocampus was processed individually in a blinded approach and in random order. One aliquot each, representing 20 mg of tissue, subjected to purification of detergent-insoluble proteins according to a protocol modified from Leliveld *et al.,* 2008 [38] and Ottis *et al.*, 2011 [39]. Briefly, the homogenates, supplemented with 2 mM phenylmethylsulfonyl fluoride (PMSF) and 1 x cOmplete, EDTA-free Protease Inhibitor Cocktail (Roche Applied Science, Mannheim, Germany), were incubated over night at 4 °C in the presence of DNase I to degrade all DNA present in the sample. The next day, the aggregome was purified via

three subsequent ultracentrifugation steps, each at 100.000 x g. Two subsequent centrifugation runs were carried out in a high-density sucrose buffer (1.1 M and 1.6 M), followed by one step in high salt buffer (1.5 M NaCl). Apart from the high salt treatment, all steps were carried out in the presence of 1.0% nonidet-P40 (NP-40) and 0.2% N-lauroylsarkosine (sarkosyl). Subsequently, the resulting pellet was washed twice in HEPES-buffer (50 mM 4-(2-hydroxyethyl)-1-piperazineethanesulfonic acid, pH 7.5) to remove salts and detergents incompatible with iTRAQ-experiments. All centrifugation steps were carried out using a TLA-55 rotor and 1.5 mL ultracentrifugation tubes (Beckman Coulter, Krefeld, Germany).

Labeling for quantitative mass spectrometry

The pellets were dried in a speed-vac and proteins were then denatured in 30 µL of 0.5 M triethyl ammonium bicarbonate (TEAB), 6 M urea, 0.8% RapiGest SF Surfactant (Waters Corporation, Milford, MA) and subjected to vigorous shaking at 25 °C for 10 min. After addition of 2 µL reducing reagent (supplied with the iTRAQ Reagent-Multiplex Buffer Kit; AB SCIEX, Darmstadt, Germany), samples were incubated at 27 °C for 2 hours with alternating shaking and pause intervals of 10 sec and 1 min, respectively. Subsequently, the reduced, free cysteines were blocked by addition of 1 µL of cysteine-blocking reagent (AB SCIEX, Darmstadt, Germany) and incubation with shaking at 25 °C for 10 min. For tryptic digestion, hydrolyzed, sequencing grade modified trypsin (Promega, Mannheim, Germany) was re-solubilized in 0.5 M TEAB to 0.4 mg/mL and 10 µL were added to each protein sample, followed by incubation at 37 °C overnight. Next day, 80 µL of HPLC-grade 2-propanol were added to each of the digests and tubes were vortexed briefly.

The denatured, reduced, blocked and digested peptides were labeled using 8-plex isobaric tagging for relative and absolute quantification (iTRAQ) [40]. To enable comparison of all 32 samples in 5 separate 8-plex analyses, 5/32 (19 µL) of each sample were pooled, split in 5 equal aliquots of 104 µL each, and were treated alongside the other samples to

serve as internal standards of all 5 experimental sets (each standard labeled with iTRAQ-reagent 121).

After addition of 1 u iTRAQ-reagent per sample, tubes were incubated at 25 °C, under constant agitation, for 2 h. Following this, labeled samples of each 8-plex experimental set were pooled and centrifuged at 18.000 x g for 5 min. Supernatants were transferred to fresh tubes and pH was adjusted to 3.0 – 3.5 using HPLC-grade 5% trifluoroacetic acid (TFA). Tubes were incubated under constant agitation at 25 °C for 30 min before being dried in a speedvac over night.

Peptide separation and mass spectrometry

Labeled samples were prepared for mass spectrometric analysis as described previously [41]. Briefly, the 5 mixtures were subjected to two-dimensional liquid chromatography (LC). Multiple LC fractions of iTRAQ labeled peptides were captured, mixed with matrix and every two consecutive LC fractions deposited as 192 spots on a single MALDI plate. Mass spectrometry (MS/MS) was performed to identify peptides and quantify the iTRAQ signal using an ABI 4800 proteomics analyzer (Applied Biosystems). This procedure was repeated 5 times for all the biological independent tissue samples.

Protein identification and statistical analyses

MS/MS spectra were searched against rat database using GPS Explorer (ABI) and Mascot (MatrixScience) with trypsin specificity and fixed iTRAQ modifications at lysine residues and N-termini of the peptides. Mass tolerance was 100 ppm for precursor ions and 0.5 Da for fragment ions; missed cleavage was allowed. For each MS/MS spectrum, a single peptide hit with the highest Mascot score in the Swissprot database (version 11/2011) was considered for further analysis. If a spectrum could not be annotated using Swissprot database, a second Mascot search was performed in the larger but more redundant NCBI database (version 11/28/2011). Next, the precursor protein sequences of all peptides from all 5 sets of samples were retrieved from the respective databases. NCBI sequences sharing more than

90% similarity over 85% of the sequence length with a Swissprot sequence were clustered as a single protein. Peptides that matched the sequence of multiple proteins were not removed from analyses. Proteins were included in analyses if at least 2 peptides had been identified with Mascot confidence > 95%, in addition to the criterion of at least 3 reliably quantified peptides (iTRAQ signature peak area above 500) in each of the 5 sets of samples. Individual peak areas of each iTRAQ signature peak of each peptide were log2 transformed, normalized to the average of all peak areas of the respective iTRAQ signature peak and mean centered. Within each set of samples, the abundance of a protein was calculated as the average of these mean centered iTRAQ values of multiple peptides, yielding 8 independent measurements of protein abundance for each of the 4 treatments.

Significance of treatment effects was evaluated using Student's t-tests. To address the problem of multiple testing, resulting p-values were converted into q-values [42] giving an estimate of the false discovery rate (FDR) for each statistical test.

Data analyses

Gene-Ontology (GO) – Analyses were performed using the online DAVID Bioinformatics Resources 6.7 tool [43,44] with a subset of rat hippocampal gene expression, provided by the Gene Expression Atlas of the European Bioinformatics institute [45,46], as background. P-values stated were calculated by the DAVID tool and were corrected according to Bonferroni.

F-actin precipitation assay

The assay was adapted from Cenni *et al.*, 2003 [47]. Briefly, human NLF neuroblastoma cells, grown to confluency and supplemented (30 min before lysis) with either DMSO only, 1 µM, or 5 µM of Mycalolide B (Santa Cruz Biotechnology, Inc.; Heidelberg, Germany), an F-actin depolymerizing substance [48]. Cells were harvested from a 10 cm culture dish by trypsination and, subsequently, were washed twice with PBS. Then 0.4 mL of lysis- and F-actin stabilization buffer (50 mM Pipes, pH 6.9; 50 mM NaCl; 5 mM $MgCl_2$; 5 mM EGTA; 5%

[v/v] glycerol; 0.1% NP-40; 0.1% Triton X-100; 1% Tween 20; 1 x cOmplete, EDTA-free Protease Inhibitor Cocktail) was added to the pelleted cells and cells were lysed by pipetting repeatedly through a 200 µL pipette-tip. After incubating the lysate for 10 min at 37 °C, a 100 µL aliquot was centrifuged at 350 x g for 5 min to pellet any cell debris. The supernatant was then transferred into a 1.5 mL ultracentrifuge tube and was subjected to centrifugation at 100.000 x g for 60 min. The supernatant containing soluble proteins and un-polymerized G-actin was carefully removed and the pellet was re-solubilized in the same volume (100 µL). Both fractions were supplemented with SDS-loading buffer and were subjected to SDS-PAGE and subsequent immuno-blotting using an α-actin antibody (A2066; Sigma-Aldrich; Munich, Germany) and an α-ARP3 antibody (ab49671; Abcam; Cambridge, UK).

Results:

Behavioral tests

Wild-type, adult and aged, male Wistar rats were characterized for their cognitive functions in the Morris-Water-Maze (MWM). For the cued version of the water maze, repeated measures ANOVA revealed a significant decrease in the distance covered to the cued platform over the four trials ($F_{3,84} = 12.725$, $p \leq 0.001$), indicative of learning, but failed to reveal significant main effects for 'age' ($F_{1,28} = 0.436$, $p = 0.515$) or 'learning performance' ($F_{1,25} = 0.018$, $p = 0.893$; data not shown). These results indicate that sensory and motor deficits did not affect the groups differentially. Thus, group differences detected in the hidden platform task are rather attributable to differences in special learning capacities, than to sensory and motor deficits [35,49].

Results of the hidden platform task are summarized in Figure 1. Repeated measures ANOVA revealed a significant decrease in the mean distance covered to platform over the course of testing ($F_{5,140} = 11.862$, $p \leq 0.001$), which significantly varied as a function of 'learning performance'($F_{5,140} = 3.720$, $p = 0.003$), but only marginally as a function of 'age' ($F_{5,140} = 2.251$, $p = 0.053$). Main effects were found for 'age' ($F_{1,28} = 44.013$, $p \leq 0.001$) and 'learning performance' ($F_{1,28} = 309.654$, $p \leq 0.001$). Also an interaction between 'age' and 'learning performance' became apparent ($F_{1,28} = 5.727$, $p = 0.029$).

Post-hoc analysis using t-tests showed that within each age group, the inferior performers, on average, moved longer distances to the hidden platform as compared to the superior performers (aged: $t = -20.409$; $p \leq 0.001$; adult: $t = -8.646$; $p \leq 0.001$). Furthermore, the aged inferior performers moved longer distances as compared to the adult inferior group ($t = 4.725$; $p \leq 0.001$). Similarly, the aged superior group moved longer distances as compared to the adult superior group ($t = -6.578$; $p \leq 0.001$). As to the slope (a_1; data not depicted) over the hidden platform training trials, the aged inferior performers exhibited a stronger decrease in the distance to the hidden platform (and therefore a steeper slope a_1) as compared to the aged superior group ($t = 3.772$; $p = 0.002$). However, such effects were

not found when the adult inferior and the adult superior group were compared ($t = 1.565$; $p = 0.140$). Similarly, the aged superior performers did not differ from the adult superior performers in the slope a_1 ($t = -1.207$; $p = 0.247$), but the aged inferior performers exhibited a steeper slope over the acquisition trials as compared to the respective adult performer group ($t = -2.321$; $p = 0.036$).

For the time spent in the platform quadrant (Figure 2), repeated measures ANOVA revealed a significant increase in the preference for the platform quadrant over the course of acquisition training ($F_{5,140} = 4.688$, $p = 0.001$), without any significant interaction effects (all $F_{5,140} \leq 1.612$, all $p \geq 0.161$). However, significant main effects were found for the factors 'age' ($F_{1,28} = 18.131$, $p \leq 0.001$) and 'learning performance' ($F_{1,28} = 17.315$, $p \leq 0.001$), indicating, that the groups also differed with respect to another direct measure of spatial learning, a preference for the reinforced platform quadrant. Post-hoc analysis using t-tests revealed that both superior performer groups exhibited a higher preference for the platform quadrant as compared to the respective inferior group of matched age (aged: $t = 2.232$, $p = 0.036$; adult: $t = 4.649$, $p \leq 0.001$; Figure 2). Furthermore, adult inferior animals exhibited a stronger preference for the platform quadrant as compared to the aged inferior animals ($t = -3.5$, $p = 0.004$). Similarly, the adult superior rats showed a stronger preference for the platform quadrant as compared to the aged superior rats ($t = -2.684$, $p = 0.018$).

Repeated measures ANOVA revealed a significant decrease in speed of swimming over hidden platform place learning ($F_{5,140} = 7.025$, $p \leq 0.001$), without any significant interaction effects (all $F_{5,140} \leq 2.046$, all $p \geq 0.076$). Furthermore, no significant main between-groups effects and interactions with the between-groups factors were revealed by ANOVA (all $F_{1,28} \leq 2.698$, all $p \geq 0.112$), ruling out the possibility that differences found during acquisition could be explained by differences in swimming speed.

Proteomic analysis

Brains from the 32 rats, each assigned to one of the four clusters 'adult inferior', 'adult superior', 'aged inferior', and 'aged superior' (Figure 3 A), were subjected to proteomic analysis. The hippocampus was selected as critical brain region since it is established to be essential for spatial memory [50] and is, therefore, an obvious brain region where molecular changes relating to impaired cognitive function, as assessed in MWM, could be present. For each of the four groups, hippocampal homogenates of the detergent-insoluble proteomes of 8 individual rats were purified to yield 32 aggregomes for quantitative mass-spectrometric analyses (Figure 3 B).

Age-specific hippocampal aggregome

Comparing the aged and adult rat cohort, we identified 52 insoluble proteins that differed as a function of age ($p < 0.05$, FDR < 11.7 %; Table 1). Amongst those proteins enriched significantly in the insoluble fraction of the aged ($p < 0.014$; FDR < 6.7%), the cluster of microtubule-associated proteins (dynactin subunit 1, cytoplasmic dynein 1 heavy chain 1, microtubule-associated protein 2, tubulin alpha-4A chain) was represented most prominently in aged compared to adult rats with a 20-fold enrichment ($p = 0.035$), as determined by gene ontology (GO) clustering analyses. Decreases in the insoluble fraction ($p \leq 0.014$) on the other hand, were found for members of the post-synaptic density, PSD, (disks large homolog 2, glutamate [NMDA] receptor subunit epsilon-1, SH3 and multiple ankyrin repeat domains protein 1-3), that were enriched by 45-fold ($p = 9.7 \times 10^{-5}$). The additional identified GO-cluster of general 'cytoskeleton' (especially actin) associated proteins, extended the PSD-cluster by the proteins actin-related protein 2/3 complex subunit 2, bassoon and SRC kinase signaling inhibitor 1. These cytoskeleton-associated components were enriched among the set of decreased proteins by 8-fold ($p = 2.1 \times 10^{-4}$).

Behavioral performance-specific hippocampal aggregome

Only three proteins differed between aged superior and aged inferior learners in their segregation to the insoluble fraction ($p < 0.05$; Table 2). These proteins were identified as: Actin-related protein 3 (ARP3), spinophilin (neurabin-2, NEB2), and the IQ motif and SEC7 domain-containing protein 1 (BRAG2). Most intriguingly, all three play crucial roles in synaptic plasticity, a phenomenon involved in memory formation [51,52,53] (Figure 4). We observed a decrease of insoluble ARP3 and NEB2, and an increase of insoluble BRAG2 in the aged inferior cohort, as compared to the group of aged superior animals.

To investigate a possible mechanism by which a higher level of a specific protein in the insoluble fraction of superior performers could be explained, we tested whether insolubility could be mediated by other proteins, more prone to sedimentation. Inspired by the joint role of the identified proteins ARP3, NEB2, and BRAG2 in synaptic plasticity, where polymerization of actin monomers to F-actin polymers plays a critical role, we performed F-actin precipitation assays and were able to validate a co-precipitation of ARP3 with F-actin (Figure 5). We could demonstrate ARP3 co-precipitation at a centrifugation speed of 100.000 x g with an intact F-actin network (Figure 5, DMSO control) but not after F-actin depolymerization by Mycalolide B (Figure 5, 5 µM Mycalolide B).

In addition to the detected changes in levels of ARP3, NEB2, and BRAG2, we also found correlations between these 3 proteins and the respective cognitive performances of the individual aged rats, as assessed by total mean swimming distance (A_0) to the hidden platform in the MWM (Table 2, Figure 6 B, E, H) corroborating their critical role in maintaining cognitive performance. ARP3 and NEB2 accumulation correlated negatively with A_0, contrary to the concentration of insoluble BRAG2. Furthermore, ARP3 and BRAG2 showed correlations to the learning rate a_1 of the individual aged animals (Table 2, Figure 6 C, F, I), with ARP3 displaying a positive correlation and BRAG2 being negatively correlated with a_1. For NEB2, the calculated (positive) correlation exceeded the significance threshold ($p = 0.066$).

The amount of ARP3 protein in the detergent-insoluble fractions of aged rats also correlated positively with the amount of NEB2 protein (Figure 7 A) identified in the same fractions. ARP3 showed a negative correlation with BRAG2 in the aged cohort (Figure 7 B), consistent with the inverse accumulation of BRAG2 and its diverse role in the post-synapse. A similar correlation was found for all aged and adult rats combined ($r = -0.377$, $p = 0.034$; data not shown).

Discussion and Conclusions

In this study, we demonstrate in a quantitative proteomics (iTRAQ) approach that the analysis of changes in the insoluble proteome of the hippocampus identifies molecular components correlating to functional systems data, here the animal's age and cognitive performance in a learning and memory task (MWM).

Our study is the first proteome-wide approach describing insoluble protein composition in the aging mammalian brain and relates to previous studies performed in the nematode *Caenorhabditis elegans* where changes in protein solubility in the course of aging were detected [19,20]. In those studies, detergent-insoluble proteins were purified from young and old, pooled whole *C. elegans*, and protein components of the aggregomes were quantified using iTRAQ. Compared to the studies of David *et al.* and Reis-Rodrigues *et al.* in *C. elegans* where changes above 10-fold were reported [19,20], the range of the detected differences between groups in our study was much smaller. One explanation for this may be the presence of different protein degradation mechanisms in mammalian cells as compared to nematodes, allowing for a more efficient clearing of protein aggregates [54], or the specific focus on a brain subregion in our study, as opposed to using the whole organism. In addition, there are important technical differences between the *C. elegans* studies and our investigations. In our study on the mammalian brain, we chose an approach with high statistical power (8 *vs.* 8 and 16 *vs.* 16 biological replicates for ‘cognition in aged’ and ‘aging’, respectively) compared to smaller numbers of biological replicates (n = 2 – 4) in refs. [19,20]. We noted that, despite normalization to input tissue-weight before purification, similar to previous studies, strong variances in total detected protein levels were detected between single animals after purification, exceeding the differences in protein levels rather than between analyzed groups. Therefore, we had to adopt a global normalization method prior to statistical testing. Finally, the aggregome purification protocols applied in these studies were distinct from ours and changes in the use of detergents, centrifugation speed, and a final extraction with formic acid, may result in differences in the set of proteins identified in the

aggregome. Compared to David *et al*. [20], we used higher centrifugation speed (100.000 x g instead of 20.000 x g), applied less ionic detergent (0.2% sarkosyl instead of 1% SDS/SDO), and performed two subsequent lipid and low molecular weight protein extractions in high-density buffer (1.1 and 1.6 M sucrose instead of 1.0 M). Furthermore, we used 1.5 M NaCl instead of 0.75 M in our high ionic strength buffer, and did not apply a final extraction in 70% formic acid, that was introduced by David and co-workers to exclude their nematode cuticular debris from the analyses. Reis-Rodriguez and colleagues [19] pre-cleared their samples by centrifugation at 3.000 x g and reduced the purification protocol to three subsequent washes with 1% SDS and centrifugation steps at 16.000 x g, followed by a final extraction with 70% formic acid.

For this initial work, in order to include more potentially altered proteins in our post-hoc analyses, we decided, upon given significance, to be less restrictive with regard to the FDRs (listed in Tables 1 and 2). For the proteins associated with the term 'aging', this resulted in the inclusion of proteins showing an FDR of 0.1163, whilst for the 'cognition in aged' analyses all three proteins identified as changed with $p \leq 0.05$ were analyzed further.

Proteins identified in the insoluble fraction of superior vs. inferior performing aged rats

ARP3 and NEB2 proteins were identified at higher concentrations in the insoluble fraction of the aged superior performers as compared to their age-matched impaired, inferior performers. In the context of synaptic plasticity, a likely explanation is that with our biochemical fractionation we pull down significant amounts of dendritic F-actin (see also the likely increased pull-down of insoluble actin in superior performers; Table 2) and associated proteins like ARP3 (Figure 5). However, other reasons such as specific post-translational modifications, or secondary effects like a specific local increase in protein density with a change in facultative protein-protein interactions should also be considered. In contrast, BRAG2, being critical for the induction of LTD [53], accumulated in the aggregome of the

aged inferior learners. The observed inverse correlation of BRAG2 with ARP3 (Figure 7 B) seems conclusive with its rather inverse role in synaptic plasticity.

The solubility changes of ARP3, NEB2, and BRAG2 detected in our proteomic analysis of aged rats are converging on an inter-related set of proteins involved in synaptic plasticity. This becomes even more intriguing, as these changes not only showed significance in the grouped comparison of aged superior and inferior performers, but, additionally, proved correlative for the cognitive performances (A_0) of the individual animals (Figure 6 B, E, H), as well as – in the case of ARP3 and BRAG2 – for the individual learning rate a_1 (Figure 6 C, I). Also inter-correlation of the solubility changes between NEB2 and ARP3, as well as between ARP3 and BRAG2 were observed (Figure 7). For ARP3, a co-precipitation with immobilized NEB2 has been described [55].

So far, these proteins have not been reported in the context of changes in cognitive performance in analyses of rodent whole synaptic protein fractions, i.e. comprising soluble and insoluble conformers [14,15,17,56,57,58]. Notably, in one study investigating differences in the whole hippocampal proteome of mice trained in different spatial memory tasks, Zheng and co-workers (2009) [16] found that ARP3, along with ARPC5 and F-actin-capping protein subunit beta, was differentially regulated in mice trained in different tasks. However, in their approach, changes were only observed comparing the different means of training, but did not correlate with any learning behavior within the trials.

The term synaptic plasticity describes structural and functional changes of dendritic spines and their postsynaptic densities (PSDs). These changes are observed following learning or the experimental induction of long-term potentiation (LTP) and long-term depression (LTD), respectively, and are believed to contribute to memory formation (reviewed by Lamprecht and LeDoux, 2004 [59]). LTP has been directly linked to performance in learning tasks such as the Morris-Water-Maze [30], and thus, can be seen as a cellular manifestation of the observed rat behavior in learning and memory [60]. Basis of LTP and LTD are changes in the molecular composition of key proteins (e.g. AMPA receptors [61,62]) and cellular structures

at synapses [52]. Both, LTP and LTD lead to the re-modeling of the actin cytoskeleton in dendritic spines [52,63]. Whereas LTP initializes the introduction of receptors into the postsynaptic membrane [64], its counter-player process LTD, induced by NMDA receptor (NMDAR) and metabotropic glutamate receptor (mGluR) activity [65], has been shown to evoke internalization of AMPA receptors (AMPARs) [64]. Like LTP, LTD is generally believed to play a crucial role in hippocampal memory formation [66].

The modulation of dendritic spine volume to mediate synaptic structural plasticity mainly involves the reorganization of the spine's actin-cytoskeleton, which is mediated by signaling proteins such as Neurabin-2 (Spinophilin) and the Ca^{2+}/calmodulin-dependent protein kinase, CAMKII [52] (Figure 4). This remodeling and the extension or degradation of the F-actin (filamentous actin) network in dendritic spines is crucial for synaptic plasticity and LTP/LTD maintenance [51,67,68], and there is a direct and crucial link of this to learning and memory formation [51,59,67,68,69,70,71].

ARP3

Actin-related protein 3 (ARP3) was found elevated in the insoluble fraction of hippocampi from aged rats displaying superior cognitive abilities. ARP3 expression is crucial to embryonic viability past the blastocyst stage [72] and is part of a protein complex, which includes ARP2 and the five subunits ARPC1-5 [73,74,75,76,77]. The complex builds the branching points of F-actin filaments [76,78] and thereby mediates the formation of branched structures within the actin cytoskeleton network [76,79] (Figure 4). Showing high concentrations in dendritic spines [80], the ARP2/3 complex is responsible for the actin network organization in spine heads and disturbances in expression of its subunits results in impaired spine and synapse formation [81,82], and in changes of synapse activity [81].

NEB2

The second protein identified as accumulating in the 'aged superior' aggregome, is spinophilin, also termed neurabin 2 (NEB2). It is a protein phosphatase I (PP-I) interacting

and PP-I – activity modulating protein [83,84] that is primarily found in dendritic spines [83,85]. Intraspinal localization of NEB2 and its F-actin binding and bundling capacity were demonstrated to be modulated via its phosphorylation by the Ca^{2+}/calmodulin dependent kinase II (CAMKII) [86] or the protein kinase A (PKA) [87], linking spinophilin action with its responsiveness to NMDA and adrenergic receptor activity [88,89] (Figure 4). The NEB2-mediated effect on F-actin organization within dendritic spines, thus, depends on Ca^{2+} as well as on cAMP signaling. It is, presumably, via modulation of the spinal F-actin network, that NEB2 modulates dendritic morphology [90] and, hence, has been found to be important for hippocampal integrity [90]. Notably, despite its effect on F-actin organization, mice, deficient in spinophilin, showed no altered LTP, but reduced LTD [90].

Previous experiments investigating a direct quantitative relation between NEB2, aging and cognitive abilities showed no positive results for the total and unfractionated protein levels [91,92]. These results, compared to our findings reported here, highlight the necessity to differentiate the solubility status of synaptic proteins for determining their function.

BRAG2

The third protein identified in our study comparing aged inferior and superior rats, BRAG2, was found increased in the aggregome of aged inferior rats. First described by Someya *et al.* in 2001 [93], this protein features an IQ-like motive and a SEC7 domain, and acts as a guanine nucleotide-exchange protein for the ADP-ribosylation factor 6 (ARF6) and, hence, is also termed IQSEC1 or ARF-GEP100. Like the other two proteins found to be changed with cognitive ability in the aggregome of aged rats – ARP3 and NEB2 – BRAG2 has been implicated in the mechanism of actin-remodeling [94] and a direct effect on LTD-maintenance has been observed [53]. NMDAR- as well as mGluR-mediated LTD was found to rely upon BRAG2 expression [53] and a mechanism of BRAG2 binding to the GluA2 C-terminal part of AMPA receptors to induce their ARF6 mediated internalization [53,95] along with changes in the actin cytoskeleton [94], has been described (Figure 4).

In our proteomic results on BRAG2, one value at 0.325 for the aged inferior cohort appeared to be standing out amongst the other values. Hence, a critical outlier-consideration was performed, where the value passed the ROUT and Grubb's test for outliers with stringency set to 5%. Furthermore, no other data derived from this particular rat appeared to be irregular. Therefore, the value was included in the post-hoc analyses. Yet, even if excluded from the analysis, the comparison of aged inferior and aged superior rats in their amounts of insoluble BRAG2 still passed the significance threshold with $p = 0.0449$ (data not shown).

Proteins identified in the insoluble fraction of aged vs. adult rats

In the approach by David *et al.*, an overall number of 461 insoluble proteins was found increased by more than two-fold in the aged samples [20], whereas Reis-Rodrigues *et al.* reported the finding of 203 insoluble proteins [19]. Elongation factor 2, heat shock protein 70, and glyceraldehyde-3-phosphate dehydrogenase showed high abundance for the aged samples both in the insoluble fractions for the nematode approaches [19,20] and in our rat hippocampal fraction. In addition, the work of David and co-workers shared the detection of up-regulated myosins with the present study [20]. The study conducted by Reis-Rodrigues *et al.* reported findings – similar to our results for rat hippocampi – of elevated levels of aggregated tubulin and mitochondrial ATP synthase subunit alpha in aged worms [19], with the latter protein component having been recognized as a common denominator in the aging-pigment lipofuscin [96,97]. The increase of 60S ribosomal protein in the in-soluble fraction of the aged animals, observed in the nematode studies [19,20], however, opposes our findings of a decrease in aged rat brain aggregome.

Reis-Rodrigues and colleagues further reported the finding of significant extensions of lifespan of *C. elegans* upon RNAi-based knockdown for almost half of the genes tested and whose products were found to be elevated in the aged aggregome [19]. Amongst those were the elongation factor 2, implicated in the ribosomal translation elongation, and tubulin, a component of the microtubular cytoskeleton [19].

Notably, there is no large overlap in the proteome from the insoluble fraction used in this study, compared to the aged rat hippocampal synaptoproteome described by Van Guilder and colleagues [12]. This corroborates the expected specificity of proteins prone to aggregate with age and accounts for the solubility changes to not be mere mirroring-effects of altered expression levels, but rather to reflect changes in the proteostasis maintaining cellular machinery. However, some commonalities could be described: Whereas dynamin-1, which appears to be downregulated in the aged rat synaptic proteome [12] and was also less abundant in the aged aggregome, other proteins rather showed an opposite trend. Synapsin-1, a phosphoprotein associated with synaptic vesicles [98], was reported to show elevated expression comparing aged and adult synaptoproteome [12], but was reduced in the aged aggregome. Heat shock protein 70, isocitrate dehydrogenase [NAD], NADH dehydrogenase (ubiquinone), and tubulins have been demonstrated to be less abundant in the soluble aged rat hippocampus synaptoproteome [12], whereas they showed elevated quantities in the detergent-insoluble fraction analyzed in this present study. This latter, inverse correlation may point towards proteins, that specifically become less soluble with age, e.g. by oxidative stress [99], and are therefore depleted of the soluble fraction analyzed by Van Guilder and colleagues [12].

In this study, we demonstrated age-associated changes of protein-solubility in the mammalian hippocampus of the rat. We used quantitative proteomics to also differentiate inferior and superior performing aged rats in a functional assay of memory and identified three proteins ARP3, NEB2, and BRAG2 involved in synaptic plasticity and long-term depression as potential molecular correlates of the age-associated memory decline. We thereby demonstrated that quantitative proteomics of the aggregome is an appropriate method for identifying molecular components of behavior related to memory/learning processes in a systems biology approach to studying the aged brain.

Abbreviations:

A_0	total mean distance swam to platform in water maze
a_1	slope of mean distance function over trial days / learning rate
AMPA-R	α-amino-3-hydroxy-5-methyl-4-isoxazolepropionic acid receptor
ANOVA	analysis of variance
ARF6	adenosine diphosphate rybosylation factor
ARP3	actin-related protein 3
CAMKII	Ca^{2+} / calmodulin-dependent protein kinase II
DMSO	Dimethyl sulfoxide
EGTA	ethylene glycol tetraacetic acid
F-actin	filamentous actin
FDR	false discovery rate
HPLC	high-performance liquid chromatography
IGF-1	insulin-like growth factor 1
iTRAQ	isobaric tag for relative and absolute quantification
LC	liquid chromatography
LTD	long-term depression
LTP	long-term potentiation
MALDI	matrix-assisted laser desorption/ionization
MCI	mild cognitive impairment
mGluR	metabotropic glutamate receptor
MS/MS	tandem mass spectrometry
MWM	Morris water maze
NEB2	neurabin 2 / spinophilin
NMDA-R	N-methyl-D-aspartate receptor
PP-I	protein phosphatase I
PSD	post synaptic density

PTP	protein tyrosine phosphatase
SEM	standard error of mean
TEAB	triethyl ammonium bicarbonate

References:

1. Blasco MA (2007) Telomere length, stem cells and aging. Nat Chem Biol 3: 640-649.

2. Terman A, Kurz T, Navratil M, Arriaga EA, Brunk UT (2010) Mitochondrial turnover and aging of long-lived postmitotic cells: the mitochondrial-lysosomal axis theory of aging. Antioxid Redox Signal 12: 503-535.

3. O'Neill C, Kiely AP, Coakley MF, Manning S, Long-Smith CM (2010) Insulin and IGF-1 signalling: longevity, protein homoeostasis and Alzheimer's disease. Biochem Soc Trans 40: 721-727.

4. Lu T, Pan Y, Kao SY, Li C, Kohane I, et al. (2004) Gene regulation and DNA damage in the ageing human brain. Nature 429: 883-891.

5. Kosik KS, Rapp PR, Raz N, Small SA, Sweatt JD, et al. (2012) Mechanisms of age-related cognitive change and targets for intervention: epigenetics. J Gerontol A Biol Sci Med Sci 67: 741-746.

6. VanGuilder HD, Freeman WM (2011) The hippocampal neuroproteome with aging and cognitive decline: past progress and future directions. Front Aging Neurosci 3: 8.

7. Carrette O, Burkhard PR, Hochstrasser DF, Sanchez JC (2006) Age-related proteome analysis of the mouse brain: a 2-DE study. Proteomics 6: 4940-4949.

8. Focking M, Boersema PJ, O'Donoghue N, Lubec G, Pennington SR, et al. (2006) 2-D DIGE as a quantitative tool for investigating the HUPO Brain Proteome Project mouse series. Proteomics 6: 4914-4931.

9. Yang S, Liu T, Li S, Zhang X, Ding Q, et al. (2008) Comparative proteomic analysis of brains of naturally aging mice. Neuroscience 154: 1107-1120.

10. Poon HF, Shepherd HM, Reed TT, Calabrese V, Stella AM, et al. (2006) Proteomics analysis provides insight into caloric restriction mediated oxidation and expression of brain proteins associated with age-related impaired cellular processes: Mitochondrial dysfunction, glutamate dysregulation and impaired protein synthesis. Neurobiol Aging 27: 1020-1034.

11. Sato Y, Yamanaka H, Toda T, Shinohara Y, Endo T (2005) Comparison of hippocampal synaptosome proteins in young-adult and aged rats. Neurosci Lett 382: 22-26.
12. VanGuilder HD, Yan H, Farley JA, Sonntag WE, Freeman WM (2010) Aging alters the expression of neurotransmission-regulating proteins in the hippocampal synaptoproteome. J Neurochem 113: 1577-1588.
13. Weinreb O, Drigues N, Sagi Y, Reznick AZ, Amit T, et al. (2007) The application of proteomics and genomics to the study of age-related neurodegeneration and neuroprotection. Antioxid Redox Signal 9: 169-179.
14. McNair K, Davies CH, Cobb SR (2006) Plasticity-related regulation of the hippocampal proteome. Eur J Neurosci 23: 575-580.
15. McNair K, Broad J, Riedel G, Davies CH, Cobb SR (2007) Global changes in the hippocampal proteome following exposure to an enriched environment. Neuroscience 145: 413-422.
16. Zheng JF, Patil SS, Chen WQ, An W, He JQ, et al. (2009) Hippocampal protein levels related to spatial memory are different in the Barnes maze and in the multiple T-maze. J Proteome Res 8: 4479-4486.
17. Chen WQ, Viidik A, Skalicky M, Hoger H, Lubec G (2007) Hippocampal signaling cascades are modulated in voluntary and treadmill exercise rats. Electrophoresis 28: 4392-4400.
18. Douglas PM, Dillin A (2010) Protein homeostasis and aging in neurodegeneration. J Cell Biol 190: 719-729.
19. Reis-Rodrigues P, Czerwieniec G, Peters TW, Evani US, Alavez S, et al. (2012) Proteomic analysis of age-dependent changes in protein solubility identifies genes that modulate lifespan. Aging Cell 11: 120-127.
20. David DC, Ollikainen N, Trinidad JC, Cary MP, Burlingame AL, et al. (2010) Widespread protein aggregation as an inherent part of aging in C. elegans. PLoS Biol 8: e1000450.

21. Reisberg B, Ferris SH, de Leon MJ, Franssen ESE, Kluger A, et al. (1988) Stage-specific behavioral, cognitive, and in vivo changes in community residing subjects with age-associated memory impairment and primary degenerative dementia of the Alzheimer type. Drug Development Research 15: 101-114.

22. Gauthier S, Reisberg B, Zaudig M, Petersen RC, Ritchie K, et al. (2006) Mild cognitive impairment. Lancet 367: 1262-1270.

23. Petersen RC (2004) Mild cognitive impairment as a diagnostic entity. Journal of Internal Medicine 256: 183-194.

24. Geslani DM, Tierney MC, Herrmann N, Szalai JP (2005) Mild cognitive impairment: an operational definition and its conversion rate to Alzheimer's disease. Dement Geriatr Cogn Disord 19: 383-389.

25. Gallagher M, Burwell RD (1989) Relationship of age-related decline across several behavioral domains. Neurobiol Aging 10: 691-708.

26. Rapp PR, Amaral DG (1992) Individual differences in the cognitive and neurobiological consequences of normal aging. Trends Neurosci 15: 340-345.

27. Lupien SJ, Wan N (2004) Successful ageing: from cell to self. Philos Trans R Soc Lond B Biol Sci 359: 1413-1426.

28. Rowe JW, Kahn RL (1987) Human aging: usual and successful. Science 237: 143-149.

29. Meijer OC, Topic B, Steenbergen PJ, Jocham G, Huston JP, et al. (2005) Correlations between hypothalamus-pituitary-adrenal axis parameters depend on age and learning capacity. Endocrinology 146: 1372-1381.

30. Schulz D, Huston JP, Jezek K, Haas HL, Roth-Harer A, et al. (2002) Water maze performance, exploratory activity, inhibitory avoidance and hippocampal plasticity in aged superior and inferior learners. Eur J Neurosci 16: 2175-2185.

31. Schulz D, Sergeeva OA, Ianovskii E, Luhmann HJ, Haas HL, et al. (2004) Behavioural parameters in aged rats are related to LTP and gene expression of ChAT and NMDA-NR2 subunits in the striatum. Eur J Neurosci 19: 1373-1383.

32. Topic B, Willuhn I, Palomero-Gallagher N, Zilles K, Huston JP, et al. (2007) Impaired maze performance in aged rats is accompanied by increased density of NMDA, 5-HT1A, and alpha-adrenoceptor binding in hippocampus. Hippocampus 17: 68-77.

33. Gallagher M, Nicolle MM (1993) Animal models of normal aging: relationship between cognitive decline and markers in hippocampal circuitry. Behav Brain Res 57: 155-162.

34. Schulz D, Huston JP, Buddenberg T, Topic B (2007) "Despair" induced by extinction trials in the water maze: relationship with measures of anxiety in aged and adult rats. Neurobiol Learn Mem 87: 309-323.

35. Topic B, Dere E, Schulz D, de Souza Silva MA, Jocham G, et al. (2005) Aged and adult rats compared in acquisition and extinction of escape from the water maze: focus on individual differences. Behav Neurosci 119: 127-144.

36. Hasenöhrl RU, Söderström S, Mohammed AH, Ebendal T, Huston JP (1997) Reciprocal changes in expression of mRNA for nerve growth factor and its receptors TrkA and LNGFR in brain of aged rats in relation to maze learning deficits. Exp Brain Res 114: 205-213.

37. Krauth J (1980) Nonparametric analysis of response curves. J Neurosci Methods 2: 239-252.

38. Leliveld SR, Bader V, Hendriks P, Prikulis I, Sajnani G, et al. (2008) Insolubility of disrupted-in-schizophrenia 1 disrupts oligomer-dependent interactions with nuclear distribution element 1 and is associated with sporadic mental disease. J Neurosci 28: 3839-3845.

39. Ottis P, Bader V, Trossbach SV, Kretzschmar H, Michel M, et al. (2011) Convergence of two independent mental disease genes on the protein level: recruitment of dysbindin to cell-invasive disrupted-in-schizophrenia 1 aggresomes. Biol Psychiatry 70: 604-610.

40. Ross PL, Huang YN, Marchese JN, Williamson B, Parker K, et al. (2004) Multiplexed protein quantitation in Saccharomyces cerevisiae using amine-reactive isobaric tagging reagents. Mol Cell Proteomics 3: 1154-1169.

41. Li KW, Miller S, Klychnikov O, Loos M, Stahl-Zeng J, et al. (2007) Quantitative proteomics and protein network analysis of hippocampal synapses of CaMKIIalpha mutant mice. J Proteome Res 6: 3127-3133.

42. Storey JD, Tibshirani R (2003) Statistical significance for genomewide studies. Proc Natl Acad Sci U S A 100: 9440-9445.

43. Huang da W, Sherman BT, Lempicki RA (2009) Bioinformatics enrichment tools: paths toward the comprehensive functional analysis of large gene lists. Nucleic Acids Res 37: 1-13.

44. Huang da W, Sherman BT, Lempicki RA (2009) Systematic and integrative analysis of large gene lists using DAVID bioinformatics resources. Nat Protoc 4: 44-57.

45. Kapushesky M, Emam I, Holloway E, Kurnosov P, Zorin A, et al. (2010) Gene expression atlas at the European bioinformatics institute. Nucleic Acids Res 38: D690-698.

46. Kapushesky M, Adamusiak T, Burdett T, Culhane A, Farne A, et al. (2012) Gene Expression Atlas update--a value-added database of microarray and sequencing-based functional genomics experiments. Nucleic Acids Res 40: D1077-1081.

47. Cenni V, Sirri A, Riccio M, Lattanzi G, Santi S, et al. (2003) Targeting of the Akt/PKB kinase to the actin skeleton. Cell Mol Life Sci 60: 2710-2720.

48. Saito S, Watabe S, Ozaki H, Fusetani N, Karaki H (1994) Mycalolide B, a novel actin depolymerizing agent. J Biol Chem 269: 29710-29714.

49. Rapp PR, Rosenberg RA, Gallagher M (1987) An evaluation of spatial information processing in aged rats. Behav Neurosci 101: 3-12.

50. O'Keefe J, Dostrovsky J (1971) The hippocampus as a spatial map. Preliminary evidence from unit activity in the freely-moving rat. Brain Res 34: 171-175.

51. Hotulainen P, Hoogenraad CC (2010) Actin in dendritic spines: connecting dynamics to function. J Cell Biol 189: 619-629.

52. Okamoto K, Bosch M, Hayashi Y (2009) The roles of CaMKII and F-actin in the structural plasticity of dendritic spines: a potential molecular identity of a synaptic tag? Physiology (Bethesda) 24: 357-366.

53. Scholz R, Berberich S, Rathgeber L, Kolleker A, Köhr G, et al. (2010) AMPA receptor signaling through BRAG2 and Arf6 critical for long-term synaptic depression. Neuron 66: 768-780.

54. Mori K (2009) Signalling pathways in the unfolded protein response: development from yeast to mammals. J Biochem 146: 743-750.

55. Barnes AP, Smith FD, 3rd, VanDongen HM, VanDongen AM, Milgram SL (2004) The identification of a second actin-binding region in spinophilin/neurabin II. Brain Res Mol Brain Res 124: 105-113.

56. Nelson TJ, Backlund PS, Jr., Alkon DL (2004) Hippocampal protein-protein interactions in spatial memory. Hippocampus 14: 46-57.

57. Henninger N, Feldmann RE, Jr., Futterer CD, Schrempp C, Maurer MH, et al. (2007) Spatial learning induces predominant downregulation of cytosolic proteins in the rat hippocampus. Genes Brain Behav 6: 128-140.

58. Freeman WM, VanGuilder HD, Bennett C, Sonntag WE (2009) Cognitive performance and age-related changes in the hippocampal proteome. Neuroscience 159: 183-195.

59. Lamprecht R, LeDoux J (2004) Structural plasticity and memory. Nat Rev Neurosci 5: 45-54.

60. Pastalkova E, Serrano P, Pinkhasova D, Wallace E, Fenton AA, et al. (2006) Storage of spatial information by the maintenance mechanism of LTP. Science 313: 1141-1144.

61. Hayashi Y, Shi S-H, Esteban JA, Piccini A, Poncer J-C, et al. (2000) Driving AMPA receptors into synapses by LTP and CaMKII: requirement for GluR1 and PDZ domain interaction. Science Signalling 287: 2262.

62. Shi S-H, Hayashi Y, Petralia RS, Zaman SH, Wenthold RJ, et al. (1999) Rapid spine delivery and redistribution of AMPA receptors after synaptic NMDA receptor activation. Science 284: 1811-1816.

63. Okamoto K, Nagai T, Miyawaki A, Hayashi Y (2004) Rapid and persistent modulation of actin dynamics regulates postsynaptic reorganization underlying bidirectional plasticity. Nat Neurosci 7: 1104-1112.

64. Kauer JA, Malenka RC (2007) Synaptic plasticity and addiction. Nat Rev Neurosci 8: 844-858.

65. Malenka RC, Bear MF (2004) LTP and LTD: an embarrassment of riches. Neuron 44: 5-21.

66. Massey PV, Bashir ZI (2007) Long-term depression: multiple forms and implications for brain function. Trends Neurosci 30: 176-184.

67. Krucker T, Siggins GR, Halpain S (2000) Dynamic actin filaments are required for stable long-term potentiation (LTP) in area CA1 of the hippocampus. Proceedings of the National Academy of Sciences 97: 6856-6861.

68. Fukazawa Y, Saitoh Y, Ozawa F, Ohta Y, Mizuno K, et al. (2003) Hippocampal LTP is accompanied by enhanced F-actin content within the dendritic spine that is essential for late LTP maintenance in vivo. Neuron 38: 447-460.

69. Ramachandran B, Frey JU (2009) Interfering with the actin network and its effect on long-term potentiation and synaptic tagging in hippocampal CA1 neurons in slices in vitro. J Neurosci 29: 12167-12173.

70. Soderling SH, Guire ES, Kaech S, White J, Zhang F, et al. (2007) A WAVE-1 and WRP signaling complex regulates spine density, synaptic plasticity, and memory. J Neurosci 27: 355-365.

71. Grove M, Demyanenko G, Echarri A, Zipfel PA, Quiroz ME, et al. (2004) ABI2-deficient mice exhibit defective cell migration, aberrant dendritic spine morphogenesis, and deficits in learning and memory. Mol Cell Biol 24: 10905-10922.

72. Vauti F, Prochnow BR, Freese E, Ramasamy SK, Ruiz P, et al. (2007) Arp3 is required during preimplantation development of the mouse embryo. FEBS Lett 581: 5691-5697.

73. Machesky LM, Atkinson SJ, Ampe C, Vandekerckhove J, Pollard TD (1994) Purification of a cortical complex containing two unconventional actins from Acanthamoeba by affinity chromatography on profilin-agarose. J Cell Biol 127: 107-115.

74. Machesky LM, Reeves E, Wientjes F, Mattheyse FJ, Grogan A, et al. (1997) Mammalian actin-related protein 2/3 complex localizes to regions of lamellipodial protrusion and is composed of evolutionarily conserved proteins. Biochem J 328 (Pt 1): 105-112.

75. Mullins RD, Stafford WF, Pollard TD (1997) Structure, subunit topology, and actin-binding activity of the Arp2/3 complex from Acanthamoeba. J Cell Biol 136: 331-343.

76. Rouiller I, Xu XP, Amann KJ, Egile C, Nickell S, et al. (2008) The structural basis of actin filament branching by the Arp2/3 complex. J Cell Biol 180: 887-895.

77. Welch MD, DePace AH, Verma S, Iwamatsu A, Mitchison TJ (1997) The human Arp2/3 complex is composed of evolutionarily conserved subunits and is localized to cellular regions of dynamic actin filament assembly. J Cell Biol 138: 375-384.

78. Svitkina TM, Borisy GG (1999) Arp2/3 complex and actin depolymerizing factor/cofilin in dendritic organization and treadmilling of actin filament array in lamellipodia. J Cell Biol 145: 1009-1026.

79. Mullins RD, Heuser JA, Pollard TD (1998) The interaction of Arp2/3 complex with actin: nucleation, high affinity pointed end capping, and formation of branching networks of filaments. Proc Natl Acad Sci U S A 95: 6181-6186.

80. Racz B, Weinberg RJ (2008) Organization of the Arp2/3 complex in hippocampal spines. J Neurosci 28: 5654-5659.

81. Hotulainen P, Llano O, Smirnov S, Tanhuanpaa K, Faix J, et al. (2009) Defining mechanisms of actin polymerization and depolymerization during dendritic spine morphogenesis. J Cell Biol 185: 323-339.

82. Wegner AM, Nebhan CA, Hu L, Majumdar D, Meier KM, et al. (2008) N-wasp and the arp2/3 complex are critical regulators of actin in the development of dendritic spines and synapses. J Biol Chem 283: 15912-15920.

83. Allen PB, Ouimet CC, Greengard P (1997) Spinophilin, a novel protein phosphatase 1 binding protein localized to dendritic spines. Proc Natl Acad Sci U S A 94: 9956-9961.

84. Hsieh-Wilson LC, Allen PB, Watanabe T, Nairn AC, Greengard P (1999) Characterization of the neuronal targeting protein spinophilin and its interactions with protein phosphatase-1. Biochemistry 38: 4365-4373.

85. Muly EC, Smith Y, Allen P, Greengard P (2004) Subcellular distribution of spinophilin immunolabeling in primate prefrontal cortex: localization to and within dendritic spines. J Comp Neurol 469: 185-197.

86. Grossman SD, Futter M, Snyder GL, Allen PB, Nairn AC, et al. (2004) Spinophilin is phosphorylated by Ca2+/calmodulin-dependent protein kinase II resulting in regulation of its binding to F-actin. J Neurochem 90: 317-324.

87. Hsieh-Wilson LC, Benfenati F, Snyder GL, Allen PB, Nairn AC, et al. (2003) Phosphorylation of spinophilin modulates its interaction with actin filaments. J Biol Chem 278: 1186-1194.

88. Uematsu K, Futter M, Hsieh-Wilson LC, Higashi H, Maeda H, et al. (2005) Regulation of spinophilin Ser94 phosphorylation in neostriatal neurons involves both DARPP-32-dependent and independent pathways. J Neurochem 95: 1642-1652.

89. Brady AE, Wang Q, Allen PB, Rizzo M, Greengard P, et al. (2005) Alpha 2-adrenergic agonist enrichment of spinophilin at the cell surface involves beta gamma subunits of Gi proteins and is preferentially induced by the alpha 2A-subtype. Mol Pharmacol 67: 1690-1696.

90. Feng J, Yan Z, Ferreira A, Tomizawa K, Liauw JA, et al. (2000) Spinophilin regulates the formation and function of dendritic spines. Proc Natl Acad Sci U S A 97: 9287-9292.

91. Leuba G, Savioz A, Vernay A, Carnal B, Kraftsik R, et al. (2008) Differential changes in synaptic proteins in the Alzheimer frontal cortex with marked increase in PSD-95 postsynaptic protein. J Alzheimers Dis 15: 139-151.

92. Calhoun ME, Fletcher BR, Yi S, Zentko DC, Gallagher M, et al. (2008) Age-related spatial learning impairment is unrelated to spinophilin immunoreactive spine number and protein levels in rat hippocampus. Neurobiol Aging 29: 1256-1264.

93. Someya A, Sata M, Takeda K, Pacheco-Rodriguez G, Ferrans VJ, et al. (2001) ARF-GEP(100), a guanine nucleotide-exchange protein for ADP-ribosylation factor 6. Proc Natl Acad Sci U S A 98: 2413-2418.

94. Hiroi T, Someya A, Thompson W, Moss J, Vaughan M (2006) GEP100/BRAG2: activator of ADP-ribosylation factor 6 for regulation of cell adhesion and actin cytoskeleton via E-cadherin and alpha-catenin. Proc Natl Acad Sci U S A 103: 10672-10677.

95. Fitzjohn SM, Bashir ZI (2010) BRAGging about mechanisms of long-term depression. Neuron 66: 627-630.

96. Schutt F, Ueberle B, Schnölzer M, Holz FG, Kopitz J (2002) Proteome analysis of lipofuscin in human retinal pigment epithelial cells. FEBS Lett 528: 217-221.

97. Ottis P, Koppe K, Onisko B, Dynin I, Arzberger T, et al. (2012) Human and rat brain lipofuscin proteome. Proteomics 12: 2445-2454.

98. Huttner WB, Schiebler W, Greengard P, De Camilli P (1983) Synapsin I (protein I), a nerve terminal-specific phosphoprotein. III. Its association with synaptic vesicles studied in a highly purified synaptic vesicle preparation. J Cell Biol 96: 1374-1388.

99. Guo J, Prokai-Tatrai K, Nguyen V, Rauniyar N, Ughy B, et al. (2011) Protein targets for carbonylation by 4-hydroxy-2-nonenal in rat liver mitochondria. J Proteomics 74: 2370-2379.

100. Collingridge GL, Peineau S, Howland JG, Wang YT (2010) Long-term depression in the CNS. Nat Rev Neurosci 11: 459-473.

Acknowledgements: Funding for this project was provided by DFG-GRK1033, KNDD BMBF 01ED1201B), EU-FP7-PRIORITY to CK, and DFG Hu 306/27-2 to JPH. ABS and KWL received funding from the EU-FP7 project ‘SynSys’ (grant # 242167).

Figure 1: Cognitive performance as distance to platform during hidden platform place learning in the Morris water maze. Shown is the distance to the platform [cm] (+ SEM) for each acquisition day as averaged for adult superior (full triangles) and adult inferior (full circles) (**A**) as well as aged superior (open triangles) and aged inferior (open circles) (**B**) learners. **C**) Depicted is the mean curve level of the distance to platform (+ SEM) for the adult and aged rats as well as their subgroups adult superior, adult inferior, aged superior, and aged inferior learners (*, **, ***: $p \leq 0.05, 0.01, 0.001$).

Figure 2: Cognitive performance place preference during hidden platform place learning in the Morris water maze. Shown is the time spent in the platform quadrant expressed as percentage of trial duration (+ SEM) for each acquisition day displayed by adult superior (full triangles) and adult inferior (full circles) (**A**) as well as aged superior (open triangles) and aged inferior (open circles) (**B**) learners. **C**) Depicted is the mean curve level [%] of the place preference (+ SEM) for adult and aged rats as well as adult superior, adult inferior, aged superior, and aged inferior learners (*, **, ***: $p \leq 0.05, 0.01, 0.001$).

Figure 3: Grouping of animals and workflow. Displayed in the left graph (**A**) is the applied grouping of the rats according to their age and learning abilities, resulting in four groups of 8 individuals, each. The right panel (**B**) depicts the workflow of the insoluble proteome purification from rat hippocampal homogenate (red: insoluble protein components; P: pellet; SN: supernatant).

Figure 4: Structural plasticity in NMDA receptor-mediated long-term depression. Depicted is a scheme of NMDA-receptor-induced LTD, bringing in context the presumably concert actions of ARP3 – localized in the ARP2/3 complex; NEB2 – being activated via phosphorylation by CAMKII and acting on catabolic and anabolic processes on the filamentous actin network; and BRAG2 – binding to the AMPA receptor-GluA2 subunit upon its de-phosphorylation by the mGluR-activated protein tyrosine phosphatase (PTP) and

inducing modulations of the actin cytoskeleton and internalization of AMPARs via its interaction with ARF6 [53,95]. Scheme based on Okamoto et al., 2009 [52], linking it to LTD [100] and including information concerning BRAG2 described by Scholz *et al.*, 2010 [53] and summarized by Fitzjohn and Bashir, 2010 [95].

Figure 5: F-actin precipitation assay. Western blot of the supernatant (SN) and insoluble pellet (P) fraction of cell lysates subjected to an F-actin precipitation assay. Visible are immunostained bands of actin and ARP3 as designated. Cells were pre-treated with 1 µM or 5 µM of the F-actin de-polymerizing agent Mycalolide B, or with the respective amount of the solvent DMSO only. Upon treatment with 5 µM Mycalolide B, actin (F-actin) and ARP3 simultaneously disappear from the pellet fraction indicating that ARP3's insolubility is dependent on F-actin.

Figure 6: Relative abundance of insoluble ARP3, NEB2, and BRAG2 comparing aged superior and aged inferior learners. Displayed are the log2-transformed relative abundances of each of the three proteins as determined for all 16 aged rats by iTRAQ mass spectrometry. Graphs **A**, **D**, and **G** show a group wise comparison of aged superior and the aged inferior rats. Panels **B**, **E**, and **H** display the log2 protein values plotted against the rats' performance in the MWM assessed as mean total distance A_0 [cm]. Drawn in graphs **C**, **F**, and **I** are the log2 protein values plotted against the rats' performance in the MWM as the learning pace, assessed as a_1-slope over the 6 trial days. Besides the Pearson correlation values (r) and the respective p-value, graphs **B**, **C**, **E**, **F**, **H**, and **I** also display the line of linear regression along with its 95%-confidence interval.

Figure 7: Protein inter-correlations. Displayed are the log2-transformed relative abundances of ARP3, NEB2, and BRAG2 plotted against one another to visualize possible correlative changes. Graphs show NEB2-values plotted against ARP3-values (**A**), BRAG2 against ARP3 (**B**), and BRAG2 against NEB2 (**C**). Besides the Pearson correlation values (r)

and the respective p-value, graphs also display the line of linear regression along with its 95%-confidence interval.

Table 1: Proteins significantly altered comparing the insoluble proteome of aged and adult rat hippocampi.

			aged vs. adult	
Entry	**Protein name**	**Change**	**p-value**	**FDR**
HPLN2_RAT	Hyaluronan and proteoglycan link protein 2	↑	2.6×10^{-9}	2.3×10^{-7}
GFAP_RAT	Glial fibrillary acidic protein	↑	2.0×10^{-6}	0.00012
MOBP_RAT	Myelin-associated oligodendrocyte basic protein	↑	5.5×10^{-6}	0.00023
DCTN1_RAT	Dynactin subunit 1	↑	2.8×10^{-5}	0.00089
BSN_RAT	Protein bassoon	↓	4.9×10^{-5}	0.00126
SHAN3_RAT	SH3 and multiple ankyrin repeat domains protein 3	↓	8.6×10^{-5}	0.00184
HOME1_RAT	Homer protein homolog 1	↓	0.00022	0.00406
SNIP_RAT	p130Cas-associated protein	↓	0.00026	0.00414
AGAP2_RAT	Arf-GAP, GTPase, ANK repeat and PH domain-containing protein 2	↓	0.00062	0.00881
gi|293342552	PREDICTED: collagen, type IV, alpha 2	↑	0.00111	0.01414
SHAN1_RAT	SH3 and multiple ankyrin repeat domains protein 1	↓	0.00122	0.01418
ERC2_RAT	ERC protein 2	↓	0.00169	0.01760
CN37_RAT	2',3'-cyclic-nucleotide 3'-phosphodiesterase	↑	0.00179	0.01760
TBA4A_RAT	Tubulin alpha-4A chain	↑	0.00247	0.02255
GLNA_RAT	Glutamine synthetase	↑	0.00326	0.02778
DLG2_RAT	Disks large homolog 2	↓	0.00377	0.03014
G3P_RAT	Glyceraldehyde-3-phosphate dehydrogenase	↑	0.00455	0.03426
BAIP2_RAT	Brain-specific angiogenesis inhibitor 1-associated protein 2	↓	0.00675	0.04665
SHAN2_RAT	SH3 and multiple ankyrin repeat domains protein 2	↓	0.00693	0.04665
DYHC1_RAT	Cytoplasmic dynein 1 heavy chain 1	↑	0.00812	0.04889
gi|157818467	Heat shock 70kDa protein 12A	↑	0.00813	0.04889
gi|293345780	PREDICTED: similar to Gene model 996	↓	0.00841	0.04889
SYN1_RAT	Synapsin-1	↓	0.01125	0.06007
MAP2_RAT	Microtubule-associated protein 2	↑	0.01127	0.06007
IDH3B_RAT	Isocitrate dehydrogenase [NAD] subunit beta, mitochondrial	↑	0.01396	0.06635
NMDE1_RAT	Glutamate [NMDA] receptor subunit epsilon-1	↓	0.01397	0.06635
ARPC2_RAT	Actin-related protein 2/3 complex subunit 2	↓	0.01400	0.06635
DLGP2_RAT	Disks large-associated protein 2	↓	0.01614	0.07203
DPYL2_RAT	Dihydropyrimidinase-related protein 2	↓	0.01707	0.07203
gi|157823479	Prickle homolog 2	↓	0.01731	0.07203
gi|33563266	NADH dehydrogenase (ubiquinone) 1 alpha subcomplex, 4	↑	0.01745	0.07203
DLGP3_RAT	Disks large-associated protein 3	↓	0.01835	0.07289
NEB2_RAT	Neurabin-2	↓	0.01937	0.07289
NCAN_RAT	Neurocan core protein	↑	0.01992	0.07289
EF2_RAT	Elongation factor 2	↑	0.01994	0.07289
ATPA_RAT	ATP synthase subunit alpha, mitochondrial	↑	0.02084	0.07365
HPLN1_RAT	Hyaluronan and proteoglycan link protein 1	↑	0.02130	0.07365
MYO1D_RAT	Myosin-Id	↑	0.02308	0.07773
GELS_RAT	Gelsolin	↑	0.02684	0.08348
TBB2C_RAT	Tubulin beta-2C chain	↑	0.02721	0.08348
RL15_RAT	60S ribosomal protein L15	↓	0.02740	0.08348
DYN1_RAT	Dynamin-1	↓	0.02544	0.08348
gi|5031595	Actin related protein 2/3 complex, subunit 4 [Mus musculus]	↓	0.02912	0.08667
AT1A1_RAT	Sodium/potassium-transporting ATPase subunit alpha-1	↑	0.03096	0.09005
RL7A_RAT	60S ribosomal protein L7a	↓	0.03515	0.09773
NMDE2_RAT	Glutamate [NMDA] receptor subunit epsilon-2	↓	0.03535	0.09773
BEGIN_RAT	Brain-enriched guanylate kinase-associated protein	↓	0.03589	0.09773
NSF_RAT	Vesicle-fusing ATPase	↑	0.04010	0.10547
gi|149066065	rCG59984	↓	0.04039	0.10547
TBB3_RAT	Tubulin beta-3 chain	↑	0.04307	0.11022
DLG4_RAT	Disks large homolog 4	↓	0.04726	0.11634
KCC2A_RAT	Calcium/calmodulin-dependent protein kinase type II alpha chain	↓	0.04728	0.11634

Table 2: Top 10 proteins altered comparing the insoluble proteome of aged inferior and aged superior rats. Values in bold are significant.

					Pearson Correlation			
		aged inferior vs. aged superior			A_0-distance (MWM)		a_1-slope (MWM)	
Entry	Protein name	Change	p-value	FDR	r	p	r	p
ARP3_RAT	**Actin-related protein 3**	↓	**0.0013**	0.2156	**-0.72**	**0.002**	**0.67**	**0.005**
NEB2_RAT	**Neurabin-2**	↓	**0.0054**	0.4662	**-0.62**	**0.010**	0.47	0.066
gi|109473862	PREDICTED: IQ motif and Sec7 domain 1-like isoform 2 (**Brag2**)	↑	**0.0310**	0.9328	**0.53**	**0.035**	**-0.73**	**0.001**
G3P_RAT	Glyceraldehyde-3-phosphate dehydrogenase	↑	0.0547	0.9328	0.45	0.080	-0.55	0.027
MYH10_RAT	Myosin-10	↑	0.0570	0.9328	-0.49	0.054	0.03	0.912
SHAN3_RAT	SH3 and multiple ankyrin repeat domains protein 3	↓	0.0729	0.9328	-0.35	0.184	0.31	0.243
ACTB_RAT	Actin, cytoplasmic 1	↓	0.0841	0.9328	-0.43	0.096	0.38	0.147
DYHC1_RAT	Cytoplasmic dynein 1 heavy chain 1	↑	0.0861	0.9328	0.40	0.125	-0.33	0.212
AGAP2_RAT	Arf-GAP, GTPase, ANK repeat and PH domain-containing protein	↑	0.0965	0.9328	0.46	0.073	-0.47	0.066
SYGP1_RAT	Ras GTPase-activating protein SynGAP	↑	0.1008	0.9328	0.43	0.096	-0.58	0.019

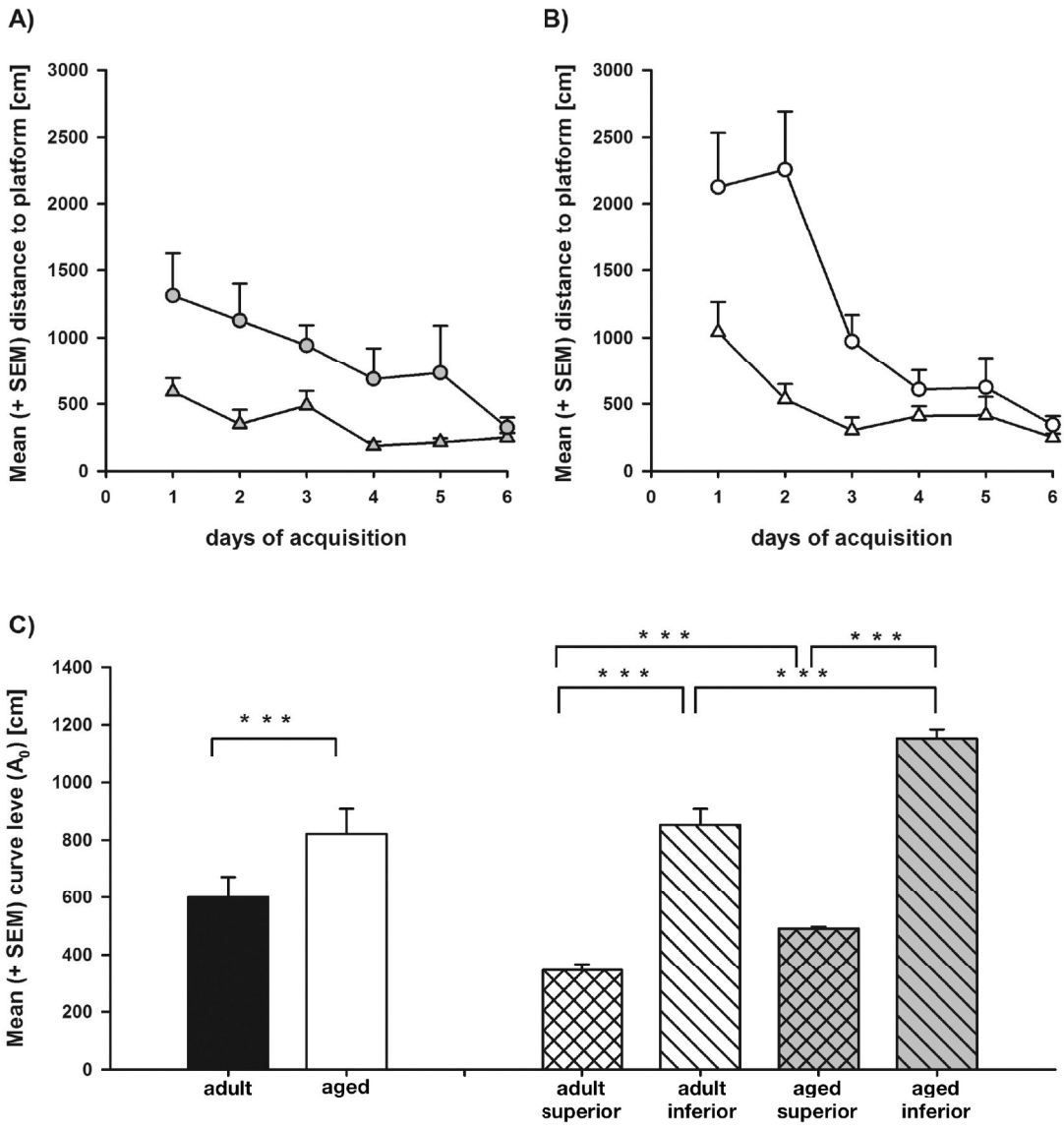
A)
B)
Mean (+ SEM) distance to platform [cm]
3000
2500
2000
1500
1000
500
0
0 1 2 3 4 5 6
days of acquisition
C)
Mean (+ SEM) curve leve (A_0) [cm]
1400
1200
1000
800
600
400
200
0
* * *
adult
aged
adult superior
adult inferior
aged superior
aged inferior

Figure 1

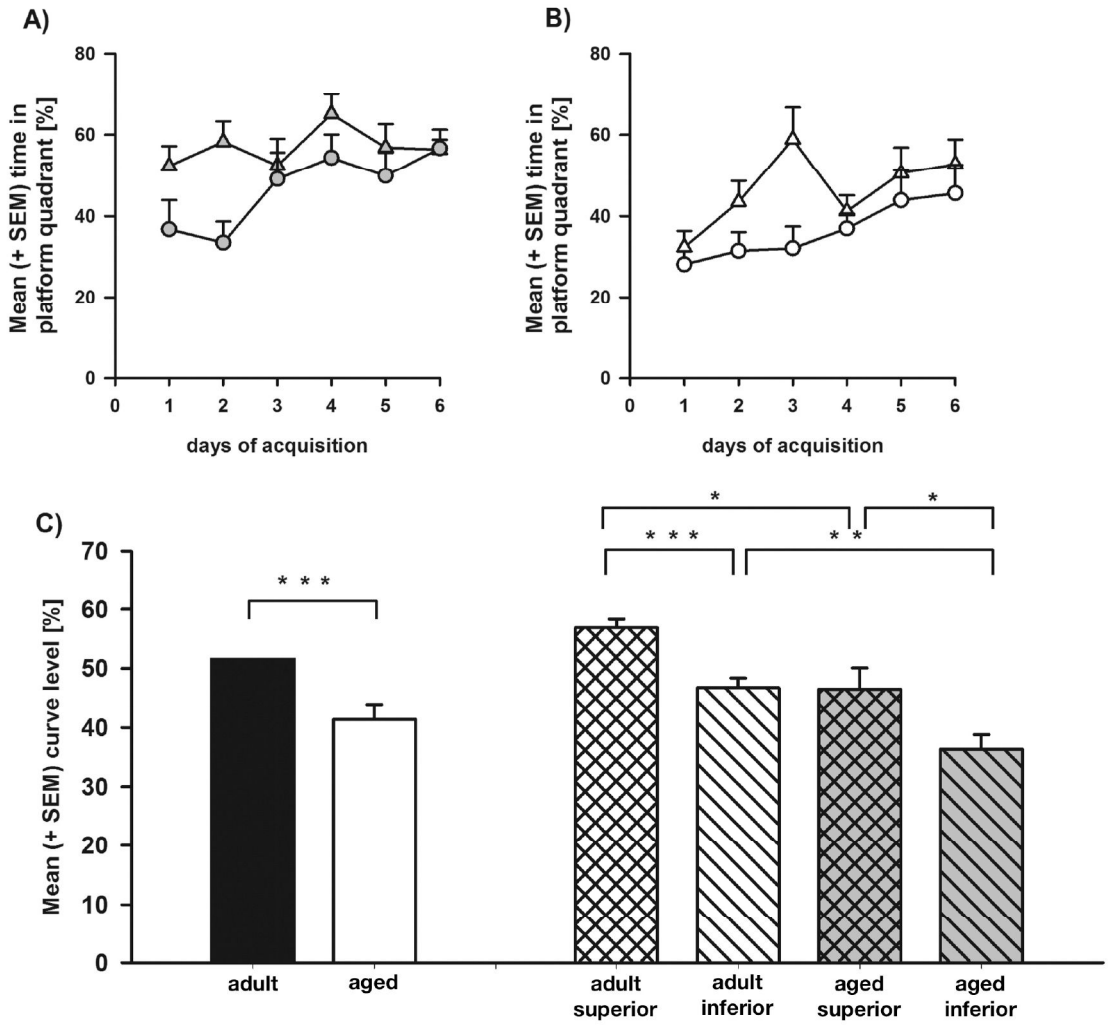
A)
B)
C)
Mean (+ SEM) time in platform quadrant [%]
days of acquisition
Mean (+ SEM) curve level [%]
adult
aged
adult superior
adult inferior
aged superior
aged inferior
* * *
* *
*

Figure 2

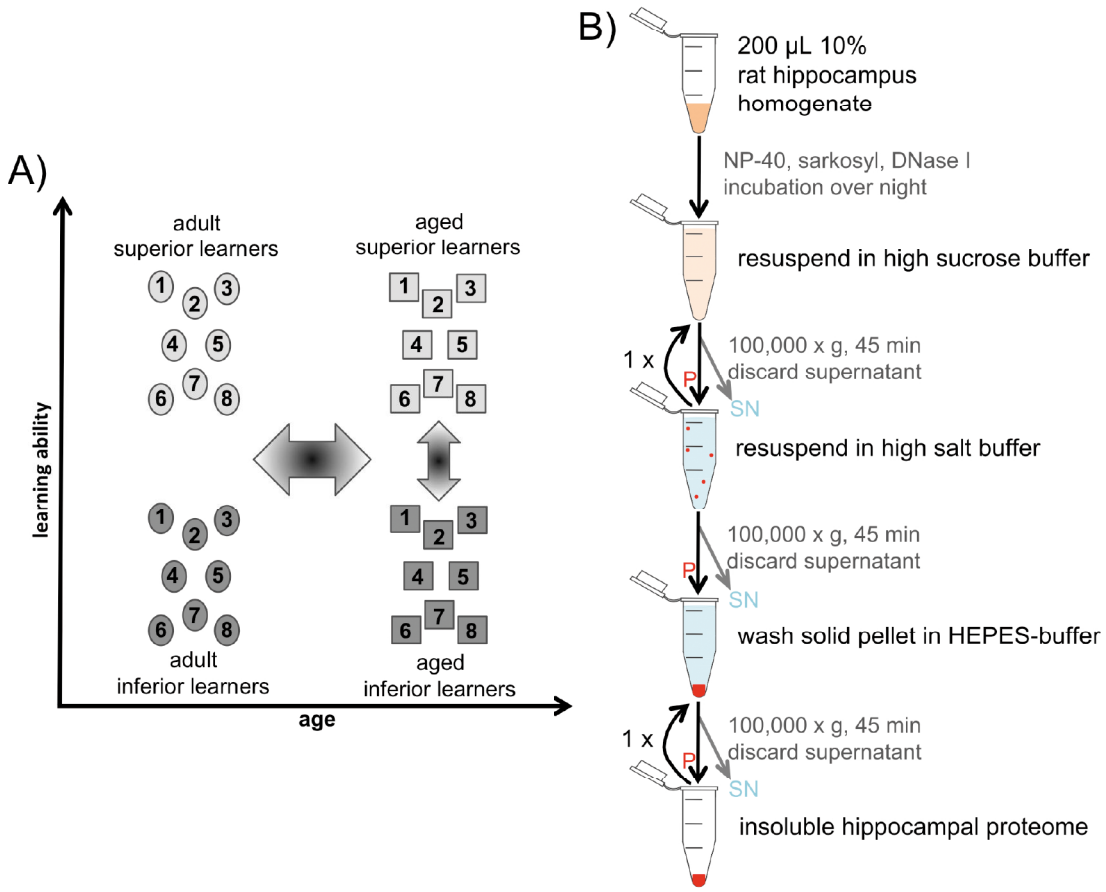
A)
adult
superior learners
aged
superior learners
learning ability
adult
inferior learners
aged
inferior learners
age
B)
200 µL 10%
rat hippocampus
homogenate
NP-40, sarkosyl, DNase I
incubation over night
resuspend in high sucrose buffer
1 x
100,000 x g, 45 min
discard supernatant
P
SN
resuspend in high salt buffer
100,000 x g, 45 min
discard supernatant
P
SN
wash solid pellet in HEPES-buffer
1 x
100,000 x g, 45 min
discard supernatant
P
SN
insoluble hippocampal proteome

Figure 3

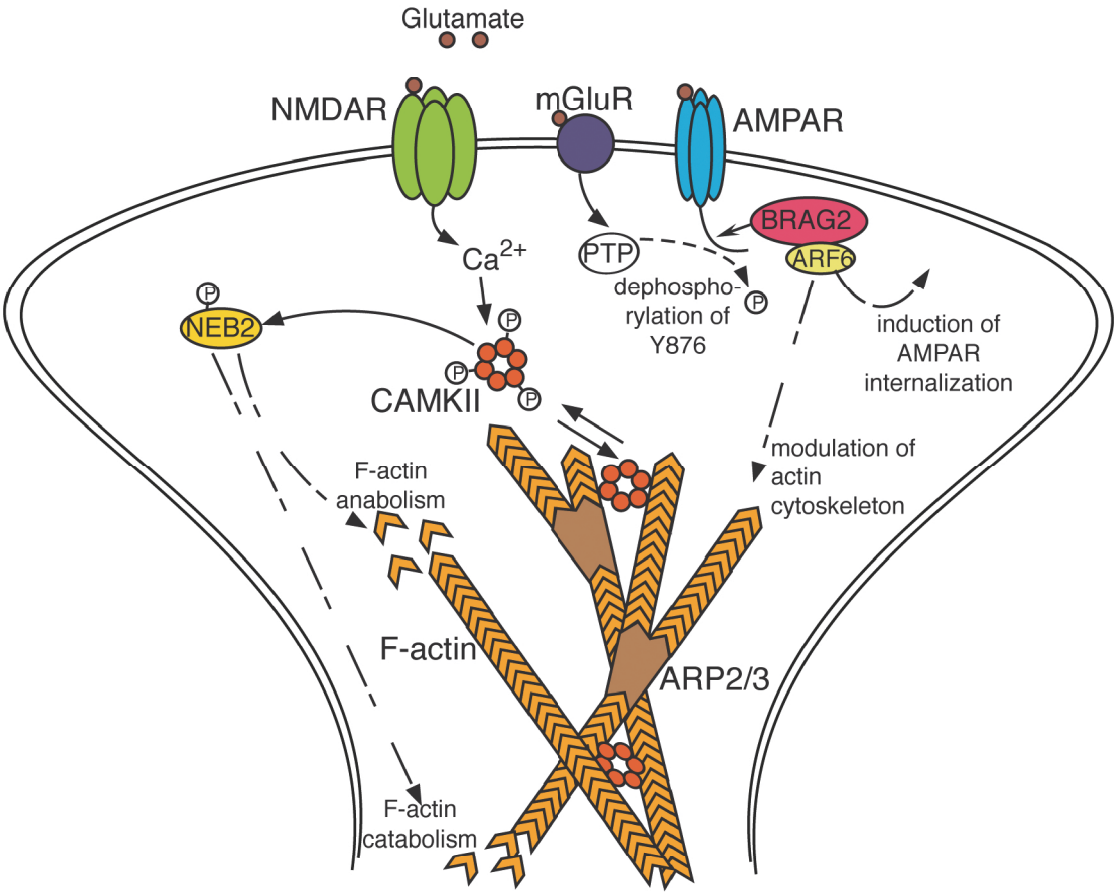
Glutamate
NMDAR
mGluR
AMPAR
BRAG2
ARF6
Ca2+
PTP
dephospho-
rylation of
Y876
induction of
AMPAR
internalization
NEB2
CAMKII
modulation of
actin
cytoskeleton
F-actin
anabolism
F-actin
ARP2/3
F-actin
catabolism

Figure 4

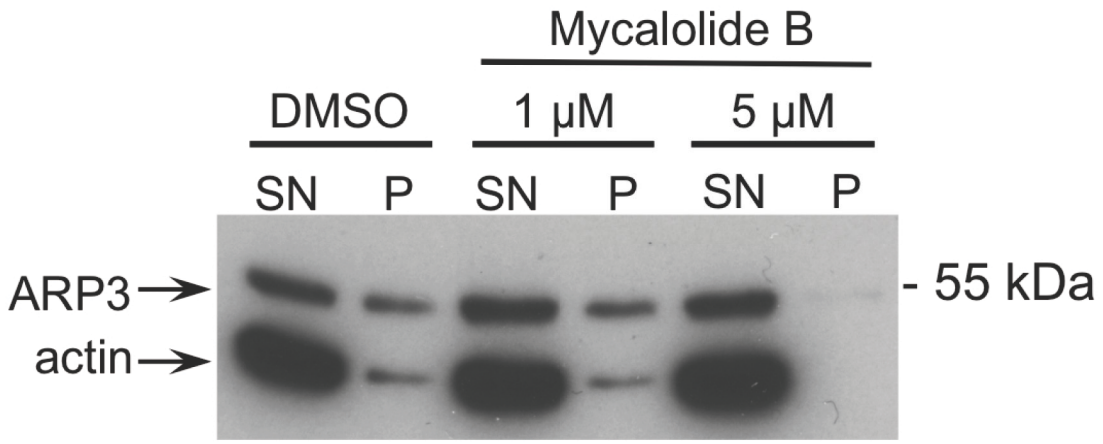

Figure 5

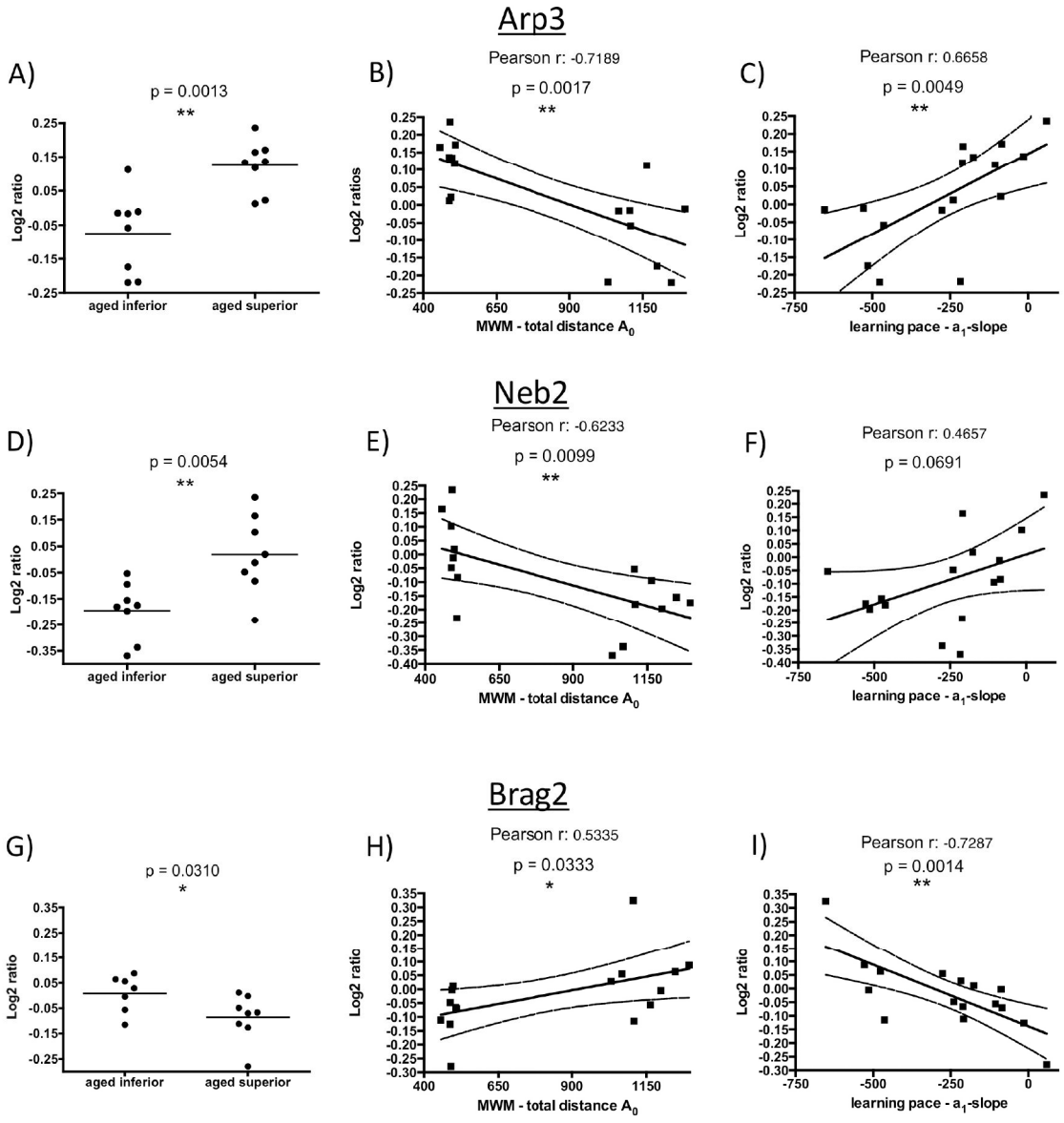
Arp3
A)
p = 0.0013
**
Log2 ratio
aged inferior
aged superior
B)
Pearson r: -0.7189
p = 0.0017
**
Log2 ratios
MWM - total distance A0
C)
Pearson r: 0.6658
p = 0.0049
**
Log2 ratio
learning pace - a1-slope
Neb2
D)
p = 0.0054
**
Log2 ratio
aged inferior
aged superior
E)
Pearson r: -0.6233
p = 0.0099
**
Log2 ratio
MWM - total distance A0
F)
Pearson r: 0.4657
p = 0.0691
Log2 ratio
learning pace - a1-slope
Brag2
G)
p = 0.0310
*
Log2 ratio
aged inferior
aged superior
H)
Pearson r: 0.5335
p = 0.0333
*
Log2 ratio
MWM - total distance A0
I)
Pearson r: -0.7287
p = 0.0014
**
Log2 ratio
learning pace - a1-slope

Figure 6

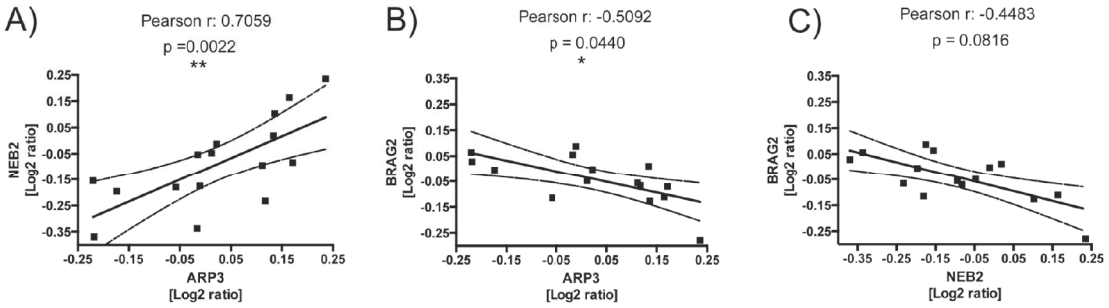
A)
Pearson r: 0.7059
p =0.0022
**
NEB2
[Log2 ratio]
ARP3
[Log2 ratio]
B)
Pearson r: -0.5092
p = 0.0440
*
BRAG2
[Log2 ratio]
ARP3
[Log2 ratio]
C)
Pearson r: -0.4483
p = 0.0816
BRAG2
[Log2 ratio]
NEB2
[Log2 ratio]

Figure 7

3.3 Publication III

Convergence of two independent mental disease genes on the protein level: Recruitment of dysbindin to cell-invasive disrupted-in-schizophrenia 1 aggresomes

Philipp Ottis, Verian Bader, Svenja V. Trossbach, Hans Kretzschmar, Max Michel, S. Rutger Leliveld and Carsten Korth

Biological Psychiatry 70 (2011): 604–610

Author's contribution:

The author performed all experiments related to the interplay of DISC1 and dysbindin with exception of the immuno-blot in Figure 3 B.

In particular, the author's contributions covered:

- Design of experimental setup
- Contribution to establishment of a protocol for the purification of DISC1 aggresomes
- Expression and purification of recombinant proteins from *E. coli*
- Generation of α-dysbindin monoclonal antibody 16G11 (e.g. mouse splenocyte isolation, hybridoma generation, ELISA and immuno-blot screening)
- Generation of protein fusion or truncation constructs
- Immuno-cytochemistry and immuno-blotting
- Analytical size-exclusion chromatography
- Circular-dichroism spectroscopy
- Purification of insoluble proteome in *post-mortem* brains
- The author generated all data leading to table 2 and figures 1 A, 2 A-C, 3 A, S2, S5-8 and S10
- Authoring the manuscript

Convergence of Two Independent Mental Disease Genes on the Protein Level: Recruitment of Dysbindin to Cell-Invasive Disrupted-In-Schizophrenia 1 Aggresomes

Philipp Ottis, Verian Bader, Svenja V. Trossbach, Hans Kretzschmar, Max Michel, S. Rutger Leliveld, and Carsten Korth

Background: Both disrupted-in-schizophrenia 1 (*DISC1*) and dysbindin have been identified as schizophrenia candidate genes in independent genetic linkage studies. The proteins have been assigned distinct subcellular locations and functions. We investigated whether both proteins converge into a common pathway specific for schizophrenia or mental diseases.

Methods: DISC1 and dysbindin were expressed as recombinant proteins with or without a fluorescent protein-tag in human or mouse neuroblastoma cells and as recombinant proteins in *E. coli*. Postmortem brains of patients with mental diseases from the Stanley Research Medical Institute's Consortium Collection were used to demonstrate molecular interactions in biochemically purified protein fractions.

Results: First, upon overexpression in neuroblastoma cells, DISC1 formed aggresomes that recruited homologous soluble C-terminal DISC1 fragment or heterologous dysbindin. Domains involved in binding could be mapped to DISC1 (316-597) and dysbindin (82-173), indicating a specific interaction. In addition, recruitment was demonstrated when externally added, purified DISC1 aggresomes penetrated recipient cells after coincubation. Second, a direct interaction between soluble DISC1 protein and dysbindin was demonstrated in a cell free system using *E. coli*-expressed proteins. Third, co-aggregation of DISC1 and dysbindin was demonstrated in postmortem brains for a subgroup of cases with chronic mental disease but not healthy control subjects.

Conclusions: A direct interaction of soluble and insoluble DISC1 protein with dysbindin protein demonstrates convergence of so far considered independent mental disease genes by direct molecular interaction. Our findings highlight protein aggregation and recruitment as a biological mechanism in mental disease.

Key Words: DISC1, DTNBP1, dysbindin, heterologous protein aggregation, protein assembly, protein conformational disease, schizophrenia pathway

The neurobiology of chronic mental diseases (CMD) like schizophrenia is becoming clearer in the wake of genetic studies establishing linkage or association to genes like disrupted-in-schizophrenia 1 (*DISC1*) (1), dysbindin (2), neuregulin 1 (3), and others (4).

Abundant evidence from genetics and reverse genetics has accumulated demonstrating a key role for DISC1 in the genesis of behavioral disorders and maintenance of mental health (5). DISC1 has a critical influence on neuronal development (6), consistent with the earlier neurodevelopmental hypothesis of the origin of schizophrenia (7). In addition, a variety of other functions for DISC1 in neuronal cell proliferation, migration, and the synapse have been demonstrated (8–10).

The independently identified, schizophrenia-linked gene dysbindin (2) has been attributed to functions distinct from *DISC1*. Originally, dysbindin was identified as a binding partner to dystrobrevin (11) and located to membranes of muscle but also pre- and postsynapses. Dysbindin is involved in dendritic spine formation through binding to WAVE-2 and Abi-1, two proteins linked to rho GTPase Rac1 regulating actin cytoskeleton reorganization (12); interestingly, DISC1 has also been identified to regulate Rac1-dependent functions (9). Dysbindin is part of the biogenesis-of-lysosome-related organelles complex (BLOC-1) that regulates generation of specialized vesicular cell organelles, including vesicle trafficking of dopamine 2 receptors (13,14).

Two important questions have remained unanswered, so far: 1) whether any of the schizophrenia-associated genes/proteins are linked to one single pathway on the cellular level, and 2) whether there is a smallest common denominator for a downstream executive function characteristic for the schizophrenia phenotype. Genetic interactions between candidate genes have been demonstrated, for example, in studies investigating additional risk for schizophrenia phenotypes in *DISC1*-conditioned genetic studies (15,16). In a recent study, we have been able to demonstrate that schizophrenia candidate gene neuregulin 1 regulated DISC1 expression in vivo (17). For DISC1 and dysbindin, an overlapping protein–protein interaction network but no direct interaction has been demonstrated (18). These findings suggested that there might be a schizophrenia-specific pathway into which several schizophrenia candidate proteins converge.

It is increasingly questioned whether the purely clinical term "schizophrenia" should be used to define biological causes of this mental disease that might in fact appear as multiple clinical phenotypes (19). From the extensive knowledge on the clinical course of disease, (20) it is already obvious that schizophrenia is likely to comprise biologically heterogenous conditions originating from different molecular causes. A majority of patients suffering from schizophrenia show signs of a progressive disease (21).

From the Department of Neuropathology (PO, VB, SVT, MM, SRL, CK), Heinrich Heine University Medical School, Düsseldorf, Germany; and the Institute of Neuropathology (HK), Ludwig-Maximilians-Universität München, Munich, Germany.

Authors PO and VB contributed equally to this work.

Address correspondence to Carsten Korth, M.D., Ph.D., Department of Neuropathology, Heinrich Heine University, Moorenstraβe 5, 40225 Düsseldorf, Germany; E-mail: ckorth@uni-duesseldorf.de.

Received Dec 20, 2010; revised Mar 15, 2011; accepted Mar 17, 2011.

0006-3223/$36.00
doi:10.1016/j.biopsych.2011.03.027

A hallmark of chronic brain conditions with a decline of intellectual abilities is the presence of aggregated proteins (22), and it was recently demonstrated that, experimentally, these protein aggregates can be transmitted between cells, even though at varying efficiencies (23–25).

We previously reported DISC1-immunoreactivity in biochemically purified insoluble fractions of brain homogenates from a subgroup of patients with chronic mental disease but not normal control subjects (26) and demonstrated that insoluble DISC1 had lost functional protein interactions (26). The aggregation propensity of DISC1 was independently confirmed by Zhou *et al.* (27).

Here, we investigated the ability of DISC1 aggresomes to recruit homologous soluble fragments of itself or heterologous as well as heterologous dysbindin.

Methods and Materials

Cell Labeling Studies

Yellow fluorescent protein (YFP)-dysbindin a and c, fluorescent green fluorescent protein (GFP)-full-length (FL) DISC1, non-tagged FL DISC1, or other constructs were cloned into the pcDNA3.1(+) vector (Invitrogen, Karlsruhe, Germany), then transfected into CAD mouse neuroblastoma cells, SH-SY5Y cells or NLF neuroblastoma cells (Children's Hospital of Philadelphia, Philadelphia, Pennsylvania) with Metafectene (Biontex, Munich, Germany) when at 70% confluency. For microscopy, cells were grown on glass coverslips. Fixation in 4% paraformaldehyde/phosphate-buffered saline (PBS) pH 7.4 was performed 24 or 48 hours after transfection, and if necessary, immunostaining for intracellular proteins was carried out as described (28). All pictures were taken on a Zeiss LSM 510 confocal microscope (Zeiss, Oberkochen, Germany).

Isolation and Purification of Green Fluorescent Protein-DISC1/Monomeric Red Fluorescence Protein-DISC1 Aggresomes and Aggresome Invasion Assay

A protocol for the purification of Lewy bodies was modified for the sucrose gradient purification of aggresomes (29). Briefly, GFP-DISC1/monomeric red fluorescence protein (mRFP)-DISC1 aggresomes from ten 10-cm dishes of transfected human neuroblastoma cells (NLF; Children's Hospital of Philadelphia) were lysed, and DNA was digested. Subsequently, the lysate (2 mL) was loaded onto a sucrose gradient consisting of 80%, 50%, 25%, and 10% sucrose in PBS pH 7.4 (2 mL each) and centrifuged (1000*g*, 30 min at 4°C). The 50%–80% interphase was collected and washed in PBS pH 7.4 (1000*g*, 15 min at 4°C) and resuspended in 500 μL PBS pH 7.4.

Recombinant Human α-Synuclein and DISC1 Labeling

Human α-synuclein # S7820 (250 μg) (Sigma-Aldrich, St. Louis, Missouri) and human DISC1 (598–854 [26]) were labeled with DyLight 594 maleimide (Thermo Scientific, Waltham, Massachusetts) according to the manufacturers' instructions. The labeled protein was dialyzed five times against 10 mmol/L sodium phosphate buffer (NaPi) in a Slide-A-Lyzer dialysis cassette (Thermo Scientific).

Invasiveness Assays of DISC1 Aggresomes and Labeled Recombinant Proteins to Recipient Cells

Inducible expression of GFP (30), GFP-DISC1 (598-854) and subsequent aggresome treatment were performed as follows: SH-SY5Y cells were permanently transfected with a retroviral, inducible expression system (pRetro X-Tight Pur, pTet-on, Clontech, Palo Alto, California) either expressing GFP alone or soluble GFP-DISC1 (598-854) with GFP fused to the DISC1 (598-854) N-terminus. Cells were kept under selection with 1 μg/mL puromycin and 400 μg/mL G418 and were induced with .5 μg/mL doxycycline. Twenty-four hours after induction, cells were treated with mRFP-DISC1 aggresomes purified as described in the preceding text. Purified aggresomes (10 μL) were added to each well, and cells were incubated for 48 hours. For uptake of recombinant protein, 5 μg/mL labeled α-synuclein and 10 μg/mL DISC1 598-854 were added to the medium, and cells were incubated for 48–72 hours. Alternatively, SH-SY5Y human neuroblastoma cells stably expressing mRFP-dysbindin a (transfected by the retroviral pLHCX system, Clontech) were seeded on coverslips and after 24 hours were incubated with DISC1 aggresomes. The cells were then washed 3× with PBS pH 7.4, and extracellular fluorescence was quenched with .04% trypan blue for 5 min. Finally, cells were fixed in 4% paraformaldehyde in PBS pH 7.4 for 10 min on ice, and the coverslips were mounted on glass slides.

Expression and Purification of Recombinant Proteins in *E. coli*, Size Exclusion Chromatography

Dysbindin a and c (31) as well as DISC1 (316-854) and DISC1 (316-854; Δ405-504) constructs were cloned into pET15b (Novagen, Madison, Wisconsin) containing an N-terminal 6-histidine tag, expressed in *E. coli* BL21-(IDE3) Rosetta (Novagen, US), and purified under denaturating conditions in 8 mol/L urea as described (32). DISC1 (598-854) was expressed similarly to that described in Leliveld *et al.* (32). Two milligrams of purified dysbindin a, DISC1 (316-854), or DISC1 (316-854; Δ405-504) were slowly refolded by overnight dialysis to 10 mmol/L NaPi buffer pH 8 plus 1 mol/L urea, 320 μmol/L dithiothreitol (DTT), and .05% 3-[(3-cholamidopropyl)dimethylammonio]-1-propanesulfonate (CHAPS) at a concentration of 2 mg/mL. The next day, two more dialysis steps to 10 mmol/L NaPi buffer pH 8 plus 320 μmol/L DTT were performed. The absence of abundant random coil or unfolded structure indicating a globular protein conformation was verified by circular dichroism spectroscopy (Figure S8A in Supplement 1) (Jasco CD Spectropolarimeter J-715, Goettingen, Germany). Size exclusion chromatography was performed at 20°C on a sephacryl S-500 HR 16/60 column (GE Healthcare, Waukesha, Wisconsin) in 10 mmol/L NaPi buffer pH 8 with 320 μmol/L DTT and .05% CHAPS at a flow of .5 mL/min, with an HPLC system (Knauer HPLC Pump 64, Berlin, Germany). The column was calibrated with gel filtration high molecular weight markers (MW-GF-1000, Sigma; and 151-1901, Bio-Rad). For single runs, 1 mg of recombinant protein was loaded onto the column. For interaction studies, equimolar amounts of precleared (5 min 20,000*g* centrifugation) DISC1 (316-854) or DISC1 (316-854; Δ405-504) and dysbindin a (1 mg) were incubated for 3 hours at room temperature before loading. Data were recorded at A = 280 nm with a BioLogic LP and visualized with the corresponding LP Data View Software v1.03 (Bio-Rad).

Purification of Insoluble Proteome in Postmortem Brains and Antibodies

Brodmann area 23 frozen cortex tissue from the Consortium Collection (33) was obtained from the Stanley Medical Research Institute, Baltimore, Maryland. The very same fractions as described in Leliveld *et al.* (26) were used, and their purification has been described (26). Brain samples were processed blinded; however, Western blot analysis was done unblinded. Rabbit antiserum to FL human DISC1 has been described (26). Rabbit antiserum to dysbindin was prepared by Prosetta Corporation (San Francisco, California) by immunizing a rabbits with two peptides, NH_2-CDKSREAKVKSKPRTV-COOH and NH_2-CTSHTDREATPD-COOH,

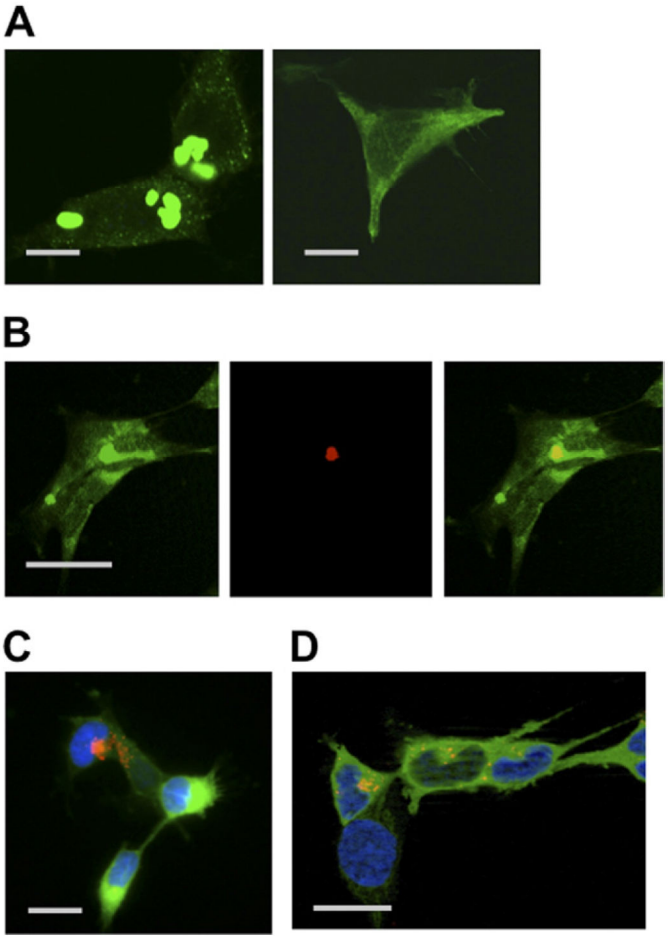

Figure 1. Laser scanning microscopy of invasive disrupted-in-schizophrenia 1 (DISC1) aggresomes and controls. **(A)** Transient transfection of green fluorescent protein (GFP)-full-length (FL) DISC1 (CAD cells) leads to several ca. 5-μm perinuclear aggresomes (left), whereas GFP-DISC1 (598-854) remains regularly dispersed throughout the cytosol (right; SH-SY5Y cells) after transfection. Same results in different cell lines (data not shown). Bar 10 μm. **(B)** Uptake of purified monomeric red fluorescence protein (mRFP)-FL DISC1 (middle) to permanently GFP-DISC1 (598-854)-expressing SH-SY5Y cells (left) leads to recruitment of soluble GFP-DISC1 (598-854) to invasive mRFP FL-DISC1 aggresomes (right). Bar 20 μm. **(C)** Cell penetration of DyLight594 (red)-tagged α-synuclein oligomers into SH-SY5Y cells permanently expressing GFP-DISC1 (598-854; green). 4′,6-diamidino-2-phenylindole (DAPI)-stained cell nucleus (blue). Bar 20 μm. **(D)** Cell penetration of DyLight594 (red)-tagged recombinant purified DISC1 (598-854) from *E. coli* into SH-SY5Y cells permanently expressing GFP-DISC1 (598-854; green). DAPI-stained cell nucleus (blue). Bar 20 μm.

corresponding to residues 25-39 and 334-344 of human dysbindin a, respectively. Rabbit antisera were then affinity purified with recombinant dysbindin before use on Western blot. For generation of α-dysbindin mouse monoclonal antibodies 16G11 and α-human DISC1 monoclonal antibody 14F2, mice were immunized with recombinant N-terminally His_6-tagged dysbindin c (see preceding text) or a recombinant C-terminal human DISC1 fragment (598-785) (32), respectively, and hybridoma were generated and screened in an enzyme-linked immunosorbent assay against the immunogen as described before (34). As secondary antibodies, anti-rabbit-Alexa Fluor 488, anti-mouse-Alexa Fluor 594, or anti-mouse-FITC (all from Invitrogen, Karlsruhe, Germany) were used for cellular stainings or an anti-rabbit-POD from Pierce (Rockford, Illinois) for Western blotting.

Results

DISC1 Forms Cell-Invasive Aggresomes That Recruit Homologous Soluble DISC1 Fragments

Upon transient overexpression in neuroblastoma cells, FL DISC1 C-terminally fused to GFP (GFP-DISC1) formed aggresomes of various sizes (Figure 1A, left) whereas N-terminally truncated GFP-DISC1 (598-854) did not (Figure 1A, right). Similar subcellular structures have been reported before (35–37). These aggresomes were not toxic to the transfected cells (Figure S1 in Supplement 1). Truncated DISC1 (1-597) did not show different aggresome formation, and those completely colocalized with FL DISC1 aggresomes (Figure S2 in Supplement 1).

When we purified the aggresomes on sucrose gradients and coincubated them with cells permanently expressing soluble GFP-DISC1 (598-854), we observed spontaneous penetration of DISC1 aggresomes into cells at very low efficiency (.3% of cells) (Figure 1B, Table 1), similar to but not as frequent as what had been observed by polyglutamine huntingtin aggregates (23) or α-synuclein oligomers (Figure 1C) (24). Z-stacking by laser-scanning microscopy clearly showed a colocalization of invasive mRFP-FL DISC1 with cytosolic GFP-DISC1 (598-854) (Figure S3 in Supplement 1). Invasiveness of DISC1 aggresomes was independent of the GFP tag (Table 1, and Figure S4A in Supplement 1). Thus, DISC1 aggresomes recruited a soluble, C-terminal DISC1 fragment through C-terminal interactions (26). For comparison, synthetic α-synuclein oligomers, refolded according to Desplats *et al.* (24), invaded cells at higher efficiency (ca. 20% of cells) but did not recruit permanently expressed DISC1 (598-854) (Figure 1C and Figure S4B in Supplement 1). However, it is difficult to compare synthetic versus aggresome-derived material, because purity seemed to play a role in the efficiency of invasiveness: similar amounts of recombinant C-terminal DISC1 had an invasive efficiency equal to α-synuclein (Figure 1D and Figure S4C in Supplement 1). These quantitative data are summarized in Table 1.

DISC1 Aggresomes Recruit Heterologous Soluble Dysbindin

To investigate whether DISC1 aggresomes could also recruit heterologous schizophrenia-relevant proteins and thereby mechanistically define a converging disease pathway on the protein level, we tested whether dysbindin could be recruited by DISC1 aggresomes. Dysbindin is expressed in several splice forms of which "dysbindin a" (hereafter termed dysbindin) is the most abundant (31) and therefore used as reference. Transiently overexpressed dysbindin expressed as a YFP fusion protein distributed equally within cells (Figure 2A, left). However, when non-tagged DISC1 and YFP-dysbindin were simultaneously overexpressed, dysbindin was recruited to DISC1 aggresomes (Figure 2A, right). Quantitative data are summarized in Table 2. Similar results were obtained when both

Table 1. Quantitative Data on the Efficiency of Invasiveness of Cellular GFP-Tagged or Untagged DISC1 Aggresomes and Recombinant DISC1(598-854) or α-Synuclein

	Aggresomes		Recombinant/Synthetic Protein	
Protein Species	GFP-DISC1	Untagged DISC1	DISC1 (598–854)	α-Synuclein
Cells Invaded, Counted by Z-Stacking in LSM (%)	.38	.31	17.86	19.15

GFP, green fluorescent protein; DISC1, disrupted-in-schizophrenia 1; LSM, laser scanning microscopy.

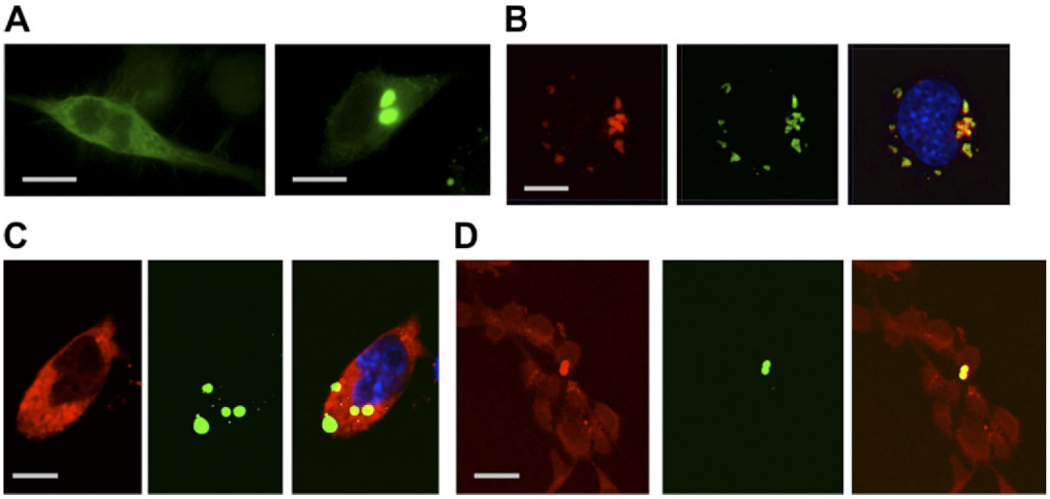

Figure 2. Laser scanning microscopy of DISC1 aggresomes recruiting dysbindin. **(A)** Expression of yellow fluorescent (YFP)-dysbindin c in CAD cells leads to a cytosol-dispersed staining (left), whereas upon cotransfection with (untagged) FL-DISC1, YFP dysbindin is recruited to aggresomes (right). Bar 20 μm. **(B)** Co-expression of untagged dysbindin a (red, left) and DISC1 (green, middle) leads to colocalization of dysbindin and DISC1 into perinuclear aggresomes (yellow for merged pictures on the right; blue, DAPI-stained nucleus) in CAD cells. Dysbindin staining with monoclonal antibodies (mAB) 16G11, DISC1 staining with affinity-purified rabbit antiserum against recombinant DISC1. Bar 10 μm. **(C)** As a negative control for an overexpressed protein, mRFP-dysbindin (173-351) stays cell-dispersed (left) and is not recruited to DISC1 aggresomes (middle), unlike FL dysbindin after coexpression with GFP-FL DISC1 in CAD cells due to the absence of the N-terminal recruitment domain within dysbindin. Because of the homogenous distribution of mRFP-dysbindin (173-351), a partial overlap in localization with the GFP-FL DISC1 aggresomes is visible (see merged pictures on the right; but compare with 2a [right] and 2b [left] for difference in aggresome recruitment). **(D)** Purified GFP-DISC1 aggresomes (middle) are taken up into permanently mRFP-dysbindin expressing SHSY5Y cells (left), and recruit mRFP dysbindin a (right). Abbreviations as in Figure 1.

proteins were expressed as FP-fusion proteins (Figure S5 in Supplement 1) or without FP-tag (Figure 2B). Of note, when DISC1 was overexpressed without GFP tag, it formed multiple smaller aggresomes instead of one or two round-shaped aggresomes (compare Figure 2A [right] and 2B [middle]).

These results demonstrated that DISC1 aggresomes, unlike aggresomes of many other proteins, could also recruit a heterologous protein. Protein domains could be mapped within DISC1 (residues 316-597) and dysbindin (82-172) that executed the heterologous recruitment (Figure S6 in Supplement 1), by using FP-tagged deletion mutants of DISC1 and dysbindin in the aggresome recruitment assay. As an important control and to rule out the possibility that overexpression could unspecifically lead to recruitment, the mRFP-linked C-terminal dysbindin fragment (residues 173-351) without the interaction domain failed to be recruited to DISC1 aggresomes (Figure 2C), just as mRFP alone (Figure S7 in Supplement 1). The existence of distinct polypeptide domains within DISC1 and dysbindin executing molecular interaction thus argued for a specific interaction.

Direct Molecular Interaction of Soluble DISC1 and Dysbindin

We expressed both proteins as refolded, soluble recombinant proteins in *E. coli* (Figure S8A in Supplement 1) and performed a cell-free interaction assay with highly purified DISC1 (316-854) and dysbindin a. After coincubation of both proteins, the emergence of a new, higher molecular weight peak in SEC demonstrated that, in addition to its recruitment to insoluble DISC1 aggresomes, dysbindin also directly interacted with soluble DISC1 (Figure 3A). These surprising data indicated that both the DISC1 and the dysbindin pathway are connected through direct molecular interactions. Recombinant DISC1 (316-854, Δ403-504) lacking the N-terminal self-interaction domain (6) did not interact with dysbindin (Figure S8B in Supplement 1), indicating that residues 403-504 within DISC1 mediate binding to dysbindin, consistent with the aggresome recruitment domain mapping (Figure S6 in Supplement 1).

To investigate whether heterologous recruitment to aggresomes could also be caused by exogenously applied, invasive DISC1 aggresomes, we used permanently transfected, low-level mRFP-dysbindin-expressing SH-SY5Y cells and incubated them with purified DISC1 aggresomes (Figure 2D, and Figure S9 in Supplement 1). Laser scanning microscopy demonstrated recruitment of dysbindin to invasive DISC1 aggresomes (Figure 2D, and Figure S9 in Supplement 1), similar to recruitment upon cotransfection (Figures 2A and 2B).

Thus, DISC1 aggresomes—similar to protein aggregates in other protein conformational diseases like polyglutamine-huntingtin or α-synuclein aggregates—are capable of invading cells, al-

Table 2. Quantitative Data on DISC1 Aggresome Formation and Recruitment of Dysbindin

Ratio GFP-DISC1/mRFP-Dysbindin in Constant 1 μg DNA	Cells Total	Co-Transfection Efficiency (%)	Aggresome Formation (>1 μm Ø) in Cotransfected Cells After 22 Hours (%)	Recruitment of Dysbindin a to DISC1-Aggresomes (%)
1:1	351	60.4	38.9	100.0
1:5	295	56.8	4.2	100.0
5:1	266	65.7	34.3	100.0

DISC1 aggresome formation is a function of time, which is why not all transfected cells show DISC1 aggresomes. However, in all cells where DISC1 aggresomes are present, dysbindin is recruited to those. Different ratios of DISC1 and dysbindin complementary DNA upon transient transfection (column 1) result in a different aggresome propensity of DISC1 in a gene dosage-dependent manner. Abbreviations as in Table 1.

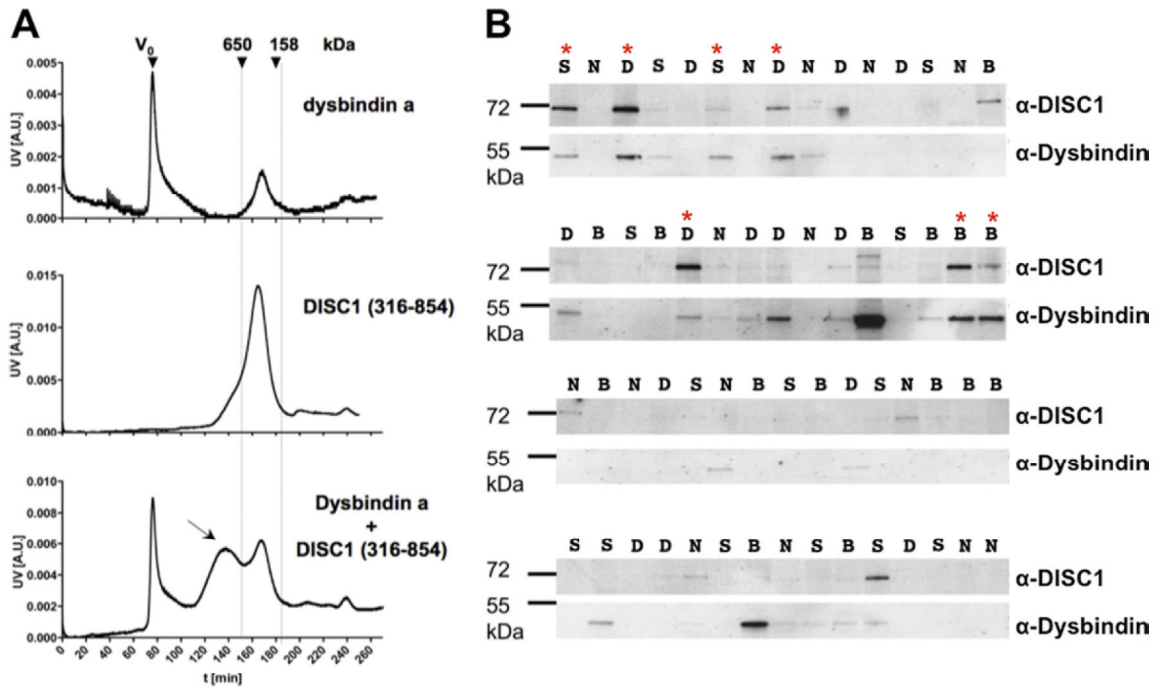

Figure 3. Interaction of disrupted-in-schizophrenia 1 (DISC1) and dysbindin in a cell-free in vitro system and in brains of patients with mental disease. **(A)** Size exclusion chromatography (SEC) of recombinant proteins expressed and purified from *E. coli*: dysbindin (top), DISC1 (316-854) (middle), coincubation of dysbindin with DISC1 (316-854) (bottom). The arrow points at the new peak of higher molecular weight, consisting of a DISC1-dysbindin complex. Dual presence of DISC1 and dysbindin was confirmed by Western blot of respective collected fractions (data not shown). **(B)** Western blot of 60 human brain homogenates biochemically purified by sequential (ultra) centrifugations, with the final, sarkosyl-insoluble fraction loaded. Brains are from individuals diagnosed with schizophrenia (S), bipolar disorder (B), depression (D), or normal control subjects without brain disease (N). From the same individuals, insoluble brain pellets are stained with α-DISC1 antibody (upper panels) or α-dysbindin antibody (lower panels). *Individuals with both DISC1 and dysbindin immunoreactivity in the insoluble pellet.

though at very low efficiency, and recruit homologous, soluble DISC1 (598-854) as well as heterologous protein dysbindin.

Dysbindin Is Copurified with Insoluble DISC1 from Postmortem Brains of a Subgroup of Patients with Chronic Mental Disease

To demonstrate relevance of dysbindin recruitment by DISC1 in mental disease, we investigated whether dysbindin co-precipitated with DISC1 aggregates in insoluble pellets purified from postmortem brains of patients with mental diseases. We analyzed the Stanley Medical Research Institute's Consortium Collection (33) of postmortem brains that has been widely characterized and that we have used before for purifying insoluble DISC1 aggregates (26). Co-precipitation of dysbindin with DISC1 could be demonstrated in 80% of cases that were positive for DISC1 immunoreactivity in the insoluble fraction (Figure 3B). Thus, the interaction of dysbindin with insoluble DISC1 could be detected in brains of a subset of patients with mental disease but not normal control subjects. Neither DISC1 nor dysbindin immunoreactivity could be detected in the insoluble fractions of a representative collection of postmortem brains with other neurodegenerative diseases, indicating that the occurrence of DISC1 and dysbindin immunoreactivity in insoluble brain fractions is specific for a subset of cases with mental disease (Figure S10 in Supplement 1).

Discussion

Mechanisms of proteostasis and protein aggregation have so far not been a focus within the context of mental disease. Our data demonstrate that a key player in maintaining mental health, the DISC1 protein: 1) forms cellular aggresomes capable of invading and penetrating cells at low efficiency; 2) recruits homologous soluble DISC1 (fragments) as well as heterologous protein dysbindin; and 3) directly interacts with soluble dysbindin, revealing convergence of thus far independently classified major schizophrenia genes on the protein level. Thus, through the possibility of a direct physical interaction, DISC1 and dysbindin converge into a common pathway. Our results support the notion that protein pathology might have a heretofore unappreciated major role in the genesis of chronic mental diseases like schizophrenia.

The recently described convergence of so far independently established schizophrenia candidate gene NRG1 into the DISC1 pathway by influencing DISC1 expression in a BACE-dependent manner (17) supports the view that schizophrenia susceptibility genes might be more closely connected than previously expected—for example, in a common DISC1 pathway (10). In such a pathway, molecular networks of schizophrenia candidate proteins intertwine, and disturbances at different nodal points—either separately or simultaneously—might result in a downstream schizophrenia phenotype.

Our three independent assays demonstrated that a DISC1-dysbindin interaction involved multimers of DISC1. However, it is unclear to what extent a direct interaction of soluble dysbindin and DISC1 takes place in the cell, since DISC1 and dysbindin are embedded in an abundant protein–protein interaction network (18). A direct competition of several proteins for the binding site of DISC1 located around the self-association domain is likely. However, our data imply that, through segregation of normally soluble dysbindin (Figure 2A), DISC1 aggresomes could impact on dysbindin-dependent functions. In such a scenario, aggresome formation would lead

to a gain-of-function sequestering a range of specific proteins similar to what has been demonstrated by Olzscha *et al.* (38).

Our finding that cell-derived DISC1 aggresomes have the potential of cell-to-cell transmission, although at very low efficiency, is surprising but could indicate that more general principles of protein aggregate cellular physiology exist, not restricted to the realm of classical neurodegenerative diseases (25). The detailed molecular mechanism of how cytosolic DISC1 protein aggresomes penetrate lipid bilayers is unclear and has not been solved for the cytosolic, cell-penetrating proteins tau, α-synuclein, or polyglutamine proteins. As possible mechanisms, direct cell penetration or endocytosis and cell penetration from late endosomes have been proposed (reviewed in Lee *et al.* [25]). The other question is how DISC1 could enter the extracellular space. In the absence of a secretory signaling sequence, DISC1 is unlikely to be translocated into the endoplasmic reticulum and to enter the secretory pathway. Whether DISC1 could be released by cell death and then be present in the extracellular space is equally unclear. Large DISC1 aggresomes (like in Figure 1A) were not released into the medium under experimental conditions of induced neurotoxicity (data not shown).

The relevance of cell-to-cell transmission of DISC1 in chronic mental diseases should be further investigated in suitable animal models of DISC1 aggregation. This will also allow comparing the morphology of DISC1 aggresomes (identified in cell culture) with DISC1 aggregates (identified in postmortem brains). Whether—in analogy to Parkinson's disease (39)—a predictable spreading pattern of insoluble DISC1 can be tracked in brains of individuals before disease onset will necessitate careful examinations of whole or half-brain sections through different ages. But even in such studies, the biological heterogeneity of schizophrenia or other CMDs might reveal that DISC1-related disorders eventually represent only a subset of all schizophrenia cases. For example, we found insoluble DISC1 as a hint of a potential involvement of DISC1 in disease pathology only in 20% of cases from the SMRI Consortium Collection (26). Nevertheless, the presence of insoluble DISC1 in this subset of cases could make DISC1 a useful biomarker for these cases. Investigations to detect CMD-associated DISC1, spliceforms, or degradation products in cerebrospinal fluid or blood are underway.

Funding from this research was obtained by the SMRI (02R-186, Baltimore), the DFG (Ko 1679/3-1, 4–1; GRK1033), NRW Biostruct, and ERANET-NEURON (DISCover, BMBF 01EW1003). Postmortem brain tissue was donated by The Stanley Medical Research Institute brain collection, courtesy of Drs. Michael B. Knable, E. Fuller Torrey, Maree J. Webster, and Robert H. Yolken. All authors report no biomedical financial interests or potential conflicts of interest.

Supplementary material cited in this article is available online.

1. Millar JK, Wilson-Annan JC, Anderson S, Christie S, Taylor MS, Semple CA, *et al.* (2000): Disruption of two novel genes by a translocation co-segregating with schizophrenia. *Hum Mol Genet* 9:1415–1423.
2. Straub RE, Jiang Y, MacLean CJ, Ma Y, Webb BT, Myakishev MV, *et al.* (2002): Genetic variation in the 6p22.3 gene DTNBP1, the human ortholog of the mouse dysbindin gene, is associated with schizophrenia. *Am J Hum Genet* 71:337–348.
3. Stefansson H, Sigurdsson E, Steinthorsdottir V, Bjornsdottir S, Sigmundsson T, Ghosh S, *et al.* (2002): Neuregulin 1 and susceptibility to schizophrenia. *Am J Hum Genet* 71:877–892.
4. Harrison PJ, Weinberger DR (2005): Schizophrenia genes, gene expression, and neuropathology: On the matter of their convergence. *Mol Psychiatry* 10:40–68.
5. Chubb JE, Bradshaw NJ, Soares DC, Porteous DJ, Millar JK (2008): The *DISC* locus in psychiatric illness. *Mol Psychiatry* 13:36–64.
6. Kamiya A, Kubo K, Tomoda T, Takaki M, Youn R, Ozeki Y, *et al.* (2005): A schizophrenia-associated mutation of *DISC1* perturbs cerebral cortex development. *Nat Cell Biol* 7:1167–1178.
7. Weinberger DR (1995): From neuropathology to neurodevelopment. *Lancet* 346:552–557.
8. Brandon N, Millar JK, Korth C, Sive H, Singh K, Sawa A, *et al.* (2009): Understanding the role of DISC1 in psychiatric disease and during normal development. *J Neurosci* 29:12768–7512775.
9. Hayashi-Takagi A, Takaki M, Graziane N, Seshadri S, Murdoch H, Dunlop AJ, *et al.* (2010): Disrupted-in-Schizophrenia 1 (DISC1) regulates spines of the glutamate synapse via Rac1. *Nat Neurosci* 13:327–332.
10. Jaaro-Peled H, Hayashi-Takagi A, Seshadri S, Kamiya A, Brandon NJ, Sawa A, *et al.* (2009): Neurodevelopmental mechanisms of schizophrenia: uUnderstanding disturbed postnatal brain maturation through neuregulin-1-ErbB4 and DISC1. *Trends Neurosci* 32:485–495.
11. Benson MA, Newey SE, Martin-Rendon E, Hawkes R, Blake DJ (2001): Dysbindin, a novel coiled-coil-containing protein that interacts with the dystrobrevins in muscle and brain. *J Biol Chem* 276:24232–24241.
12. Ito H, Morishita R, Shinoda T, Iwamoto I, Sudo K, Okamoto K, *et al.* (2010): Dysbindin-1, WAVE2 and Abi-1 form a complex that regulates dendritic spine formation. *Mol Psychiatry* 15:976–986.
13. Iizuka Y, Sei Y, Weinberger DR, Straub RE (2007): Evidence that the BLOC-1 protein dysbindin modulates dopamine D2 receptor internalization and signaling but not D1 internalization. *J Neurosci* 27:12390–12395.
14. Ghiani CA, Starcevic M, Rodriguez-Fernandez IA, Nazarian R, Cheli VT, Chan LN, *et al.* (2009): The dysbindin-containing complex (BLOC-1) in brain: Developmental regulation, interaction with SNARE proteins and role in neurite outgrowth. *Mol Psychiatry* 15:204–15215.
15. Hennah W, Tomppo L, Hiekkalinna T, Palo OM, Kilpinen H, Ekelund J, *et al.* (2007): Families with the risk allele of *DISC1* reveal a link between schizophrenia and another component of the same molecular pathway, NDE1. *Hum Mol Genet* 16:453–462.
16. Tomppo L, Hennah W, Lahermo P, Loukola A, Tuulio-Henriksson A, Suvisaari J, *et al.* (2009): Association between genes of Disrupted in schizophrenia 1 (*DISC1*) interactors and schizophrenia supports the role of the DISC1 pathway in the etiology of major mental illnesses. *Biol Psychiatry* 65:1055–1062.
17. Seshadri S, Kamiya A, Yokota Y, Prikulis I, Kano SI, Hayashi-Takagi A, *et al.* (2010): Disrupted-in-Schizphrenia-1 expression is regulated by beta-site amyloid precursor protein cleaving enzyme-1-neuregulin cascade. *Proc Natl Acad Sci U S A* 107:5622–75627.
18. Camargo LM, Collura V, Rain JC, Mizuguchi K, Hermjakob H, Kerrien S, *et al.* (2007): Disrupted in Schizophrenia 1 Interactome: Evidence for the close connectivity of risk genes and a potential synaptic basis for schizophrenia. *Mol Psychiatry* 12:74–86.
19. Owen MJ, Craddock N, Jablensky A (2007): The genetic deconstruction of psychosis. *Schizophr Bull* 33:905–911.
20. an der Heiden W, Häfner H (2000): The epidemiology of onset and course of schizophrenia. *Eur Arch Psychiatry Clin Neurosci* 250:292–303.
21. van Haren NE, Cahn W, Hulshoff Pol HE, Kahn RS (2008): Schizophrenia as a progressive brain disease. *Eur Psychiatry* 23:245–254.
22. Prusiner SB (2001): Shattuck Lecture—neurodegenerative diseases and prions. *N Engl J Med* 344:1516–1526.
23. Ren PH, Lauckner JE, Kachirskaia I, Heuser JE, Melki R, Kopito RR, *et al.* (2009): Cytoplasmic penetration and persistent infection of mammalian cells by polyglutamine aggregates. *Nat Cell Biol* 11:219–225.
24. Desplats P, Lee HJ, Bae EJ, Patrick C, Rockenstein E, Crews L, *et al.* (2009): Inclusion formation and neuronal cell death through neuron-to-neuron transmission of alpha-synuclein. *Proc Natl Acad Sci U S A* 106:13010–13015.
25. Lee SJ, Desplats P, Sigurdson C, Tsigelny I, Masliah E (2010): Cell-to-cell transmission of non-prion protein aggregates. *Nat Rev Neurol* 6:702–706.
26. Leliveld SR, Bader V, Hendriks P, Prikulis I, Sajnani G, Requena JR, *et al.* (2008): Insolubility of disrupted-in-schizophrenia 1 disrupts oligomer-dependent interactions with nuclear distribution element 1 and is associated with sporadic mental disease. *J Neurosci* 28:3839–3845.
27. Zhou X, Chen Q, Schaukowitch K, Kelsoe JR, Geyer MA (2010): Insoluble DISC1-Boymaw fusion proteins generated by DISC1 translocation. *Mol Psychiatry* 15:669–672.

28. Korth C, Kaneko K, Prusiner SB (2000): Expression of unglycosylated mutated prion protein facilitates PrP^{Sc} formation in neuroblastoma cells infected with different prion strains. *J Gen Virol* 81:2555–2563.
29. Iwatsubo T, Yamaguchi H, Fujimuro M, Yokosawa H, Ihara Y, Trojanowski JQ, *et al.* (1996): Purification and characterization of Lewy bodies from the brains of patients with diffuse Lewy Body disease. *Am J Pathol* 148:1517–1529.
30. Hanson GT, Aggeler R, Oglesbee D, Cannon M, Capaldi RA, Tsien RY, *et al.* (2004): Investigating mitochondrial redox potential with redox-sensitive green fluorescent protein indicators. *J Biol Chem* 279:13044–13053.
31. Guo AY, Sun J, Riley BP, Thiselton DL, Kendler KS, Zhao Z, *et al.* (2009): The dystrobrevin-binding protein 1 gene: Features and networks. *Mol Psychiatry* 14:18–29.
32. Leliveld SR, Hendriks P, Michel M, Sajnani G, Bader V, Trossbach S, *et al.* (2009): Oligomer assembly of the C-terminal DISC1 domain (640–854) is controlled by self-association motifs and disease-associated polymorphism. *Biochemistry* 48:7746–7755.
33. Torrey EF, Webster M, Knable M, Johnston N, Yolken RH (2000): The Stanley Foundation Brain Collection and neuropathology consortium. *Schizophr Res* 44:151–155.
34. Korth C, Stierli B, Streit P, Moser M, Schaller O, Fischer R, *et al.* (1997): Prion (PrP^{Sc})-specific epitope defined by a monoclonal antibody. *Nature* 389:74–77.
35. Morris JA, Kandpal G, Ma L, Austin CP (2003): DISC1 (Disrupted-In-Schizophrenia 1) is a centrosome-associated protein that interacts with MAP1A, MIPT3, ATF4/5 and NUDEL: Regulation and loss of interaction with mutation. *Hum Mol Genet* 12:1591–1608.
36. Brandon NJ, Handford EJ, Schurov I, Rain JC, Pelling M, Duran-Jimeniz B, *et al.* (2004): Disrupted in Schizophrenia 1 and Nudel form a neurodevelopmentally regulated protein complex: iImplications for schizophrenia and other major neurological disorders. *Mol Cell Neurosci* 25:42–55.
37. Brandon NJ, Schurov I, Camargo LM, Handford EJ, Duran-Jimeniz B, Hunt P, *et al.* (2005): Subcellular targeting of DISC1 is dependent on a domain independent from the Nudel binding site. *Mol Cell Neurosci* 28:613–624.
38. Olzscha H, Schermann SM, Woerner AC, Pinkert S, Hecht MH, Tartaglia GG, *et al.* (2011): Amyloid-like aggregates sequester numerous metastable proteins with essential cellular functions. *Cell* 144:67–78.
39. Braak H, Del Tredici K, Rub U, de Vos RA, Jansen Steur EN, Braak E, *et al.* (2003): Staging of brain pathology related to sporadic Parkinson's disease. *Neurobiol Aging* 24:197–211.

Supplemental Information

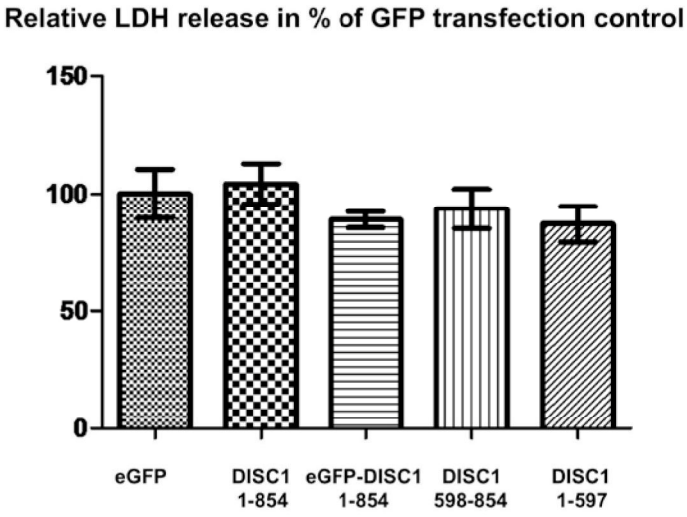

Figure S1. Measurement for potential neurotoxicity of transiently transfected construct on lacatate dehydrogenase (LDH) release into the cell culture supernatant. This analysis did not show a significant increase on the neurotoxicity-related release of LDH relative to the eGFP control after expression of several tagged or untagged DISC1 constructs (as depicted), indicating that the observed DISC1 aggresomes were not toxic to NLF human neuroblastoma cells (Children's Hospital of Philadelphia, Philadelphia, PA). One day before transfection 1 x 10^5 cells were seeded in 12 well plates, each well was transfected with 1 µg DNA using Metafectene (Biontex, Martinsried, Germany). Forty-eight hours after transfection, relative LDH release was measured with the CytoTox 96 Non-Radioactive Cytotoxicity Assay (Promega, Madison, WI).

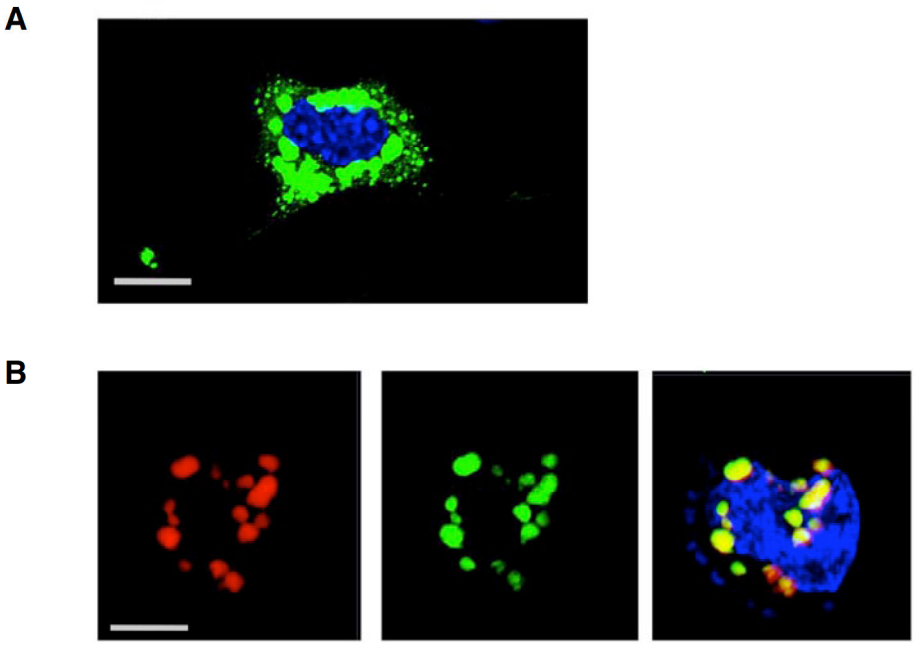

Figure S2. Laser scanning microscopy of CAD cells co-transfected with GFP-DISC1 (1-597) (**A**; green) or simultaneously with GFP-DISC1 (1-597)/green and mRFP-FL DISC1 (1-854)/red (**B**). DISC1 (1-597) (**A**) formed aggresomes similar to FL DISC1, and both constructs perfectly co-localized into merged (yellow) aggresomes (**B**, rightmost picture). Bar 10 μm. DISC1, disrupted-in-schizophrenia 1; FL, full length; GFP, green fluorescent protein; mRFP, monomeric red fluorescence protein.

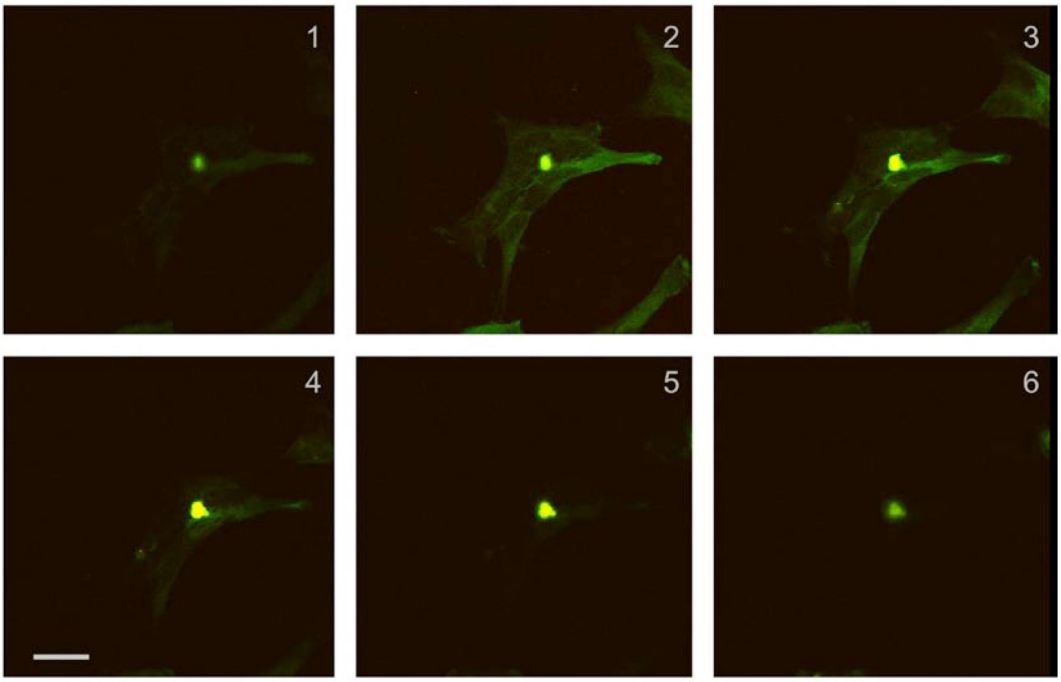

Figure S3. Laser scanning microscopy Z-scan through an invasive, SH-SY5Y-penetrating mRFP-FL DISC1 aggresome recruiting homologous GFP-DISC1 (598-854) (same image as Figure 1B[right] with additional Z-stacks serially numbered 1-6). The Z scan clearly shows that the aggresome is co-localized with cytosolic, permanently expressed GFP-DISC1 (598-854) supporting the cytosol-invasive ability of DISC1 aggresomes. Bar 20 μm. Abbreviations as in Figure S2.

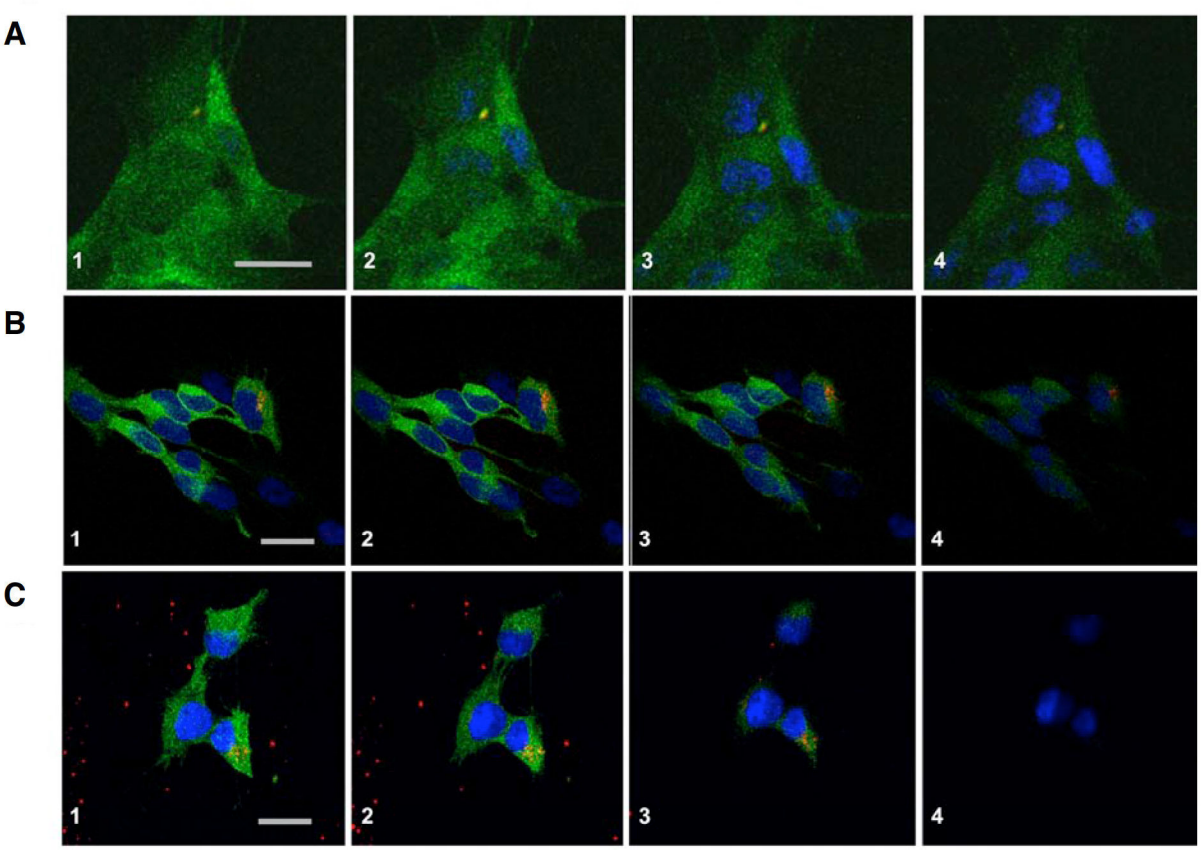

Figure S4. Laser scanning microscopy Z-scan through an invasive, cell-penetrating untagged DISC1 aggresome (**A**), synthetic α-synuclein oligomers, or recombinant DISC1 (598-854) in permanently GFP-DISC1 (598-854) expressing SH-SY5Y cells. (**A**) The Z scan clearly shows that the aggresome (stained with α-DISC1 mAB 14F2, and anti-mouse-Alexa Fluor 594; Invitrogen, Germany) is co-localized with cytosolic, permanently expressed GFP-DISC1 (598-854) indicating cytosol-invasion of untagged DISC1 aggresomes. (**B**) Synthetic α-synuclein oligomers (covalently tagged with DyLight594) penetrate SH-SY5Y cells, stain at the same z-stack as cytosolic GFP-DISC1 (598-854) similar to described before (1), but do not merge indicating absence of binding to GFP-DISC1(598-854). (**C**) Recombinant purified DISC1 (598-854), DyLight594 tagged, penetrates cells and merges to yellow with GFP-DISC (598-854); red spots are extracellular deposits of excess non-penetrated recombinant DISC1 (598-854). Bar 20 μm. Abbreviations as in Figure S2.

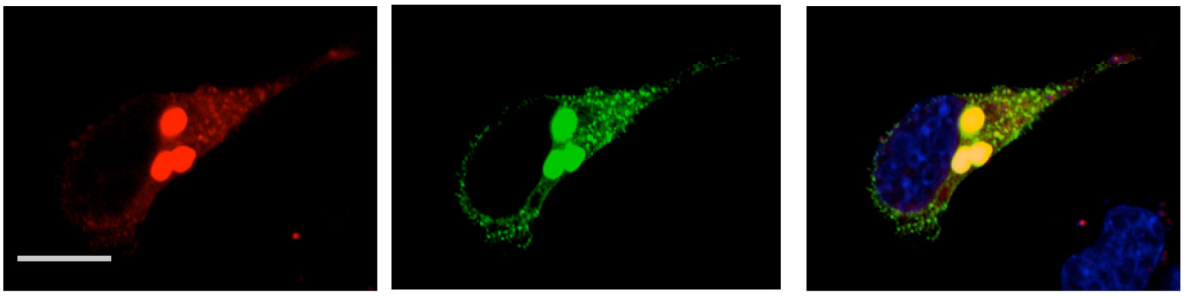

Figure S5. Laser scanning microscopy of CAD cells co-transfected with mRFP-dysbindin a (left), and GFP-FL DISC1 (middle), and the merged picture (right) demonstrates recruitment of dysbindin to DISC1 aggresomes similar to Figures 2A and B. Bar 20 μm. Abbreviations as in Figure S2.

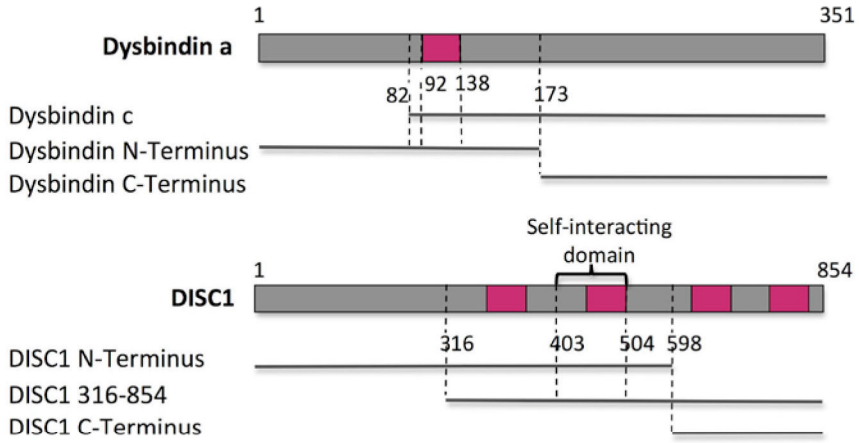

	Dysbindin a	Dysbindin c	Dysbindin (1-173)	Dysbindin (174-351)
FL DISC1	+	+	+	-

	FL DISC1	DISC1 (316-854)	DISC1 (1-597)	DISC1 (598-854)
Dysbindin a	+	+	+	-

Figure S6. Scheme and table depicting the deletion constructs of dysbindin and DISC1 (top), and the positive recruitment (denominated "+" as shown, for example, in Figure 2A, B), or absence of recruitment (denominated "-" as shown, for example, in Figure 2C) of FP-tagged dysbindin to FP-tagged DISC1 aggresomes. The interaction table demonstrates that the recruitment domain is comprised by residues 82-173 within dysbindin, and by residues 316-597 within DISC1. Abbreviations as in Figure S2.

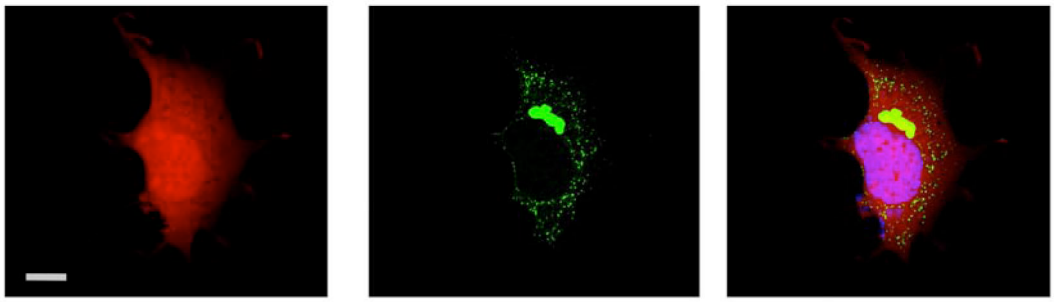

Figure S7. Laser scanning microscopy of CAD cells co-transfected with mRFP (left), and GFP-FL DISC1 (middle), and the merged picture (right) demonstrating lack of recruitment of mRFP to DISC1 aggresomes. Bar 10 μm. Abbreviations as in Figure S2.

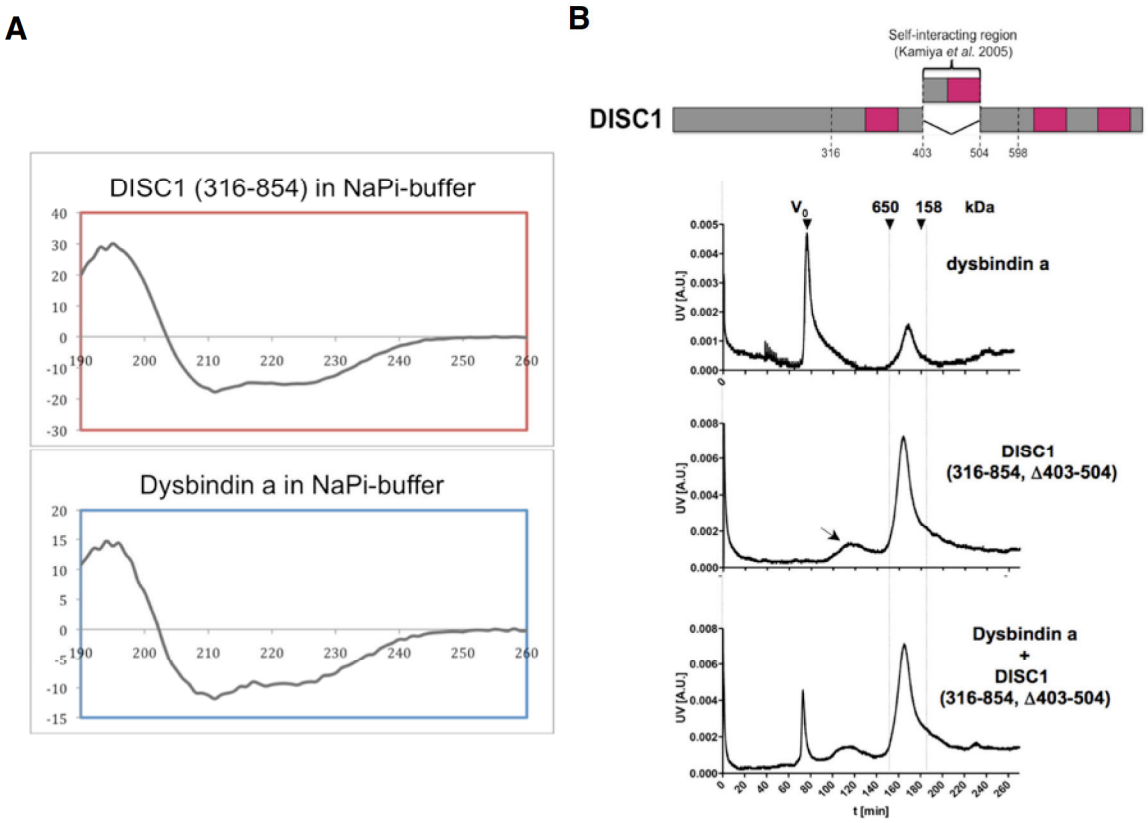

Figure S8. Protein characteristics and interaction of recombinant dysbindin a and DISC1 (316-854) expressed and purified from E. coli. **(A)** Circular dichroism (CD) spectroscopy of purified recombinant proteins DISC1 (316-854) (top) and dysbindin a (bottom) showing that both proteins do not show extended stretches of β-sheets or random coil, thus indicating a sound refolding. **(B)** Size exclusion chromatography (SEC) of recombinant dysbindin a and DISC1 (316-854, Δ403-504). SEC profile of DISC1 (316-854, Δ403-504) lacking the N-terminal self-association domain (2) was slightly different from DISC1 (316-854) in that an additional high molecular weight peak appeared (arrow), likely as the result of uncoordinated self-association. Co-incubation of dysbindin a with DISC1 (316-854, Δ403-504) did not lead to an additional high molecular weight peak as in Figure 2A indicating that the interaction mediating domain within DISC1 had been deleted.

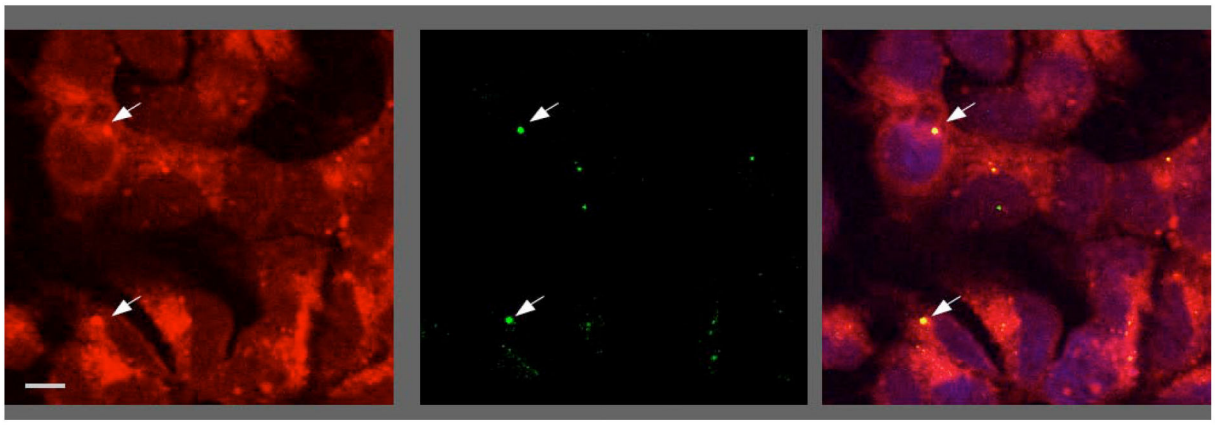

Figure S9. Laser scanning microscopy of invasive DISC1 aggresomes in SH-SY5Y cells. Purified GFP-DISC1 aggresomes (middle) are taken up into permanently mRFP-dysbindin a-expressing SH-SY5Y cells (left), and recruit mRFP dysbindin a (right). Arrows indicate the largest DISC1 aggresomes (middle and right) recruiting mRFP-dysbindin a (left). Abbreviations as in Figure S2.

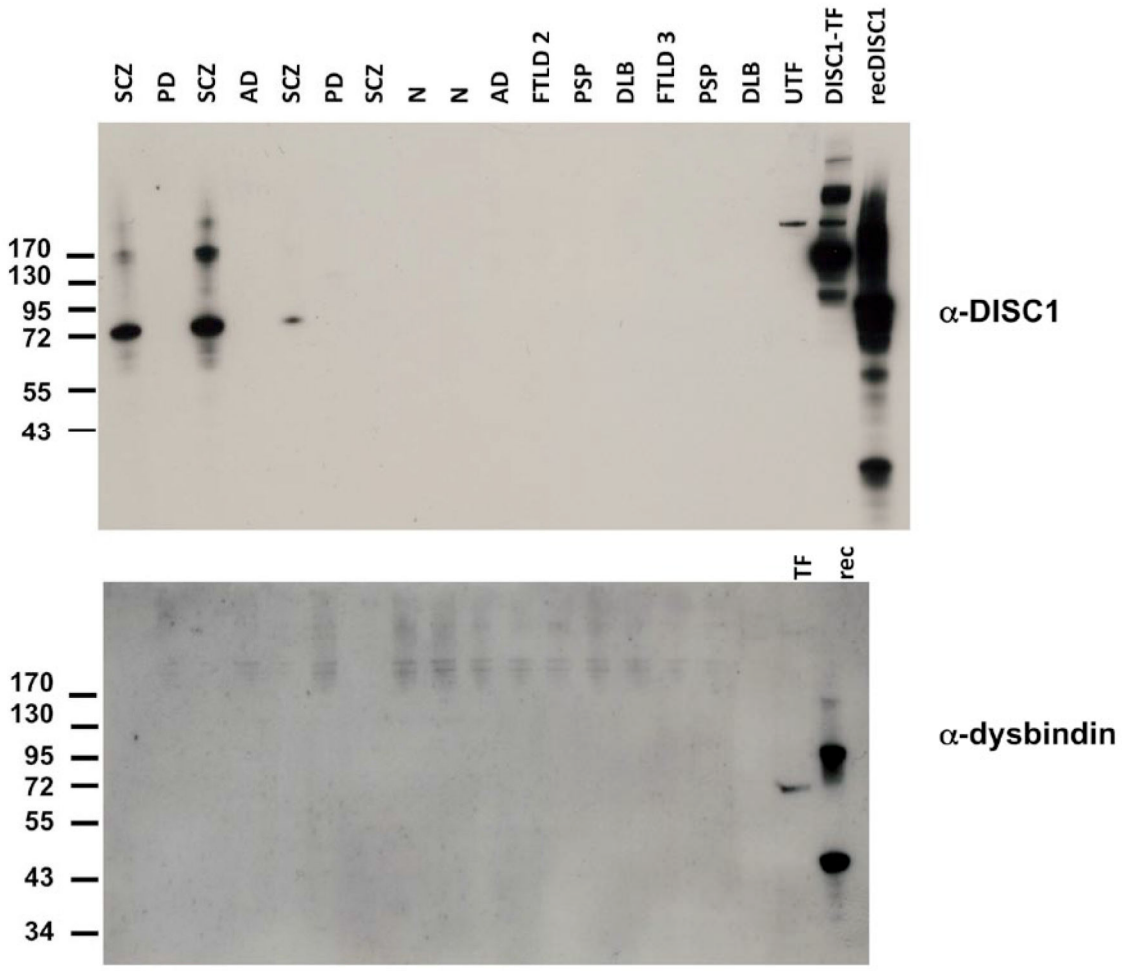

Figure S10. Western blot of insoluble fractions from post mortem brains of patients with schizophrenia (SCZ) or neuropathologically diagnosed neurodegenerative disorders: Parkinson's disease (PD), Alzheimer's disease (AD), no brain disease (N), frontotemporal dementia (FTLD2, FTLD3), progressive supranuclear palsy (PSP), or dementia with Lewy bodies (DLB). Western blots were probed with mAB14F2 for DISC1 immunoreactivity (top) or commercial antibody for dysbindin (D-20; #sc-46931, Santa Cruz Biotechnology Inc, Santa Cruz, CA). While some schizophrenia brain pellets displayed DISC1 immunoreactivity, those from neurodegenerative disorders did not. For dysbindin, no imunoreactivity was detected, except for the positive controls. UTF = untransfected (negative) control, TF = neuroblastoma cells transfected with DISC1 (top) or mRFP-dysbindin (bottom), rec = recombinant DISC1 (316-854; top) or dysbindin (bottom).

The brains were donated following informed consent of the deceased or their next of kin according to local Brain Bank regulations, and the Guidelines for Brain Banking of BrainNet Europe (www.brainnet-europe.org). Following fixation in formalin and paraffin embedding, histological and immunohistochemical investigations were performed according to the published standard procedures "Guidelines for neuropathological diagnoses" at www.brainnet-europe.org.

Processing of brain tissue and subsequent purification of the insoluble proteome was performed as described in Leliveld *et al.* (3) except for the following changes: homogenization was performed under presence of 1 x protease inhibitor cocktail (PI, Roche, Indianapolis, IN) and 2 mM PMSF. 0.5% Triton X-100 were added to the 10% homogenate prior to the first centrifugation step (1) at 20.000 x g - Steps (1) and (3) were performed only once. In step (2) no layer of 2.3 M sucrose at the bottom of the tube was applied. In step (3) the sample was treated with DNaseI in the presence of 10 mM $MgCl_2$. For step (4) the pellet was resuspended in 50 mM HEPES, pH 7.5 supplemented with 0.5% N-lauroylsarkosine (Sarkosyl). Centrifugations of this final step were carried out in a TLA-55 rotor (Beckman Coulter, Fullerton, CA).

Supplemental References

1. Desplats P, Lee HJ, Bae EJ, Patrick C, Rockenstein E, Crews L, *et al.* (2009): Inclusion formation and neuronal cell death through neuron-to-neuron transmission of alpha-synuclein. *Proc Natl Acad Sci U S A*. 106:13010-13015.
2. Kamiya A, Kubo K, Tomoda T, Takaki M, Youn R, Ozeki Y, *et al.* (2005): A schizophrenia-associated mutation of DISC1 perturbs cerebral cortex development. *Nat Cell Biol*. 7:1167-1178.
3. Leliveld SR, Bader V, Hendriks P, Prikulis I, Sajnani G, Requena JR, *et al.* (2008): Insolubility of disrupted-in-schizophrenia 1 disrupts oligomer-dependent interactions with nuclear distribution element 1 and is associated with sporadic mental disease. *J Neurosci*. 28:3839-3845.

4 Discussion

The results of the present study demonstrate that disturbed proteostasis during physiological (aging) and pathophysiological (mental illness) conditions lead to a distinct and defined accumulation of proteins.

Regarding the novel description of neuronal lipofuscin proteomic composition in humans and rats, the results demonstrated that the cellular mechanism of aging-related lipofuscin accumulation is conserved across species. This is highlighted, not only by the fact that lipofuscin accumulates as a function of biological age, rather than absolute time (21 months for rats, 65-85 years for humans) (Nakano et al., 1995), but also by the large overlap of proteins identified in the lipofuscin fractions of both species (64%). Another finding, the broad overlap of proteins identified in this approach on brain lipofuscin with the proteomic contents of lipofuscin derived from retinal pigment epithelial cells, described by Schutt et al. (Schutt et al., 2002), further indicates a general cellular mechanism underlying lipofuscin accumulation in different tissues.

Taken together, this agues for an inherent imperfection of lysosomal degradation (Brunk and Terman, 2002), already present in young organisms and causative for gradual accumulation of lipofuscin material. It therefore constitutes an impairment in proteostasis occurring early in life and – in the case of brain lipofuscin – without immediate cytotoxic effects, similar to the described non-pathology associated, gradual accumulation of amyloid-β peptide and tau protein (Braak et al., 2011). Whether these pre-pathological phenomenons, nevertheless, may gain relevance upon the global, age-

associated decline in proteostasis, remains subject of future investigations. Yet, like the Alzheimer's disease for the accumulation of Aβ and tau, diseases such as neuronal ceroid lipofuscinoses (Anderson et al., 2012) and age-related macular degeneration (Suter et al., 2000) represent pathologies characterized by the accumulation of lipofuscin-like material, which, in the case of AMD, could be demonstrated to directly confer cytotoxic properties.

It could, therefore, be reasonable to argue that aging itself constitutes a specific state of pathology and that this pathology is, at leased in parts, attributable to lipofuscin accumulation (Brunk and Terman, 2002; Terman et al., 2010). According to this hypothesis, postulated by Ulf Brunk and Alexei Terman, the accumulation of lipofuscin leads to an increase in reactive oxygen production and subsequent damage of proteins and organelles, further contributing to lipofuscin buildup, which gradually reduces lysosomal activity (Terman et al., 2010). This progressive decline in protein degradation systems in relation to age and environmental stressors, here intracellular ROS, stands in concordance with the postulated theory of "aging as an event of proteostasis collapse" (Taylor and Dillin, 2011). However, further investigations will have to clarify the apparent inconsistency of reported linear increase of lipofuscin (Ju et al., 2001; Nakano et al., 1995) versus the anticipated exponential accumulation implied by the model of Brunk and Terman (Terman et al., 2010).

The changes in proteostasis in the course of normal aging, reflected as changes in aggregome composition, described in this present study, show such age-related proteostatic alterations, previously demonstrated in the nematode *C. elegans* (David et al., 2010; Reis-Rodrigues et al., 2012), to be also present in rat hippocampus.

The finding of differential maintenance of solubility for specific neuronal proteins correlative with cognitive abilities in aged rats, supports the idea of neurons being especially vulnerable to impairments in proteostasis (Drummond and Wilke, 2008; Lee et al., 2006). Identification of the three proteins ARP3, NEB2 and BRAG2 to segregate in

aged rats relative to the observed individual scores in a special memory test, indicates the potentially far-reaching effects of even minor changes in proteostasis: Initial alterations in proteostasis may lead to changes in solubility for ARP3, NEB2 and BRAG2. Changes on these three post-synaptic proteins, in turn, could affect the integrity and function in the dendritic spine and post-synaptic density, again leading to alterations in induction and maintenance of long-term potentiation and depression. This, on the other hand, could influence synaptic transmission, on its part affecting information handling and storage – learning and memory – eventually reflected in the animal's behavior in trials intended to test these cognitive parameters, such as the Morris Water Maze used for classification of the animals in this experiment.

Future, analogous studies, carefully designed to match the needs for statistical power and sufficient hippocampal material, will have to substantiate the findings of this initial study in terms of cognition related changes in protein solubility of ARP3, NEB2 and BRAG2. Successive investigations also will have to promote answers to the question, which of the observed precipitations are primary events and which are a result of secondary, passive co-aggregation.

Not only aging, but also disease conditions may trigger a decrease in proteostasis maintenance. Besides the known diseases such as Parkinson's or type II diabetes (Chiti and Dobson, 2006), more and more pathologic states are recognized as being associated with changes in proteostasis and protein solubility (Dobson, 2001; Thomas et al., 1995). Whether these pathognomonic impairments in proteostasis are to be placed at the beginning or the end of the molecular cascades involved in the various pathophysiologies remains to be determined separately for each individual disease.

Leliveld and colleagues demonstrated the disease-specific insolubility of DISC1 in chronic mental illnesses (Leliveld et al., 2008). The study presented, investigated possible consequences of the loss of solubility for DISC1. With DISC1 being considered a hub protein (Camargo et al., 2007; Korth, 2012; Mackie et al., 2007; Yerabham et al.,

2013), its aggregation can be assumed to lead to a multitude of changed interactions, losses as well as gains.

Here, the investigations uncovered a gain of interaction with another, previously separately identified schizophrenia susceptibility protein, dysbindin, demonstrating how the loss of solubility for one particular protein (DISC1) can lead to subsequent precipitation of other, unrelated proteins, similar to what was observed by the work of Olzscha et al. (Olzscha et al., 2011). This second, co-aggregating protein being another product of a gene strongly linked to the disease of schizophrenia (Straub et al., 2002), highlights how potential secondary effects may contribute and add up to downstream effects of disease pathology. These far-reaching ramifications of DISC1 aggregation were further demonstrated in the most recent findings of Verian Bader and co-workers, who demonstrated the facultative interaction and co-aggregation of another protein implicated in critical neuronal/neurodevelopmental processes, CRMP1 (Bader et al., 2012).

Taken together, impairments in the maintenance of a functional, soluble proteome, either by inherent imperfection of components of the proteostasis network, or by its gradual decline with age and disease, are reflected in the accumulation of damaged, misfolded and hardly degradable proteins. Be it as simple conglomerates massing up in organelles, or as tightly packed aggresomes and amyloids, these accumulations or oligomeric subunits thereof have been indicated to be involved in multiple maladies from devastating neurodegenerational diseases to the pathophysiology of normal aging. Understanding the nature of these aberrant protein accumulations will help defining the pathognomonic bottlenecks in the proteostasis network, in order to uncover potential targets of therapeutic intervention (Balch et al., 2008). It is the intention of this study, to contribute to this understanding.

Bibliography

Åkerfelt, M., Morimoto, R.I., and Sistonen, L. (2010). Heat shock factors: integrators of cell stress, development and lifespan. Nat Rev Mol Cell Biol 11, 545-555.

Alzheimer, A. (1907). Über eine eigenartige Erkrankung der Hirnrinde [Concerning a novel disease of the cortex]. Allgemeine Zeitschrift für Psychiatrie Psychisch-Gerichtliche Medizin 64, 146-148.

Amaducci, L., and Tesco, G. (1994). Aging as a Major Risk for Degenerative Diseases of the Central-Nervous-System - Editorial Commentary. Curr Opin Neurol 7, 283-286.

Amieva, H., Le Goff, M., Millet, X., Orgogozo, J.M., Peres, K., Barberger-Gateau, P., Jacqmin-Gadda, H., and Dartigues, J.F. (2008). Prodromal Alzheimer's disease: successive emergence of the clinical symptoms. Annals of neurology 64, 492-498.

Anderson, G.W., Goebel, H.H., and Simonati, A. (2012). Human pathology in NCL. Biochim Biophys Acta.

Anfinsen, C.B. (1973). Principles that govern the folding of protein chains. Science 181, 223-230.

Anton, L.C., Schubert, U., Bacik, I., Princiotta, M.F., Wearsch, P.A., Gibbs, J., Day, P.M., Realini, C., Rechsteiner, M.C., Bennink, J.R., et al. (1999). Intracellular localization of proteasomal degradation of a viral antigen. J Cell Biol 146, 113-124.

Bader, V., Tomppo, L., Trossbach, S.V., Bradshaw, N.J., Prikulis, I., Leliveld, S.R., Lin, C.Y., Ishizuka, K., Sawa, A., Ramos, A., et al. (2012). Proteomic, genomic and translational approaches identify CRMP1 for a role in schizophrenia and its underlying traits. Human Molecular Genetics 21, 4406-4418.

Balch, W.E., Morimoto, R.I., Dillin, A., and Kelly, J.W. (2008). Adapting proteostasis for disease intervention. Science 319, 916-919.

Behrends, C., Langer, C.A., Boteva, R., Bottcher, U.M., Stemp, M.J., Schaffar, G., Rao, B.V., Giese, A., Kretzschmar, H., Siegers, K., et al. (2006). Chaperonin TRiC promotes the assembly of polyQ expansion proteins into nontoxic oligomers. Molecular cell 23, 887-897.

Beiser, A., D'Agostino, R.B., Seshadri, S., Sullivan, L.M., and Wolf, P.A. (2000). Computing estimates of incidence, including lifetime risk: Alzheimer's disease in the Framingham Study. The Practical Incidence Estimators (PIE) macro. Statistics in Medicine 19, 1495-1522.

Ben-Zvi, A., Miller, E.A., and Morimoto, R.I. (2009). Collapse of proteostasis represents an early molecular event in Caenorhabditis elegans aging. Proc Natl Acad Sci U S A 106, 14914-14919.

Benaroudj, N., Zwickl, P., Seemuller, E., Baumeister, W., and Goldberg, A.L. (2003). ATP hydrolysis by the proteasome regulatory complex PAN serves multiple functions in protein degradation. Molecular cell 11, 69-78.

Bence, N.F., Sampat, R.M., and Kopito, R.R. (2001). Impairment of the Ubiquitin-Proteasome System by Protein Aggregation. Science 292, 1552-1555.

Bjorkoy, G., Lamark, T., Brech, A., Outzen, H., Perander, M., Overvatn, A., Stenmark, H., and Johansen, T. (2005). p62/SQSTM1 forms protein aggregates degraded by autophagy and has a protective effect on huntingtin-induced cell death. Journal of Cell Biology 171, 603-614.

Bolognesi, B., Kumita, J.R., Barros, T.P., Esbjorner, E.K., Luheshi, L.M., Crowther, D.C., Wilson, M.R., Dobson, C.M., Favrin, G., and Yerbury, J.J. (2010). ANS binding reveals common features of cytotoxic amyloid species. ACS chemical biology 5, 735-740.

Bossy-Wetzel, E., Schwarzenbacher, R., and Lipton, S.A. (2004). Molecular pathways to neurodegeneration. Nat Med 10 Suppl, S2-9.

Braak, H., Thal, D.R., Ghebremedhin, E., and Del Tredici, K. (2011). Stages of the pathologic process in Alzheimer disease: age categories from 1 to 100 years. Journal of neuropathology and experimental neurology 70, 960-969.

Brooks, r., C L, Onuchic, J.N., and Wales, D.J. (2001). Statistical thermodynamics. Taking a walk on a landscape. Science 293, 612-613.

Brunk, U.T., and Terman, A. (2002). The mitochondrial-lysosomal axis theory of aging: accumulation of damaged mitochondria as a result of imperfect autophagocytosis. European journal of biochemistry / FEBS 269, 1996-2002.

Buchberger, A., Bukau, B., and Sommer, T. (2010). Protein Quality Control in the Cytosol and the Endoplasmic Reticulum: Brothers in Arms. Molecular cell 40, 238-252.

Camargo, L.M., Collura, V., Rain, J.-C., Mizuguchi, K., Hermjakob, H., Kerrien, S., Bonnert, T.P., Whiting, P.J., and Brandon, N.J. (2007). Disrupted in Schizophrenia 1 Interactome: evidence for the close connectivity of risk genes and a potential synaptic basis for schizophrenia. Mol Psychiatry 12, 74-86.

Carew, J.S., Medina, E.C., Esquivel Ii, J.A., Mahalingam, D., Swords, R., Kelly, K., Zhang, H., Huang, P., Mita, A.C., Mita, M.M., et al. (2010). Autophagy inhibition enhances vorinostat-induced apoptosis via ubiquitinated protein accumulation. Journal of Cellular and Molecular Medicine 14, 2448-2459.

Carrard, G., Bulteau, A.L., Petropoulos, I., and Friguet, B. (2002). Impairment of proteasome structure and function in aging. The international journal of biochemistry & cell biology 34, 1461-1474.

Cattaneo, E., Rigamonti, D., Goffredo, D., Zuccato, C., Squitieri, F., and Sipione, S. (2001). Loss of normal huntingtin function: new developments in Huntington's disease research. Trends in Neurosciences 24, 182-188.

Chen, Y.W., and Dokholyan, N.V. (2008). Natural selection against protein aggregation on self-interacting and essential proteins in yeast, fly, and worm. Mol Biol Evol 25, 1530-1533.

Chiti, F., and Dobson, C.M. (2006). Protein misfolding, functional amyloid, and human disease. Annu Rev Biochem 75, 333-366.

Cohen, E., Bieschke, J., Perciavalle, R.M., Kelly, J.W., and Dillin, A. (2006). Opposing Activities Protect Against Age-Onset Proteotoxicity. Science 313, 1604-1610.

Connell, P., Ballinger, C.A., Jiang, J., Wu, Y., Thompson, L.J., Hohfeld, J., and Patterson, C. (2001). The co-chaperone CHIP regulates protein triage decisions mediated by heat-shock proteins. Nat Cell Biol 3, 93-96.

Creutzfeldt, H.G. (1920). Über eine eigenartige herdförmige Erkrankung des Zentralnervensystems (vorläufige Mitteilung). Zeitschrift für die gesamte Neurologie und Psychiatrie 57, 1-18.

Cuervo, A.M., and Dice, J.F. (2000). Age-related decline in chaperone-mediated autophagy. J Biol Chem 275, 31505-31513.

Cuervo, A.M., Palmer, A., Rivett, A.J., and Knecht, E. (1995). Degradation of Proteasomes by Lysosomes in Rat Liver. European Journal of Biochemistry 227, 792-800.

Cuervo, A.M., Wong, E.S.P., and Martinez-Vicente, M. (2010). Protein degradation, aggregation, and misfolding. Mov Disord 25 Suppl 1, S49-54.

David, D.C., Ollikainen, N., Trinidad, J.C., Cary, M.P., Burlingame, A.L., and Kenyon, C. (2010). Widespread protein aggregation as an inherent part of aging in C. elegans. PLoS Biol 8, e1000450.

De Baets, G., Reumers, J., Delgado Blanco, J., Dopazo, J., Schymkowitz, J., and Rousseau, F. (2011). An evolutionary trade-off between protein turnover rate and protein aggregation favors a higher aggregation propensity in fast degrading proteins. PLoS computational biology 7, e1002090.

De Duve, C., and Wattiaux, R. (1966). Functions of lysosomes. Annual review of physiology 28, 435-492.

DePristo, M.A., Weinreich, D.M., and Hartl, D.L. (2005). Missense meanderings in sequence space: a biophysical view of protein evolution. Nature reviews Genetics 6, 678-687.

Ding, W.X., and Yin, X.M. (2008). Sorting, recognition and activation of the misfolded protein degradation pathways through macroautophagy and the proteasome. Autophagy 4, 141-150.

Dobson, C.M. (1999). Protein misfolding, evolution and disease. Trends Biochem Sci 24, 329-332.

Dobson, C.M. (2001). The structural basis of protein folding and its links with human disease. Philos T Roy Soc B 356, 133-145.

Dobson, C.M. (2003). Protein folding and misfolding. Nature 426, 884-890.

Douglas, P.M., and Dillin, A. (2010). Protein homeostasis and aging in neurodegeneration. J Cell Biol 190, 719-729.

Douglas, P.M., Treusch, S., Ren, H.-Y., Halfmann, R., Duennwald, M.L., Lindquist, S., and Cyr, D.M. (2008). Chaperone-dependent amyloid assembly protects cells from prion toxicity. Proceedings of the National Academy of Sciences 105, 7206-7211.

Dragatsis, I., Levine, M.S., and Zeitlin, S. (2000). Inactivation of Hdh in the brain and testis results in progressive neurodegeneration and sterility in mice. Nat Genet 26, 300-306.

Drummond, D.A., and Wilke, C.O. (2008). Mistranslation-induced protein misfolding as a dominant constraint on coding-sequence evolution. Cell 134, 341-352.

Drummond, D.A., and Wilke, C.O. (2009). The evolutionary consequences of erroneous protein synthesis. Nature reviews Genetics 10, 715-724.

Elbaz, A., Bower, J.H., Maraganore, D.M., McDonnell, S.K., Peterson, B.J., Ahlskog, J.E., Schaid, D.J., and Rocca, W.A. (2002). Risk tables for parkinsonism and Parkinson's disease. Journal of Clinical Epidemiology 55, 25-31.

Fargnoli, J., Kunisada, T., Fornace, A.J., Schneider, E.L., and Holbrook, N.J. (1990). Decreased expression of heat shock protein 70 mRNA and protein after heat treatment in cells of aged rats. Proceedings of the National Academy of Sciences 87, 846-850.

Farina, M., Avila, D.S., da Rocha, J.B.T., and Aschner, M. (2013). Metals, oxidative stress and neurodegeneration: A focus on iron, manganese and mercury. Neurochemistry International 62, 575-594.

Ferrington, D.A., Husom, A.D., and Thompson, L.V. (2005). Altered proteasome structure, function, and oxidation in aged muscle. FASEB journal : official publication of the Federation of American Societies for Experimental Biology 19, 644-646.

Fink, A.L. (1998). Protein aggregation: folding aggregates, inclusion bodies and amyloid. Fold Des 3, R9-23.

García-Mata, R., Bebök, Z., Sorscher, E.J., and Sztul, E.S. (1999). Characterization and dynamics of aggresome formation by a cytosolic GFP-chimera. J Cell Biol 146, 1239-1254.

Garcia-Mata, R., Gao, Y.-S., and Sztul, E. (2002). Hassles with taking out the garbage: Aggravating aggresomes. Traffic 3, 388-396.

Gidalevitz, T., Ben-Zvi, A., Ho, K.H., Brignull, H.R., and Morimoto, R.I. (2006). Progressive disruption of cellular protein folding in models of polyglutamine diseases. Science 311, 1471-1474.

Gidalevitz, T., Krupinski, T., Garcia, S., and Morimoto, R.I. (2009). Destabilizing protein polymorphisms in the genetic background direct phenotypic expression of mutant SOD1 toxicity. PLoS genetics 5, e1000399.

Gidalevitz, T., Prahlad, V., and Morimoto, R.I. (2011). The stress of protein misfolding: from single cells to multicellular organisms. Cold Spring Harb Perspect Biol 3.

Groll, M., Bajorek, M., Kohler, A., Moroder, L., Rubin, D.M., Huber, R., Glickman, M.H., and Finley, D. (2000). A gated channel into the proteasome core particle. Nature structural biology 7, 1062-1067.

Gupta, R., Kasturi, P., Bracher, A., Loew, C., Zheng, M., Villella, A., Garza, D., Hartl, F.U., and Raychaudhuri, S. (2011). Firefly luciferase mutants as sensors of proteome stress. Nat Meth 8, 879-884.

Haase-Pettingell, C.A., and King, J. (1988). Formation of aggregates from a thermolabile in vivo folding intermediate in P22 tailspike maturation. A model for inclusion body formation. J Biol Chem 263, 4977-4983.

Hartl, F.U. (1996). Molecular chaperones in cellular protein folding. Nature 381, 571-580.

Hartl, F.U., Bracher, A., and Hayer-Hartl, M. (2011). Molecular chaperones in protein folding and proteostasis. Nature 475, 324-332.

Haynes, C.M., and Ron, D. (2010). The mitochondrial UPR – protecting organelle protein homeostasis. Journal of Cell Science 123, 3849-3855.

Herbst, R., Schafer, U., and Seckler, R. (1997). Equilibrium intermediates in the reversible unfolding of firefly (Photinus pyralis) luciferase. J Biol Chem 272, 7099-7105.

Hershko, A., and Ciechanover, A. (1998). The ubiquitin system. Annu Rev Biochem 67, 425-479.

Heydari, A.R., Wu, B., Takahashi, R., Strong, R., and Richardson, A. (1993). Expression of heat shock protein 70 is altered by age and diet at the level of transcription. Molecular and Cellular Biology 13, 2909-2918.

Hiller, M.M., Finger, A., Schweiger, M., and Wolf, D.H. (1996). ER degradation of a misfolded luminal protein by the cytosolic ubiquitin-proteasome pathway. Science 273, 1725-1728.

Hirano, K., Guhl, B., Roth, J., and Ziak, M. (2009). A cell culture system for the induction of Mallory bodies: Mallory bodies and aggresomes represent different types of inclusion bodies. Histochem Cell Biol 132, 293-304.

Hsu, A.-L., Murphy, C.T., and Kenyon, C. (2003). Regulation of aging and age-related disease by DAF-16 and heat-shock factor. Science 300, 1142-1145.

Huntington, G. (1872). On chorea. The Medical and Surgigal Reporter: A Weekly Journal 26, 317-321.

Johnston, J.A., Dalton, M.J., Gurney, M.E., and Kopito, R.R. (2000). Formation of high molecular weight complexes of mutant Cu, Zn-superoxide dismutase in a mouse model for familial amyotrophic lateral sclerosis. Proc Natl Acad Sci U S A 97, 12571-12576.

Johnston, J.A., Illing, M.E., and Kopito, R.R. (2002). Cytoplasmic dynein/dynactin mediates the assembly of aggresomes. Cell Motil Cytoskeleton 53, 26-38.

Johnston, J.A., Ward, C.L., and Kopito, R.R. (1998). Aggresomes: a cellular response to misfolded proteins. J Cell Biol 143, 1883-1898.

Ju, S.-J., Secor, D.H., and Harvey, H.R. (2001). Growth rate variability and lipofuscin accumulation rates in the blue crab Callinectes sapidus. Marine Ecology Progress Series 224, 197-205.

Jung, T., Catalgol, B., and Grune, T. (2009). The proteasomal system. Molecular aspects of medicine 30, 191-296.

Kaganovich, D., Kopito, R., and Frydman, J. (2008). Misfolded proteins partition between two distinct quality control compartments. Nature 454, 1088-1095.

Kamerzell, T.J., and Middaugh, C.R. (2008). The complex inter-relationships between protein flexibility and stability. J Pharm Sci-Us 97, 3494-3517.

Keller, J.N., Dimayuga, E., Chen, Q., Thorpe, J., Gee, J., and Ding, Q. (2004). Autophagy, proteasomes, lipofuscin, and oxidative stress in the aging brain. The international journal of biochemistry & cell biology 36, 2376-2391.

Kim, I., Rodriguez-Enriquez, S., and Lemasters, J.J. (2007). Selective degradation of mitochondria by mitophagy. Archives of biochemistry and biophysics 462, 245-253.

Kopito, R.R. (2000). Aggresomes, inclusion bodies and protein aggregation. Trends Cell Biol 10, 524-530.

Korth, C. (2012). Aggregated proteins in schizophrenia and other chronic mental diseases DISC1opathies. Prion 6, 134-141.

Kryukov, G.V., Pennacchio, L.A., and Sunyaev, S.R. (2007). Most rare missense alleles are deleterious in humans: Implications for complex disease and association studies. American Journal of Human Genetics 80, 727-739.

Kubelka, J., Hofrichter, J., and Eaton, W.A. (2004). The protein folding 'speed limit'. Curr Opin Struct Biol 14, 76-88.

Lee, H.J., Shin, S.Y., Choi, C., Lee, Y.H., and Lee, S.J. (2002). Formation and removal of alpha-synuclein aggregates in cells exposed to mitochondrial inhibitors. J Biol Chem 277, 5411-5417.

Lee, J.W., Beebe, K., Nangle, L.A., Jang, J., Longo-Guess, C.M., Cook, S.A., Davisson, M.T., Sundberg, J.P., Schimmel, P., and Ackerman, S.L. (2006). Editing-defective tRNA synthetase causes protein misfolding and neurodegeneration. Nature 443, 50-55.

Leliveld, S.R., Bader, V., Hendriks, P., Prikulis, I., Sajnani, G., Requena, J.R., and Korth, C. (2008). Insolubility of disrupted-in-schizophrenia 1 disrupts oligomer-dependent interactions with nuclear distribution element 1 and is associated with sporadic mental disease. J Neurosci 28, 3839-3845.

Lemere, C.A., Blusztajn, J.K., Yamaguchi, H., Wisniewski, T., Saido, T.C., and Selkoe, D.J. (1996). Sequence of deposition of heterogeneous amyloid beta-peptides and APO E in Down syndrome: implications for initial events in amyloid plaque formation. Neurobiology of disease 3, 16-32.

Leverenz, J.B., and Raskind, M.A. (1998). Early amyloid deposition in the medial temporal lobe of young Down syndrome patients: a regional quantitative analysis. Exp Neurol 150, 296-304.

London, J., Skrzynia, C., and Goldberg, M.E. (1974). Renaturation of Escherichia coli tryptophanase after exposure to 8 M urea. Evidence for the existence of nucleation centers. European journal of biochemistry / FEBS 47, 409-415.

Lopez-Otin, C., Blasco, M.A., Partridge, L., Serrano, M., and Kroemer, G. (2013). The hallmarks of aging. Cell 153, 1194-1217.

Luzio, J.P., Pryor, P.R., and Bright, N.A. (2007). Lysosomes: fusion and function. Nat Rev Mol Cell Biol 8, 622-632.

Mackie, S., Millar, J.K., and Porteous, D.J. (2007). Role of DISC1 in neural development and schizophrenia. Current opinion in neurobiology 17, 95-102.

Matthews, B.W. (1993). Structural and genetic analysis of protein stability. Annu Rev Biochem 62, 139-160.

Mayeux, R. (2003). Epidemiology of neurodegeneration. Annual review of neuroscience 26, 81-104.

Min, J.N., Whaley, R.A., Sharpless, N.E., Lockyer, P., Portbury, A.L., and Patterson, C. (2008). CHIP deficiency decreases longevity, with accelerated aging phenotypes accompanied by altered protein quality control. Molecular and Cellular Biology 28, 4018-4025.

Mizushima, N., Levine, B., Cuervo, A.M., and Klionsky, D.J. (2008). Autophagy fights disease through cellular self-digestion. Nature 451, 1069-1075.

Mizushima, N., Ohsumi, Y., and Yoshimori, T. (2002). Autophagosome formation in mammalian cells. Cell structure and function 27, 421-429.

Monsellier, E., and Chiti, F. (2007). Prevention of amyloid-like aggregation as a driving force of protein evolution. EMBO Rep 8, 737-742.

Monsellier, E., Ramazzotti, M., de Laureto, P.P., Tartaglia, G.G., Taddei, N., Fontana, A., Vendruscolo, M., and Chiti, F. (2007). The distribution of residues in a polypeptide sequence is a determinant of aggregation optimized by evolution. Biophysical journal 93, 4382-4391.

Morawe, T., Hiebel, C., Kern, A., and Behl, C. (2012). Protein Homeostasis, Aging and Alzheimer's Disease. Mol Neurobiol 46, 41-54.

Morimoto, R.I. (2008). Proteotoxic stress and inducible chaperone networks in neurodegenerative disease and aging. Genes & development 22, 1427-1438.

Morrow, G., Samson, M., Michaud, S., and Tanguay, R.M. (2004). Overexpression of the small mitochondrial Hsp22 extends Drosophila life span and increases resistance to

oxidative stress. FASEB journal : official publication of the Federation of American Societies for Experimental Biology 18, 598-599.

Nakano, M., Oenzil, F., Mizuno, T., and Gotoh, S. (1995). Age-related changes in the lipofuscin accumulation of brain and heart. Gerontology 41 Suppl 2, 69-79.

Narayanaswamy, R., Levy, M., Tsechansky, M., Stovall, G.M., O'Connell, J.D., Mirrielees, J., Ellington, A.D., and Marcotte, E.M. (2009). Widespread reorganization of metabolic enzymes into reversible assemblies upon nutrient starvation. P Natl Acad Sci USA 106, 10147-10152.

Nelson, P.T., Braak, H., and Markesbery, W.R. (2009). Neuropathology and cognitive impairment in Alzheimer disease: a complex but coherent relationship. Journal of neuropathology and experimental neurology 68, 1-14.

Nelson, R., Sawaya, M.R., Balbirnie, M., Madsen, A.O., Riekel, C., Grothe, R., and Eisenberg, D. (2005). Structure of the cross-beta spine of amyloid-like fibrils. Nature 435, 773-778.

Netzer, W.J., and Ulrich Hartl, F. (1998). Protein folding in the cytosol: chaperonin-dependent and-independent mechanisms. Trends in biochemical sciences 23, 68-73.

Newby, G.A., and Lindquist, S. (2013). Blessings in disguise: biological benefits of prion-like mechanisms. Trends Cell Biol 23, 251-259.

Ohm, T.G., Müller, H., Braak, H., and Bohl, J. (1995). Close-meshed prevalence rates of different stages as a tool to uncover the rate of Alzheimer's disease-related neurofibrillary changes. Neuroscience 64, 209-217.

Olzscha, H., Schermann, S.M., Woerner, A.C., Pinkert, S., Hecht, M.H., Tartaglia, G.G., Vendruscolo, M., Hayer-Hartl, M., Hartl, F.U., and Vabulas, R.M. (2011). Amyloid-like Aggregates Sequester Numerous Metastable Proteins with Essential Cellular Functions. Cell 144, 67 - 78.

Pace, C., and Hermans, J. (1975). The stability of globular protein. Critical Reviews in Biochemistry and Molecular Biology 3, 1-43.

Pakula, A.A., and Sauer, R.T. (1989). Genetic-Analysis of Protein Stability and Function. Annu Rev Genet 23, 289-310.

Parkinson, J. (1817). An essay on the shaking palsy (Printed by Whittingham and Rowland for Sherwood, Neely, and Jones).

Princiotta, M.F., Finzi, D., Qian, S.B., Gibbs, J., Schuchmann, S., Buttgereit, F., Bennink, J.R., and Yewdell, J.W. (2003). Quantitating protein synthesis, degradation, and endogenous antigen processing. Immunity 18, 343-354.

Rajan, R.S., Illing, M.E., Bence, N.F., and Kopito, R.R. (2001). Specificity in intracellular protein aggregation and inclusion body formation. Proceedings of the National Academy of Sciences 98, 13060-13065.

Ravikumar, B., Duden, R., and Rubinsztein, D.C. (2002). Aggregate-prone proteins with polyglutamine and polyalanine expansions are degraded by autophagy. Hum Mol Genet 11, 1107-1117.

Ravikumar, B., Vacher, C., Berger, Z., Davies, J.E., Luo, S., Oroz, L.G., Scaravilli, F., Easton, D.F., Duden, R., O'Kane, C.J., et al. (2004). Inhibition of mTOR induces autophagy and reduces toxicity of polyglutamine expansions in fly and mouse models of Huntington disease. Nat Genet 36, 585-595.

Reis-Rodrigues, P., Czerwieniec, G., Peters, T.W., Evani, U.S., Alavez, S., Gaman, E.A., Vantipalli, M., Mooney, S.D., Gibson, B.W., Lithgow, G.J., et al. (2012). Proteomic analysis of age-dependent changes in protein solubility identifies genes that modulate lifespan. Aging Cell 11, 120-127.

Ron, D., and Walter, P. (2007). Signal integration in the endoplasmic reticulum unfolded protein response. Nat Rev Mol Cell Biol 8, 519-529.

Rosen, D.R., Siddique, T., Patterson, D., Figlewicz, D.A., Sapp, P., Hentati, A., Donaldson, D., Goto, J., Oregan, J.P., Deng, H.X., et al. (1993). Mutations in Cu/Zn superoxide dismutase gene are associated with familial amyotrophic lateral sclerosis. Nature 362, 59-62.

Rüdiger, S., Buchberger, A., and Bukau, B. (1997a). Interaction of Hsp70 chaperones with substrates. Nature structural & molecular biology 4, 342-349.

Rüdiger, S., Germeroth, L., Schneider-Mergener, J., and Bukau, B. (1997b). Substrate specificity of the DnaK chaperone determined by screening cellulose-bound peptide libraries. EMBO J 16, 1501-1507.

Schubert, U., Anton, L.C., Gibbs, J., Norbury, C.C., Yewdell, J.W., and Bennink, J.R. (2000). Rapid degradation of a large fraction of newly synthesized proteins by proteasomes. Nature 404, 770-774.

Schutt, F., Ueberle, B., Schnölzer, M., Holz, F.G., and Kopitz, J. (2002). Proteome analysis of lipofuscin in human retinal pigment epithelial cells. FEBS letters 528, 217-221.

Sharma, S.K., Christen, P., and Goloubinoff, P. (2009). Disaggregating Chaperones: An Unfolding Story. Current Protein & Peptide Science 10, 432-446.

Sigler, P.B., Xu, Z., Rye, H.S., Burston, S.G., Fenton, W.A., and Horwich, A.L. (1998). Structure and function in GroEL-mediated protein folding. Annu Rev Biochem 67, 581-608.

Simonsen, A., Cumming, R.C., Brech, A., Isakson, P., Schubert, D.R., and Finley, K.D. (2008). Promoting basal levels of autophagy in the nervous system enhances longevity and oxidant resistance in adult Drosophila. Autophagy 4, 176-184.

Speed, M.A., Wang, D.I., and King, J. (1996). Specific aggregation of partially folded polypeptide chains: the molecular basis of inclusion body composition. Nature biotechnology 14, 1283-1287.

Straub, R.E., Jiang, Y., MacLean, C.J., Ma, Y., Webb, B.T., Myakishev, M.V., Harris-Kerr, C., Wormley, B., Sadek, H., Kadambi, B., et al. (2002). Genetic variation in the 6p22.3 gene DTNBP1, the human ortholog of the mouse dysbindin gene, is associated with schizophrenia. Am J Hum Genet 71, 337-348.

Suter, M., Remé, C., Grimm, C., Wenzel, A., Jäättela, M., Esser, P., Kociok, N., Leist, M., and Richter, C. (2000). Age-related Macular Degeneration: The lipofuscin component N-retinyl-N-retinylidene ethanolamine detaches proapoptotic proteins from mitochondria and induces apoptosis in mammalian retinal pigment epithelial cells. Journal of Biological Chemistry 275, 39625-39630.

Swindell, W.R., Masternak, M.M., Kopchick, J.J., Conover, C.A., Bartke, A., and Miller, R.A. (2009). Endocrine regulation of heat shock protein mRNA levels in long-lived dwarf mice. Mechanisms of ageing and development 130, 393-400.

Tanaka, M., Kim, Y.M., Lee, G., Junn, E., Iwatsubo, T., and Mouradian, M.M. (2004). Aggresomes formed by alpha-synuclein and synphilin-1 are cytoprotective. J Biol Chem 279, 4625-4631.

Tartaglia, G.G., Pechmann, S., Dobson, C.M., and Vendruscolo, M. (2007). Life on the edge: a link between gene expression levels and aggregation rates of human proteins. Trends Biochem Sci 32, 204-206.

Tartaglia, G.G., Pechmann, S., Dobson, C.M., and Vendruscolo, M. (2009). A relationship between mRNA expression levels and protein solubility in E. coli. J Mol Biol 388, 381-389.

Tartaglia, G.G., and Vendruscolo, M. (2009). Correlation between mRNA expression levels and protein aggregation propensities in subcellular localisations. Molecular bioSystems 5, 1873-1876.

Taylor, J.P., Hardy, J., and Fischbeck, K.H. (2002). Toxic Proteins in Neurodegenerative Disease. Science 296, 1991-1995.

Taylor, J.P., Tanaka, F., Robitschek, J., Sandoval, C.M., Taye, A., Markovic-Plese, S., and Fischbeck, K.H. (2003). Aggresomes protect cells by enhancing the degradation of toxic polyglutamine-containing protein. Human Molecular Genetics 12, 749-757.

Taylor, R.C., and Dillin, A. (2011). Aging as an event of proteostasis collapse. Cold Spring Harb Perspect Biol 3.

Terman, A., and Brunk, U.T. (2004). Aging as a catabolic malfunction. The international journal of biochemistry & cell biology 36, 2365-2375.

Terman, A., Gustafsson, B., and Brunk, U.T. (2006). The lysosomal-mitochondrial axis theory of postmitotic aging and cell death. Chem Biol Interact 163, 29-37.

Terman, A., Gustafsson, B., and Brunk, U.T. (2007). Autophagy, organelles and ageing. J Pathol 211, 134-143.

Terman, A., Kurz, T., Navratil, M., Arriaga, E.A., and Brunk, U.T. (2010). Mitochondrial turnover and aging of long-lived postmitotic cells: the mitochondrial-lysosomal axis theory of aging. Antioxidants & redox signaling 12, 503-535.

Terman, A., and Sandberg, S. (2002). Proteasome Inhibition Enhances Lipofuscin Formation. Annals of the New York Academy of Sciences 973, 309-312.

Thomas, P.J., Qu, B.H., and Pedersen, P.L. (1995). Defective Protein-Folding as a Basis of Human-Disease. Trends in Biochemical Sciences 20, 456-459.

Uversky, V.N. (2003). Protein folding revisited. A polypeptide chain at the folding-misfolding-nonfolding cross-roads: Which way to go? Cell Mol Life Sci 60, 1852-1871.

Vendruscolo, M. (2012). Proteome folding and aggregation. Current Opinion in Structural Biology 22, 138-143.

Vendruscolo, M., Knowles, T.P.J., and Dobson, C.M. (2011). Protein solubility and protein homeostasis: a generic view of protein misfolding disorders. Cold Spring Harb Perspect Biol 3.

Waelter, S., Boeddrich, A., Lurz, R., Scherzinger, E., Lueder, G., Lehrach, H., and Wanker, E.E. (2001). Accumulation of Mutant Huntingtin Fragments in Aggresome-like Inclusion Bodies as a Result of Insufficient Protein Degradation. Molecular Biology of the Cell 12, 1393-1407.

Walker, G.A., and Lithgow, G.J. (2003). Lifespan extension in C-elegans by a molecular chaperone dependent upon insulin-like signals. Aging Cell 2, 131-139.

Wang, Y., Meriin, A.B., Zaarur, N., Romanova, N.V., Chernoff, Y.O., Costello, C.E., and Sherman, M.Y. (2009). Abnormal proteins can form aggresome in yeast: aggresome-targeting signals and components of the machinery. The FASEB Journal 23, 451-463.

Ward, C.L., Omura, S., and Kopito, R.R. (1995). Degradation of CFTR by the ubiquitin-proteasome pathway. Cell 83, 121-127.

Wetzel, R. (1994). Mutations and off-pathway aggregation of proteins. Trends in biotechnology 12, 193-198.

Wickner, S., Maurizi, M.R., and Gottesman, S. (1999). Posttranslational quality control: folding, refolding, and degrading proteins. Science 286, 1888-1893.

Wigley, W.C., Fabunmi, R.P., Lee, M.G., Marino, C.R., Muallem, S., DeMartino, G.N., and Thomas, P.J. (1999). Dynamic association of proteasomal machinery with the centrosome. J Cell Biol 145, 481-490.

Winkelmann, J., Calloni, G., Campioni, S., Mannini, B., Taddei, N., and Chiti, F. (2010). Low-level expression of a folding-incompetent protein in Escherichia coli: search for the molecular determinants of protein aggregation in vivo. J Mol Biol 398, 600-613.

Winklhofer, K.F., Tatzelt, J., and Haass, C. (2008). The two faces of protein misfolding: gain- and loss-of-function in neurodegenerative diseases. EMBO J 27, 336-349.

Wolfe, K.J., and Cyr, D.M. (2011). Amyloid in neurodegenerative diseases: Friend or foe? Seminars in Cell & Developmental Biology 22, 476-481.

Yerabham, A.S., Weiergraber, O.H., Bradshaw, N.J., and Korth, C. (2013). Revisiting Disrupted in Schizophrenia 1 as a scaffold protein. Biological chemistry.

Zettlmeissl, G., Rudolph, R., and Jaenicke, R. (1979). Reconstitution of lactic dehydrogenase. Noncovalent aggregation vs. reactivation. 1. Physical properties and kinetics of aggregation. Biochemistry 18, 5567-5571.

Acknowledgment

I owe my sincere gratitude to all people who made this dissertation possible.

First and foremost, I want to thank Prof. Dr. Carsten Korth for giving me the opportunity to work on such highly interesting projects, for his support and guidance throughout my doctoral work and for countless stimulating discussions.

I would also like to thank Prof. Dr. Dieter Willbold who courteously agreed to evaluate this thesis.

Further, I want to thank my colleagues for creating a continuously pleasant and joyful atmosphere and for their contribution in my work and their participation in most fruitful and stimulating discussions. In particular, I would like to mention in this context Dr. Verian Bader, Dr. Andreas Müller-Schiffmann, Svenja Troßbach.

Special thanks also to all my external collaborators who contributed such wealthy information to my work and thereby made this cumulative thesis possible.

I thank the Deutsche Forschungsgesellschaft, the graduate school GRK1033 and the National Contest for Life (NCL) for funding.

And last but not least, I want to express my deepest and everlasting gratitude towards my parents for their continuous support and love and their imperturbable believe in me.